

Transcutaneous auricular vagus nerve stimulation: New vistas in assessing the consequences and underlying principles.

Thesis

for the degree of
doctor rerum naturalium (Dr. rer. nat.)

approved by the Faculty of Natural Sciences of Otto von Guericke
University Magdeburg

by: M.Sc. Christian Wienke born on 21.01.1987 in Schwedt / Oder

Examiner: Prof. Dr. Tino Zähle
Prof. Dr. Matthias Weymar

submitted on: 18.12.2023

defended on: 27.06.2024

Table of content

List of abbreviations.....	III
Abstract	IV
German Abstract (Zusammenfassung)	VI
1 General Introduction	1
1.1 Basics of vagus nerve stimulation	1
1.2 Transcutaneous auricular vagus nerve stimulation as an alternative.....	2
1.3 The working mechanism of taVNS	3
1.4 The challenges in taVNS	4
1.5 Aim of this thesis	6
2 General Discussion.....	8
2.1 Summary.....	8
2.2 Phasic versus tonic taVNS.....	9
2.3 Acute taVNS biomarkers	10
2.4 Limitations.....	11
2.5 Future research	12
2.6 Conclusion	14
2.7 References	14
3 Appendix: Included peer-reviewed publications	24

List of abbreviations

μ s	<i>Microseconds</i>
ABVN	<i>Auricular Branch of the Vagus Nerve</i>
ERP	<i>Event Related Potential</i>
EWN	<i>Edinger-Westphal Nucleus</i>
FDA	<i>Food and Drug Administration</i>
Hz	<i>Hertz</i>
iVNS	<i>invasive Vagus Nerve Stimulation</i>
LC	<i>Locus Coeruleus</i>
mA	<i>Milliampere</i>
NTS	<i>Nucleus Tractus Solitarius</i>
PD	<i>Pupil Diameter</i>
tACS	<i>transcranial Alternating Current Stimulation</i>
taVNS	<i>transcutaneous auricular Vagus Nerve Stimulation</i>
tcVNS	<i>transcutaneous cervical Vagus Nerve Stimulation</i>
tDCS	<i>transcranial Direct Current Stimulation</i>
VN	<i>Vagus Nerve</i>

Abstract

Transcutaneous auricular vagus nerve stimulation (taVNS) is a relatively new stimulation method that holds promising potential as a non-invasive way to modulate brain activity. In this technique, small electrodes are attached to regions of the auricle innervated by a branch of the vagus nerve and weak electric pulses are applied to stimulate the underlying nerve fibers. Via the vagus nerve, the stimulation then reaches the brain where it can modulate activity in different cortical and subcortical areas. Despite extensive research in the last years, the exact working mechanism is still not fully understood. One likely target system is the Locus coeruleus – Noradrenaline (LC-NA) system. Much research has been conducted to investigate taVNS effects on markers of LC-NA activity. Unfortunately, many studies failed to induce observable effects, which threatens the potential of taVNS as an easy-to-use, non-invasive tool to modulate brain activity. Therefore, this thesis investigated (I) new variables that could serve as indicators of taVNS effects and (II) the potential of new stimulation paradigms to systematically modulate known markers of LC-NA activity.

This thesis contains one review article and three empirical studies. In the review article, I describe the current challenges facing the field of taVNS as well as possible ways that could, in my eyes, help to overcome these challenges. One of these challenges that could explain the large number of heterogeneous results is probably the widespread use of non-validated stimulation parameters that seem to be ineffective in modulating LC activity in experimental scenarios. The article discusses the use of phasic, event-related stimulation in contrast to the more often used tonic stimulation. The first empirical study investigated the effects of taVNS on cortical oscillations related to γ -aminobutyric acid (GABA), namely beta oscillations in the motor cortex and gamma oscillations in the visual cortex. Here, no effects of taVNS on either of these oscillatory parameters could be observed. The second empirical study investigated the effects of taVNS on markers of primary auditory perception. Previous animal research has shown that the repeated combination of short sine tones and phasic, event-related vagus nerve stimulation led to plastic changes in the animal's primary auditory cortex. Therefore, this study used a similar paradigm in humans where short sine tones were either paired with taVNS or sham stimulation. In a third condition, tones of random frequencies were presented to control for adaptation effects due to repeated presentation of the same tones. TaVNS specifically inhibited the reduction of the N1 event related potential after repeated stimulus presentation. The third empirical study investigated effects of phasic, event-related taVNS on pupillary and

oscillatory parameters during a cognitive task and during the pupil light reflex. During the cognitive task, I observed improved performance during taVNS, a stimulation specific increase in pupil diameter, as well as increased frontal theta and reduced occipital alpha oscillations. Furthermore, taVNS reduced the amplitude and delayed the onset of the pupil light reflex, showing that this parameter can be used as a proxy of LC-NA activity in future studies.

In conclusion, I present in this thesis important insights that help to advance the field of taVNS. I present results that show the effectiveness of phasic taVNS in modulating physiological parameters in experimental settings as well as a new and so far overlooked parameter that can be used in future studies to further elucidate the exact working mechanism of taVNS and to improve current stimulation paradigms.

German Abstract (Zusammenfassung)

Transkutane aurikuläre Vagusnervstimulation (taVNS) ist eine relativ neue Stimulationsmethode, die vielversprechendes Potenzial als nicht-invasive Möglichkeit zur Modulation der Gehirnaktivität bietet. Bei dieser Technik werden kleine Elektroden an Regionen der Ohrmuschel befestigt, die von einem Ast des Vagusnervs versorgt werden. Schwache elektrische Impulse werden dann appliziert um die darunterliegenden Nervenfasern zu stimulieren. Über den Vagusnerv erreicht die Stimulation das Gehirn, wo sie die Aktivität in verschiedenen kortikalen und subkortikalen Bereichen modulieren kann. Trotz umfangreicher Forschung in den letzten Jahren ist der genaue Wirkmechanismus immer noch nicht vollständig verstanden. Ein wahrscheinliches Zielsystem ist das Locus coeruleus - Noradrenalin (LC-NA) System. Es wurde viel Forschung betrieben, um die Auswirkungen von taVNS auf Marker der LC-NA-Aktivität zu untersuchen. Leider konnten viele Studien keine beobachtbaren Effekte erzielen, was das Potenzial von taVNS als einfach zu verwendendes, nicht-invasives Werkzeug zur Modulation der Gehirnaktivität in Frage stellt. Daher untersuchte diese Arbeit (I) neue Variablen, die als Indikatoren für taVNS-Effekte dienen könnten, und (II) das Potenzial neuer Stimulationsparameter zur systematischen Modulation bekannter Marker der LC-NA-Aktivität.

Diese Arbeit enthält einen Übersichtsartikel sowie drei empirische Studien. Im Übersichtsartikel beschreibe ich die aktuellen Herausforderungen, denen das Gebiet der taVNS gegenübersteht, sowie mögliche Wege, die meiner Meinung nach dazu beitragen könnten, diese Herausforderungen zu bewältigen. Eine dieser Herausforderungen, die die große Anzahl heterogener Ergebnisse erklären könnte, ist wahrscheinlich die weit verbreitete Verwendung von nicht validierten Stimulationsparametern, die in experimentellen Szenarien offenbar unwirksam zu sein scheinen. Der Artikel diskutiert die Verwendung von phasischer, ereigniskorrelierter Stimulation im Gegensatz zur häufiger verwendeten tonischen Stimulation. Die erste empirische Studie untersuchte die Auswirkungen von taVNS auf kortikale Oszillationen in Bezug auf γ -Aminobuttersäure (GABA), nämlich Beta-Oszillationen im motorischen Cortex und Gamma-Oszillationen im visuellen Cortex. Hier konnten keine Effekte von taVNS auf diese oszillatorischen Parameter beobachtet werden. Die zweite empirische Studie untersuchte die Auswirkungen von taVNS auf Marker der primären auditorischen Wahrnehmung. Frühere Tierforschung hat gezeigt, dass die wiederholte Kombination von kurzen Sinustönen und phasischer, ereigniskorrelierter Vagusnervstimulation zu plastischen Veränderungen im primären auditorischen Cortex der Tiere führte. Daher verwendete diese

Studie ein ähnliches Paradigma bei Menschen, bei dem kurze Sinustöne entweder mit taVNS oder Placebo-Stimulation gekoppelt wurden. Eine dritte Bedingung mit Tönen zufälliger Frequenzen wurde verwendet, um für Adaptationseffekte aufgrund wiederholter Präsentation der gleichen Töne zu kontrollieren. TaVNS hemmte spezifisch die Reduktion des N1 ereigniskorrelierten Potenzials nach wiederholter Reizpräsentation. Die dritte empirische Studie untersuchte die Auswirkungen phasischer, ereigniskorrelierter taVNS auf pupilläre und oszillatorische Parameter während einer kognitiven Aufgabe und während des Pupillen-Lichtreflexes. Während der kognitiven Aufgabe beobachtete ich eine verbesserte Leistung während der taVNS, eine stimulationsspezifische Zunahme des Pupillendurchmessers sowie erhöhte frontale Theta- und reduzierte okzipitale Alpha-Oszillationen. Darüber hinaus reduzierte taVNS die Amplitude und verzögerte das Einsetzen des Pupillen-Lichtreflexes, was zeigt, dass dieser Parameter in zukünftigen Studien als Indikator für die LC-NA-Aktivität verwendet werden kann.

Zusammenfassend präsentiere ich in dieser Arbeit wichtige Erkenntnisse, die dazu beitragen, das Gebiet der taVNS voranzubringen. Ich zeige Ergebnisse, die die Wirksamkeit phasischer taVNS bei der Modulation physiologischer Parameter in experimentellen Situationen zeigt sowie einen neuen und bisher übersehenen Parameter, der in zukünftigen Studien zur weiteren Aufklärung des genauen Wirkmechanismus von taVNS und zur Verbesserung aktueller Stimulationsparadigmen verwendet werden kann.

1 General Introduction

1.1 Basics of vagus nerve stimulation

The vagus nerve (VN; 10th cranial nerve) is a major part of the parasympathetic nervous system. Vagal afferent and efferent fibers innervate multiple thoracic and abdominal organs, where they play an important role in maintaining homeostasis (Butt et al., 2020). Its afferent fibers enter the brain primarily via the Nucleus tractus solitarius (NTS) of the brainstem. The NTS, in turn, projects to several different other nuclei, including the serotonergic raphe nuclei and the noradrenergic Locus coeruleus (LC) (Dolphin et al., 2022). Via these structures, vagally transmitted information then reaches large parts of the brain.

Clinical and physiological effects of vagus nerve stimulation have been investigated throughout the 20th century mainly using invasive vagus nerve stimulation (iVNS) (Badran & Austelle, 2022). Bailey and Bremer (1938) first recorded changes in orbitofrontal potentials in anesthetized cats after direct stimulation of the isolated VN. Later, a similar feline model was used to demonstrate that vagus nerve stimulation reduced chemically induced epileptic brain activity (Zanchetti et al., 1952). Main contributions were provided in the 1980s and 1990s by the group around Jacob Zabara, who showed the anti-epileptic effects of iVNS in canine models (Zabara, 1985, 1992). During this time also, Penry and Dean (1990) implanted the first four human patients, suffering from intractable epilepsy, with iVNS devices. This resulted in a complete seizure control in two patients and a 40% seizure reduction in a third patient, proving the anti-epileptic potential of vagus nerve stimulation also in humans (Penry & Dean, 1990). In humans, iVNS entails the surgical implantation of a cuff electrode, typically around the left cervical VN, as well as an implantable stimulator with battery under the collarbone. The left VN is targeted to avoid cardiac side effects like bradycardia (Goggins et al., 2022). Weak electric currents in the form of short, rectangular pulses are then delivered directly to VN (Yap et al., 2020). Further research was conducted that also demonstrated the anti-depressive effects of iVNS, leading to the approval of iVNS by the US Food and Drug Administration (FDA) as an adjunctive treatment option for pharmaco-resistant epilepsy in 1997 (Morris et al., 2013) and treatment resistant major depression disorder in 2005 (Cristancho et al., 2011).

1.2 Transcutaneous auricular vagus nerve stimulation as an alternative

Although iVNS has been proven to be feasible and effective in a number of conditions (Goggins et al., 2022), the surgical procedure necessary to implant the iVNS devices comes with certain risks for the patients. This includes nerve damage, post-operative infection or failure of single components (Butt et al., 2020). In addition to the relatively high costs, these are strong incentives to develop an equivalent, non-invasive procedure. Ventureya (2000) was the first to suggest transcutaneous vagus nerve stimulation as an alternative approach to circumvent these drawbacks. This suggestion was based on the knowledge that cutaneous information from areas of the inner auricle is transmitted to the brain via the VN. Following the seminal paper by Peuker & Filler (2002), which investigated the precise innervation of the auricle in seven body donors, interest in this technique grew. The authors showed that the cymba conchae, a region of the auricle close to the ear canal, is solely innervated by the auricular branch of the vagus nerve (ABVN), whereas other parts, such as the tragus, are at least largely innervated by the ABVN. Due to this distinct distribution of vagal fibers, the cymba conchae and the tragus are popular locations, targeted for non-invasive stimulation of the VN (Butt et al., 2020). At present, various expressions exist that describe the same technique, i.e., stimulating the ABVN via the auricle. The most common ones are *transcutaneous vagus nerve stimulation* or *transcutaneous auricular vagus nerve stimulation* (Wang et al., 2022). Because of the more precise anatomical description, I will use the term transcutaneous auricular vagus nerve stimulation (taVNS) for the rest of this thesis.

In taVNS, small surface electrodes are attached to the cymba concha or tragus region of the auricle. As with iVNS, the left auricle is commonly used to avoid cardiac side effects (Farmer et al., 2021). Although one study showed no cardiac effects after stimulation of the right ear (De Couck et al., 2017), a systematic investigation of cardiac side effects following left or right ear stimulation is still lacking (Farmer et al., 2021). Via the electrodes, weak electric pulses in the form of brief, rectangular, mono- or biphasic pulses are delivered to stimulate the underlying fibers of the ABVN (Farmer et al., 2021). The electric pulses are characterized by a combination of different parameters: pulse width, frequency and intensity. Additional parameters are the duty cycle and the duration of the stimulation (Thompson et al., 2021). *Pulse width* refers to the temporal duration of the individual stimulation pulses, typically in the range

of a few hundred microseconds (μs). *Intensity* measures the amplitude of each pulse in units of milliamperes (mA). *Frequency* indicates the number of pulses per seconds in Hertz (Hz). Additionally, many studies apply stimulation with a specific *duty cycle*, which is a time where stimulation is actually applied (ON period) followed by a time of non-stimulation (OFF period). A common duty cycles is 30 s ON followed by 30 s OFF, rhythmically changing. Finally, the *duration* describes the total time of stimulation (i.e., the summation of each ON period) (Thompson et al., 2021).

Next to taVNS, also transcutaneous cervical vagus nerve stimulation (tcVNS) was developed. In this procedure, a small hand-held stimulator is pressed against the neck over the path of the cervical VN. The stimulator then applies a weak sinusoidal current to stimulate the underlying VN (Farmer et al., 2021). However, as this thesis focusses on taVNS, tcVNS is only mentioned here for the sake of completeness.

1.3 The working mechanism of taVNS

Despite its widespread use and numerous conducted studies, the exact working mechanisms of taVNS are still not completely understood (Farmer et al., 2021). Unlike other noninvasive neuromodulation techniques like transcranial alternating current stimulation (tACS) or transcranial direct current stimulation (tDCS), taVNS does not rely on the direct modulation of neuronal reactivity (Ruhnau & Zaehle, 2021). Rather, it likely results in an increased activity in the Locus coeruleus – Noradrenaline (LC-NA) system (Burger, D’Agostini, et al., 2020; Butt et al., 2020; Farmer et al., 2021). The LC is a small, bilateral, pontine nucleus and its widespread cortical, subcortical and cerebellar projections are the main source of the brain for NA, a neuromodulatory transmitter (Sara, 2009). The LC-NA system is involved in a large number of cognitive and physiological processes (Samuels & Szabadi, 2008a, 2008b) and a loss of noradrenergic neurons in the LC is common in neurodegenerative diseases like Alzheimer’s or Parkinson’s disease (Holland et al., 2021). NA exerts its effects through α_1 -, α_2 -, and β -adrenoreceptors with α_1 - and β -adrenoreceptors causing excitatory effects while α_2 -adrenoreceptors have an inhibitory effect on the neuron (Samuels & Szabadi, 2008a).

Activation of the LC by taVNS is anatomically plausible given the large amount of input it receives from the NTS, the major relay station for the VN in the brain stem (Dolphin et al., 2022). Indeed, studies using functional magnetic resonance imaging (fMRI) have shown

increased activity along the vagal afferent pathway, including the NTS (Badran, Dowdle, et al., 2018; Frangos et al., 2015; Yakunina et al., 2017).

However, NA is likely not the only transmitter system modulated in response to taVNS. The inhibitory neurotransmitter γ – aminobutyric acid (GABA) seems to play a part in the working mechanism of taVNS as well. It has been shown, for example, that long term iVNS increased the concentration of GABA in the cerebrospinal fluid (CSF) of patients (Ben-Menachem et al., 1995; Carpenter et al., 2004) as well as the density of GABA-A receptors (Marrosu et al., 2003). Nevertheless, these connections lack sufficient investigation in taVNS, as many studies focus on NA as the main contributor of its effects.

1.4 The challenges in taVNS

As described in the previous section, modulation of the LC-NA system is one prospective target mechanism through which taVNS exerts its effects. For this reason, many studies have investigated effects of taVNS on indirect markers of LC-NA activity in humans. These include, for example, the pupil diameter (PD), the P3 event related potential (ERP) or the enzyme salivary alpha amylase (Burger, D'Agostini, et al., 2020). The most promising of these markers is probably the PD due to its close relation to the LC-NA system. The rationale to use the PD as an indicator of LC-NA activity and taVNS effects is as follows: Two antagonizing muscles in the iris regulate the PD. A sympathetically innervated dilator muscle causes pupil dilation and a parasympathetically innervated sphincter muscle causes the pupil to constrict. Under constant light conditions, both systems are in balance, allowing the PD to remain stable (Eckstein et al., 2017). As light exposure increases, higher activity in the Edinger-Westphal Nucleus (EWN), located in the midbrain, shifts this balance towards the parasympathetic side, leading to pupil constriction (Eckstein et al., 2017; Hall & Chilcott, 2018). Importantly, activity in the EWN can be inhibited via α_2 -adrenoreceptors (Hall & Chilcott, 2018; Samuels & Szabadi, 2008a, 2008b). Therefore, an increase in LC-NA activity should inhibit activity in EWN, causing a shift towards a relatively stronger activation of the sympathetically innervated dilator muscle, which results in a dilation of the pupil even under constant lighting conditions. Results, however, are heterogeneous. Despite this clear anatomical pathway, many studies failed to show modulating effects of taVNS on PD (e.g., Burger, Van der Does, et al., 2020; D'Agostini et al., 2022; Keute et al., 2019).

One challenge that factors into this could be the lack of validated stimulation parameters. The most commonly used parameter combinations are 200 – 250 μ s pulse width, frequencies between 20 and 30 Hz and duty cycles of 30 to 60 s ON (Ludwig et al., 2021; Thompson et al., 2021; Yap et al., 2020). However, previous studies using this setup often failed to achieve observable modulations in the outcome measure. Originally, these parameter combinations stem from experience with iVNS. There, frequencies between 20 and 30 Hz were arbitrarily chosen to avoid nerve damage that can occur in excess of 50 Hz. Duty cycles of around 30 s followed by an OFF period were chosen to prolong battery life and the stimulation intensity was adjusted based on patients' comfort (Thompson et al., 2021). Systematic investigations of optimal parameter settings for taVNS, however, are lacking (Ludwig et al., 2021). Although individual studies modulated one (Capone et al., 2021) or two parameters (Badran, Mithoefer, et al., 2018; Urbin et al., 2021), their methodologies differ and their results are far from conclusive.

Especially the timing in form of these long and stimulus-independent stimulations seems to be a major issue in previous studies. For instance, animal research has shown that short, phasic trains of stimulation systematically increased LC firing rates (Collins et al., 2021; Hulsey et al., 2017; Mridha et al., 2021; Rembado et al., 2021) and caused plastic changes in the rats' auditory cortices when combined with acoustic stimuli (Borland et al., 2016; C. T. Engineer et al., 2015; N. D. Engineer et al., 2011; Shetake et al., 2012). In line with this, recent taVNS studies in humans have also shown promising results in response to short trains of stimulation (D'Agostini et al., 2023; Sharon et al., 2021; Urbin et al., 2021; Villani et al., 2022). These studies used stimulation durations between 600 and 5000 ms and observed systematic modulation of the PD, showing the promising connection between taVNS and modulated LC-NA activity. However, stimulation was largely applied in the absence of a specific task (D'Agostini et al., 2023; Sharon et al., 2021; Urbin et al., 2021) or started before the onset of a relevant stimulus (Villani et al., 2022). Therefore, the question remains how phasic taVNS affects noradrenergic outcome measures in an event-related fashion (i.e., coinciding with a relevant stimulus).

Furthermore, studies have so far focused on the PD in response to stimulation itself. The pupil light reflex (PLR), however, has not been considered as proxy of noradrenergic activity even though it is also modulated by the NA concentration (Bitsios et al., 1999; Hysek & Liechti, 2012). Previous studies have shown that increased NA concentrations, e.g. after pharmacological intervention (Bitsios et al., 1999; Hysek & Liechti, 2012) or in subjects with

high arousal due to anxiety (Bakes et al., 1990) or threat of electric shock (Bitsios et al., 1996) led to a reduction in the physiological PLR. In light of these observations, it is reasonable to investigate the PLR as a further marker of LC-NA activation in taVNS studies.

1.5 Aim of this thesis

This thesis aggregates four separate studies. Following the challenges outlined in chapter 1.4, the aim of this thesis was to (I) validate phasic, event-related taVNS as a non-invasive tool to modulate LC-NA activity in experimental settings, (II) transfer a paradigm from animal research onto human subjects and (III) investigate the effects of taVNS on so far under-appreciated parameters like GABA-associated cortical oscillations or the PLR.

In study 1 (Ludwig / Wienke et al., 2021), I reviewed the previous literature on taVNS and summarized the challenges facing the field of taVNS. Furthermore, I aimed to present possible ways how to conquer these.

In study 2 (Keute et al., 2020), I investigated the effects of taVNS on GABA associated brain oscillations. As mentioned above, the effects of taVNS on markers of GABAergic activation lack investigation. However, certain oscillatory frequency ranges in the motor and visual cortex are tightly linked to GABAergic activity (Edden et al., 2009; Muthukumaraswamy et al., 2013) and could thus possibly be used to index taVNS effects. In concrete, we hypothesized that taVNS would modulate movement-associated oscillations in the beta range and gamma oscillations in the primary visual cortex related to visual processing.

In Study 3 (Rufener / Wienke et al., 2023), I aimed to transfer a paradigm with known effects in the animal model onto humans. NA plays a crucial role in plastic adaptation processes in the brain. Studies combining iVNS in rodents with the repeated presentation of pure sine tones were able to show plastic changes in the primary auditory cortex of these animals (Adcock et al., 2020; Borland et al., 2016; Shetake et al., 2012) and were even able to reverse pathological activity induced by tinnitus (N. D. Engineer et al., 2011). Therefore, I investigated whether similar effects can be induced in humans using non-invasive, phasic taVNS. Sham stimulation or taVNS were combined with the repeated presentation of pure sine tones in a sample of healthy, adult subjects. Brain activity in response to these tones was recorded to analyze cortical

response patterns. I hypothesized that taVNS would reduce the typically observed reduction in the N1 amplitude, an ERP marker of primary auditory processing (Näätänen & Picton, 1987) .

Finally, in study 4 (Wienke et al., 2023), I aimed to investigate the effects of phasic taVNS on electrophysiological, pupillary and behavioral parameters of LC-NA activity. As mentioned above, many previous studies failed to induce modulations in PD via taVNS despite the clear anatomical connection (e.g., Burger, Van der Does, et al., 2020; D'Agostini et al., 2022; Keute et al., 2019). Given the aforementioned effects induced by short-term, phasic stimulation in animals (e.g., C. T. Engineer et al., 2015; N. D. Engineer et al., 2011) and humans (D'Agostini et al., 2023; Sharon et al., 2021) and the results from our own study (Rufener et al., 2023), I hypothesized that the event-related application of short-term taVNS (500 ms) would systematically modulate behavioral, pupillary, and electrophysiological parameters in a cognitive processing task. In concrete, I hypothesized that the stimulation would improve accuracy and reaction time. For the pupil, I expected increased PD during cognitive processing and a reduced amplitude of the PLR. For the electrophysiological parameters, I hypothesized increased frontal-midline theta power as well as reduced occipital alpha power.

2 General Discussion

2.1 Summary

The first study in this thesis (Ludwig / Wienke et al., 2021) provided a review of recent taVNS literature with the aim to identify current challenges facing the field. We discussed how the use of suboptimal stimulation parameters might be limiting current research, particularly in identifying adequate biomarkers of LC-NA activity and improving stimulation parameters. To address this issue, we proposed the use of phasic stimulation, a method that has shown promising results in animal research, recent human taVNS studies, and the research presented in this thesis. Furthermore, we outline the potential of animal research to investigate effects of vagus nerve stimulation in translational, cross species approaches.

The second study (Keute et al., 2020) aimed to investigate modulating effects of taVNS on cortical, GABA associated oscillations. Much research over the last few years has focused on NA associated effects but the role of GABA in taVNS remains under-explored. Following a 30 minute stimulation period, subjects performed cued button presses with either the left or right index finger and passively viewed simple Gabor gratings. We hypothesized that taVNS would modulate resting beta power, peri- and post-movement related beta power as well as visual gamma power. Against our hypotheses, we observed no stimulation specific effects on beta or gamma as well as no lateralization effect.

The third study (Rufener / Wienke et al., 2023) aimed to transfer a paradigm with known results in animal research onto human subjects using taVNS. Animal research has shown that the repeated combination of phasic iVNS with pure sine tones led to plastic changes in the A1 of these animals. We adapted this paradigm for a single session in humans where we recorded brain activity using EEG before and after pairing pure sine tones with taVNS or sham stimulation. According to our hypotheses, we observed that phasic taVNS, coinciding with tone presentation, inhibited the known reduction of the N1 ERP after repeated tone presentation.

Finally, the fourth study (Wienke et al., 2023) aimed to further investigate the potential of phasic, event related taVNS on electrophysiological, pupillary, and behavioral parameters during a cognitive task. Additionally, this study investigated the potential of the PLR as an indirect marker of taVNS effects. According to my hypotheses, phasic, event related taVNS improved behavioral accuracy during the cognitive task and led to increased PD. Regarding

cortical oscillations, the stimulation increased frontal theta and alpha oscillations and reduced occipital alpha power. During the PLRT, also in accordance with my hypothesis, phasic event related taVNS reduced the amplitude of the PLR. Further analyses revealed that also the onset of the PLR was delayed. Importantly, these results are in agreement with an increased activity in the LC-NA system.

In summary, I have demonstrated in this thesis the potential of event-related, phasic taVNS to modulate activity in the LC-NA system in experimental settings. This was shown in two separate studies with different parameters under investigation. Further, I was able to show that the PLR can be used as a valid parameter to investigate the modulation of the LC-NA system by taVNS. On the other hand, no effects of taVNS on GABA associated oscillations could be observed.

2.2 Phasic versus tonic taVNS

As described above, one problem in current taVNS research is the usage of largely unverified and potentially suboptimal stimulation parameters (Ludwig et al., 2021; Thompson et al., 2021). Many studies rely on commercially available stimulation devices with a predefined set of stimulation parameters (Yap et al., 2020). Although this provides an easy-to-use and economic way to apply stimulation, it often restricts researchers to the stimulation parameters set by the manufacturers.

One aim of this thesis is to argue, that this approach needs to be reconsidered. Especially the temporal duration of the stimulation seems to be a crucial parameter. Research on animals (Borland et al., 2018; C. T. Engineer et al., 2015; N. D. Engineer et al., 2011; Shetake et al., 2012) and humans (D'Agostini et al., 2023; Sharon et al., 2021; Urbin et al., 2021) has shown the potential of shorter stimulation durations to modulate activity in the LC-NA system. The reason for this could lie in the different activity modes of the LC. In general, the LC shows two patterns of activity: First, a tonic baseline activity and second, a phasic burst-like activity mode in response to salient or behaviorally relevant stimuli (Aston-Jones & Bloom, 1981; Aston-Jones & Cohen, 2005; Berridge & Waterhouse, 2003). Regarding the PD, for example, the tonic baseline activity is more related to baseline PD while the phasic activation is reflected in transient increases in PD (Aston-Jones & Cohen, 2005). Furthermore, animal research has shown that especially the phasic activity mode was associated with an increase in NA concentration (Florin-Lechner et al., 1996). Therefore, I argue that the phasic stimulation

applied in this and other recent work (D'Agostini et al., 2023; Sharon et al., 2021; Urbin et al., 2021) was better able to enhance the activity in the LC and thus lead to stimulation specific effects. Especially the event related, phasic stimulation used in study three and four of this thesis might have been able to enhance the naturally occurring phasic activity in the LC in response to the stimuli. This would then lead to transiently increased levels of NA that, in turn, led to the observed results in these studies. This seems plausible as the nearly identical stimulation regime led to distinct, stimulation specific effects in different target regions, i.e., primary auditory processing, PD or frontal theta power.

Tonic LC activity on the other hand is strongly correlated with the current vigilance level (Rajkowski et al., 1994) and forms an inverted-U function between activity and task performance when selective attention is required (Aston-Jones & Cohen, 2005). In monkeys, low tonic LC activity corresponds to inattentiveness while high tonic LC-activity leads to heightened distractibility, which also impairs performance. During intermediate tonic LC activity, however, performance is optimal (Aston-Jones et al., 1999; Aston-Jones & Cohen, 2005). In humans, higher tonic LC activity, indexed by baseline pupil diameter, was related to measures of attention-deficit / hyperactivity disorder (Kim et al., 2022).

2.3 Acute taVNS biomarkers

As described above, much of taVNS research has focused on indirect markers of NA activity. This includes electrophysiological parameters like the P3 ERP, enzymatic ones like salivary alpha amylase or the PD (Burger, D'Agostini, et al., 2020; Farmer et al., 2021). For all these parameters, previous study results are highly heterogeneous, with some studies showing modulating effects, while others failed to observe stimulation specific effects (Burger, D'Agostini, et al., 2020; Farmer et al., 2021). Based on anatomical considerations, the PD seems to be the most valid proxy of LC-NA activity but these heterogeneous results threatened the validity of taVNS to systematically modulate activity in the LC. This thesis, as well as other recent publications (D'Agostini et al., 2023; Sharon et al., 2021; Urbin et al., 2021; Villani et al., 2022), have shown evidence that this problem might be rooted in the use of suboptimal stimulation parameters. Using phasic, event-related stimulation, I was able to systematically modulate the PD in the expected manner. That is, an increase in PD as sign for an increased LC activity. This shows that phasic taVNS is indeed able to modulate brain activity in experimental settings and that the PD remains a valid readout of short-term stimulation effects.

Furthermore, I was able to show that the PLR is a similarly good indicator of stimulation effects. Surprisingly, this was not investigated earlier as pharmacological studies already showed a connection between the PLR and increased LC-NA activity (Bakes et al., 1990; Bitsios et al., 1996, 1999; Hysek & Liechti, 2012). The use of the PLR could give future studies an easy-to-use tool to check whether their stimulation setup works, as it is relatively easy and fast to measure. This can also be used in clinical settings when taVNS is supposed to be used as an adjunctive therapy option. Here also, proper function in the stimulation setup could be tested in advance. Altogether, the PLR could provide for a new proxy in taVNS studies as it is easy to measure and provides a stereotypical response where systematic modulations are easy to observe.

Apart from pupillary parameters, cortical low-frequency oscillations have been considered as indicators of LC activity. One recent taVNS study reported decreased power in the alpha range at parieto-occipital electrodes (Sharon et al., 2021) which is in line with observations from previous iVNS studies (Bodin et al., 2015; Lewine et al., 2019). Note however, that a more recent study failed to replicate the alpha effect from the Sharon et al. (2021) paper (Lloyd et al., 2023). Study four in this thesis also observed an effect of taVNS on occipital alpha during both the EST as well as the PLRT. We also observed an effect on FM-theta oscillations during the EST. FM-theta power is also associated with the LC-NA system (Dippel et al., 2017) and has been successfully modulated in a previous taVNS study during cognitive processing (Keute et al., 2020). These results further underlie the potential of phasic taVNS to modulate low-frequency cortical oscillations and the use of these oscillations as markers of noradrenergic activity.

2.4 Limitations

Of course, this work is not free of limitations. Like many other studies, I dedicated large parts of this thesis to effects associated with the LC-NA system. However, as with most things, reality is likely far more complex and includes more than just this one neurotransmitter. The NTS, the major relay station for the VN in the brain stem, exhibits widespread connections to other nuclei like the serotonergic Raphe nuclei or to basal and forebrain areas (Frangos et al., 2015; Krahl & Clark, 2012). It is also known that cholinergic projections from the basal forebrain play a role in modulating PD (Mridha et al., 2021; Reimer et al., 2016). Hence, a cholinergic

interaction cannot be ruled out. However, as with GABA, the involvement of these other transmitter systems is currently not studied well enough to make any definitive conclusions.

Although study two in this thesis (Keute et al., 2021) aimed to investigate taVNS effects on GABA associated oscillations, we did not observe any stimulation specific effect of taVNS. There are several possible explanations for this. For instance, based on the success of the phasic stimulation in study three and four, it is possible that the tonic stimulation of 60 s, unrelated to any stimulus or movement was insufficient to systematically increase GABA concentrations. Whether a phasic stimulation paradigm can lead to observable effects on these parameters remains to be investigated. On the other hand, it is possible that the stimulation was still not long enough. This means that increased NA and GABA concentrations may occur on different temporal scales. Evidence for the involvement of GABA in the effects of vagus nerve stimulation stems from studies using iVNS in humans that received this form of stimulation over a prolonged period of time (Ben-Menachem et al., 1995; Carpenter et al., 2004; Marrosu et al., 2003). It is thus possible that an increased level of GABA can only be achieved by longer stimulation paradigms.

Another limitation is also mentioned in study four (Wienke et al., 2023) and stems from the stimulation itself. When using concurrent electrical stimulation and electrophysiological recordings of brain activity, one is confronted with an enormous stimulation artifact that contaminates the data. Therefore, the number of studies that used this approach is limited (Hyvärinen et al., 2015; Keatch et al., 2022; Lehtimäki et al., 2013). Although the approach used in study four to clean the artifact from the data has been used elsewhere (Keatch et al., 2022, 2023), results have to be interpreted with care as all interpolation bears the risk of data alterations. To reliably estimate online effects of taVNS on brain activity, more sophisticated methods are required to clean the data from the stimulation artefact.

2.5 Future research

In the introduction of this thesis, I mentioned that the largely unverified stimulation parameters might be a major reason why so many studies have failed to observe stimulation-specific effects of taVNS. Although this thesis and other studies (D'Agostini et al., 2023; Sharon et al., 2021; Urbin et al., 2021; Villani et al., 2022) have shown the potential of shorter stimulation duration, this does not mean that the search for optimal stimulation parameters is at or near its ending. In my opinion, this was just the first step in this endeavor. More research is needed to improve

stimulation settings in order to maximize its potential for future clinical and research oriented approaches. One way to achieve this might be the use of more sophisticated statistical approaches to deduce optimal stimulation parameters. For instance, Bayesian optimization techniques have been used in tACS research to improve stimulation outcomes (Lorenz et al., 2019). As described above, the combination of several stimulation parameters like intensity, pulse width, frequency, and stimulation duration spans a multidimensional parameter space from which researchers have to choose. Picking parameters at random is thus unlikely to produce meaningful results and exhaustively testing all parameter combinations is not feasible. In Bayesian optimization approaches, existing data from previous studies or trials with different parameter settings can be used in an iterative process to model the objective function, i.e. the relationship between the stimulation parameters and the outcome under scrutiny. This surrogate model is then used to make prediction about the models behavior and to choose stimulation parameters for the next block or subject (Lorenz et al., 2019). The drawback of this technique is that it requires large amounts of data to estimate the most optimal parameters. This means that for the first iterations, random parameter combinations can be used until the surrogate model can be estimated. The advantage on the other hand is that already existing data from e.g. previous studies can be used to expedite this process. Furthermore, the accuracy of the model improves with each new iteration. This can help researches to optimize their stimulation paradigm and to investigate whether the different outcomes require different optimal stimulation parameter settings.

Another important aspect that requires further investigation are the long term effects of phasic taVNS. The studies conducted in this thesis, as many other studies, focus only on the effects of short term stimulation. In the animal research that formed the basis for study three, iVNS and auditory stimuli were repeatedly combined multiple times a day over a 20 day period and led to longer lasting effects of at least three weeks (N. D. Engineer et al., 2011). As we have seen observable results after already 1 stimulation session, it seems plausible to assume that longer lasting effects could be achieved by repeating this procedure over several days. Based on the relative simplicity of the task and the fact that taVNS has already been used in self-administered at home treatments (Badran et al., 2022), this assumption could easily be tested.

Furthermore, future research should try to incorporate inter-individual differences in parameter settings. As mentioned, most studies use very similar frequency and pulse width settings (Thompson et al., 2021; Yap et al., 2020). Regarding the stimulation intensity, there are currently two different approaches: (I) Using the same intensity for all subjects (e.g., Höper

et al., 2022; Keute et al., 2020; Warren et al., 2019) or (II) individually adjusting the intensity for each subjects to the same subjective perception (e.g., Giraudier et al., 2020; Kühnel et al., 2020; Neuser et al., 2020). The first approach poses the risk of different perceptions between subjects based on inter-individual differences in e.g., skin thickness that could influence the perception of the stimulation. The second approach, on the other hand, poses the risk of widely differing stimulation intensities among subjects. Badran et al. (2019) proposed a standardized procedure to individually adjust stimulation intensities based on subjective ratings. However, as of now there is no clear consensus which of the two approaches is preferable.

Finally, the role of other transmitter systems in the effects of taVNS requires further investigation. As mentioned before other transmitter systems are likely involved due to the widespread connections from the NTS. Some animal studies exist that show an involvement of the cholinergic system (Hulseley et al., 2016; Lu et al., 2017) but this aspect lacks investigation in human studies.

2.6 Conclusion

Taken together, I have shown in this thesis that taVNS remains a valid stimulation technique with promising potential for experimental and clinical settings. I presented two compelling studies showing the potential of phasic, event related stimulation to modulate activity in the LC-NA system in experimental settings. As a result, this thesis helps to further our understanding of the working mechanisms of taVNS and the LC-NA system in general. Future research can exploit these results to further investigate the working mechanisms of taVNS and to improve the experimental and therapeutic potential of taVNS. Considering the high potential of taVNS as a non-invasive, easy-to-use treatment additive, this work contributes to the ever growing literature that emphasizes the use of new stimulation paradigms. I am optimistic that this work can play its part in encouraging new studies that will further improve this exciting technology and make it accessible to a larger group of people.

2.7 References

Adcock, K. S., Chandler, C., Buell, E. P., Solorzano, B. R., Loerwald, K. W., Borland, M. S., & Engineer, C. T. (2020). Vagus nerve stimulation paired with tones restores auditory processing in a rat model of Rett syndrome. *Brain Stimulation*, *13*(6), 1494–1503. <https://doi.org/10.1016/j.brs.2020.08.006>

- Aston-Jones, G., & Bloom, F. E. (1981). Activity of norepinephrine-containing locus coeruleus neurons in behaving rats anticipates fluctuations in the sleep-waking cycle. *The Journal of Neuroscience*, *1*(8). <https://doi.org/10.1523/JNEUROSCI.01-08-00876.1981>
- Aston-Jones, G., & Cohen, J. D. (2005). An integrative theory of locus coeruleus-norepinephrine function: Adaptive gain and optimal performance. *Annual Review of Neuroscience*, *28*(1), 403–450. <https://doi.org/10.1146/annurev.neuro.28.061604.135709>
- Aston-Jones, G., Rajkowski, J., & Cohen, J. (1999). Role of locus coeruleus in attention and behavioral flexibility. *Biological Psychiatry*, *46*(9), 1309–1320. [https://doi.org/10.1016/S0006-3223\(99\)00140-7](https://doi.org/10.1016/S0006-3223(99)00140-7)
- Badran, B. W., & Austelle, C. W. (2022). The Future Is Noninvasive: A Brief Review of the Evolution and Clinical Utility of Vagus Nerve Stimulation. *FOCUS*, *20*(1), 3–7. <https://doi.org/10.1176/appi.focus.20210023>
- Badran, B. W., Dowdle, L. T., Mithoefer, O. J., LaBate, N. T., Coatsworth, J., Brown, J. C., DeVries, W. H., Austelle, C. W., McTeague, L. M., & George, M. S. (2018). Neurophysiologic effects of transcutaneous auricular vagus nerve stimulation (taVNS) via electrical stimulation of the tragus: A concurrent taVNS/fMRI study and review. *Brain Stimulation*, *11*(3), 492–500. <https://doi.org/10.1016/j.brs.2017.12.009>
- Badran, B. W., Huffman, S. M., Dancy, M., Austelle, C. W., Bikson, M., Kautz, S. A., & George, M. S. (2022). A pilot randomized controlled trial of supervised, at-home, self-administered transcutaneous auricular vagus nerve stimulation (taVNS) to manage long COVID symptoms. *Bioelectronic Medicine*, *8*(1), 13. <https://doi.org/10.1186/s42234-022-00094-y>
- Badran, B. W., Mithoefer, O. J., Summer, C. E., LaBate, N. T., Glusman, C. E., Badran, A. W., DeVries, W. H., Summers, P. M., Austelle, C. W., McTeague, L. M., Borckardt, J. J., & George, M. S. (2018). Short trains of transcutaneous auricular vagus nerve stimulation (taVNS) have parameter-specific effects on heart rate. *Brain Stimulation*, *11*(4), 699–708. <https://doi.org/10.1016/j.brs.2018.04.004>
- Badran, B. W., Yu, A. B., Adair, D., Mappin, G., DeVries, W. H., Jenkins, D. D., George, M. S., & Bikson, M. (2019). Laboratory Administration of Transcutaneous Auricular Vagus Nerve Stimulation (taVNS): Technique, Targeting, and Considerations. *Journal of Visualized Experiments*, *143*, 58984. <https://doi.org/10.3791/58984>
- Bailey, P., & Bremer, F. (1938). A SENSORY CORTICAL REPRESENTATION OF THE VAGUS NERVE: WITH A NOTE ON THE EFFECTS OF LOW BLOOD PRESSURE ON THE CORTICAL ELECTROGRAM. *Journal of Neurophysiology*, *1*(5), 405–412. <https://doi.org/10.1152/jn.1938.1.5.405>
- Bakes, A., Bradshaw, C., & Szabadi, E. (1990). Attenuation of the pupillary light reflex in anxious patients. *British Journal of Clinical Pharmacology*, *30*(3), 377–381. <https://doi.org/10.1111/j.1365-2125.1990.tb03787.x>
- Ben-Menachem, E., Hamberger, A., Hedner, T., Hammond, E. J., Uthman, B. M., Slater, J., Treig, T., Stefan, H., Ramsay, R. E., Wernicke, J. F., & Wilder, B. J. (1995). Effects of

- vagus nerve stimulation on amino acids and other metabolites in the CSF of patients with partial seizures. *Epilepsy Research*, 20(3), 221–227. [https://doi.org/10.1016/0920-1211\(94\)00083-9](https://doi.org/10.1016/0920-1211(94)00083-9)
- Berridge, C. W., & Waterhouse, B. D. (2003). The locus coeruleus–noradrenergic system: Modulation of behavioral state and state-dependent cognitive processes. *Brain Research Reviews*, 42(1), 33–84. [https://doi.org/10.1016/S0165-0173\(03\)00143-7](https://doi.org/10.1016/S0165-0173(03)00143-7)
- Bitsios, P., Szabadi, E., & Bradshaw, C. M. (1996). The inhibition of the pupillary light reflex by the threat of an electric shock: A potential laboratory model of human anxiety. *Journal of Psychopharmacology*, 10(4), 279–287. <https://doi.org/10.1177/026988119601000404>
- Bitsios, P., Szabadi, E., & Bradshaw, C. M. (1999). Comparison of the effects of venlafaxine, paroxetine and desipramine on the pupillary light reflex in man. *Psychopharmacology*, 143(3), 286–292. <https://doi.org/10.1007/s002130050949>
- Bodin, C., Aubert, S., Daquin, G., Carron, R., Scavarda, D., McGonigal, A., & Bartolomei, F. (2015). Responders to vagus nerve stimulation (VNS) in refractory epilepsy have reduced interictal cortical synchronicity on scalp EEG. *Epilepsy Research*, 113, 98–103. <https://doi.org/10.1016/j.eplepsyres.2015.03.018>
- Borland, M. S., Engineer, C. T., Vrana, W. A., Moreno, N. A., Engineer, N. D., Vanneste, S., Sharma, P., Pantalia, M. C., Lane, M. C., Rennaker, R. L., & Kilgard, M. P. (2018). The Interval Between VNS-Tone Pairings Determines the Extent of Cortical Map Plasticity. *Neuroscience*, 369, 76–86. <https://doi.org/10.1016/j.neuroscience.2017.11.004>
- Borland, M. S., Vrana, W. A., Moreno, N. A., Fogarty, E. A., Buell, E. P., Sharma, P., Engineer, C. T., & Kilgard, M. P. (2016). Cortical Map Plasticity as a Function of Vagus Nerve Stimulation Intensity. *Brain Stimulation*, 9(1), 117–123. <https://doi.org/10.1016/j.brs.2015.08.018>
- Burger, A. M., D’Agostini, M., Verkuil, B., & Van Diest, I. (2020). Moving beyond belief: A narrative review of potential biomarkers for transcutaneous vagus nerve stimulation. *Psychophysiology*, 57(6). <https://doi.org/10.1111/psyp.13571>
- Burger, A. M., Van der Does, W., Brosschot, J. F., & Verkuil, B. (2020). From ear to eye? No effect of transcutaneous vagus nerve stimulation on human pupil dilation: A report of three studies. *Biological Psychology*, 152, 107863. <https://doi.org/10.1016/j.biopsycho.2020.107863>
- Butt, M. F., Albusoda, A., Farmer, A. D., & Aziz, Q. (2020). The anatomical basis for transcutaneous auricular vagus nerve stimulation. *Journal of Anatomy*, 236(4), 588–611. <https://doi.org/10.1111/joa.13122>
- Capone, F., Motolese, F., Di Zazzo, A., Antonini, M., Magliozzi, A., Rossi, M., Marano, M., Pilato, F., Musumeci, G., Coassin, M., & Di Lazzaro, V. (2021). The effects of transcutaneous auricular vagal nerve stimulation on pupil size. *Clinical Neurophysiology*, 132(8), 1859–1865. <https://doi.org/10.1016/j.clinph.2021.05.014>

- Carpenter, L. L., Moreno, F. A., Kling, M. A., Anderson, G. M., Regenold, W. T., Labiner, D. M., & Price, L. H. (2004). Effect of vagus nerve stimulation on cerebrospinal fluid monoamine metabolites, norepinephrine, and gamma-aminobutyric acid concentrations in depressed patients. *Biological Psychiatry*, *56*(6), 418–426. <https://doi.org/10.1016/j.biopsych.2004.06.025>
- Collins, L., Boddington, L., Steffan, P. J., & McCormick, D. (2021). Vagus nerve stimulation induces widespread cortical and behavioral activation. *Current Biology*, *31*(10), 2088–2098.e3. <https://doi.org/10.1016/j.cub.2021.02.049>
- Cristancho, P., Cristancho, M. A., Baltuch, G. H., Thase, M. E., & O’Reardon, J. P. (2011). Effectiveness and Safety of Vagus Nerve Stimulation for Severe Treatment-Resistant Major Depression in Clinical Practice After FDA Approval: Outcomes at 1 Year. *The Journal of Clinical Psychiatry*, *72*(10), 1376–1382. <https://doi.org/10.4088/JCP.09m05888blu>
- D’Agostini, M., Burger, A. M., Franssen, M., Perkovic, A., Claes, S., von Leupoldt, A., Murphy, P. R., & Van Diest, I. (2023). Short bursts of transcutaneous auricular vagus nerve stimulation enhance evoked pupil dilation as a function of stimulation parameters. *Cortex*, *159*, 233–253. <https://doi.org/10.1016/j.cortex.2022.11.012>
- D’Agostini, M., Burger, A. M., Villca Ponce, G., Claes, S., Leupoldt, A., & Van Diest, I. (2022). No evidence for a modulating effect of continuous transcutaneous auricular vagus nerve stimulation on markers of noradrenergic activity. *Psychophysiology*, *59*(4). <https://doi.org/10.1111/psyp.13984>
- De Couck, M., Cserjesi, R., Caers, R., Zijlstra, W. P., Widjaja, D., Wolf, N., Luminet, O., Ellrich, J., & Gidron, Y. (2017). Effects of short and prolonged transcutaneous vagus nerve stimulation on heart rate variability in healthy subjects. *Autonomic Neuroscience*, *203*, 88–96. <https://doi.org/10.1016/j.autneu.2016.11.003>
- Dippel, G., Mückschel, M., Ziemssen, T., & Beste, C. (2017). Demands on response inhibition processes determine modulations of theta band activity in superior frontal areas and correlations with pupillometry – Implications for the norepinephrine system during inhibitory control. *NeuroImage*, *157*, 575–585. <https://doi.org/10.1016/j.neuroimage.2017.06.037>
- Dolphin, H., Dukelow, T., Finucane, C., Commins, S., McElwaine, P., & Kennelly, S. P. (2022). “The Wandering Nerve Linking Heart and Mind” – The Complementary Role of Transcutaneous Vagus Nerve Stimulation in Modulating Neuro-Cardiovascular and Cognitive Performance. *Frontiers in Neuroscience*, *16*, 897303. <https://doi.org/10.3389/fnins.2022.897303>
- Eckstein, M. K., Guerra-Carrillo, B., Miller Singley, A. T., & Bunge, S. A. (2017). Beyond eye gaze: What else can eyetracking reveal about cognition and cognitive development? *Developmental Cognitive Neuroscience*, *25*, 69–91. <https://doi.org/10.1016/j.dcn.2016.11.001>
- Edden, R. A. E., Muthukumaraswamy, S. D., Freeman, T. C. A., & Singh, K. D. (2009). Orientation Discrimination Performance Is Predicted by GABA Concentration and Gamma Oscillation Frequency in Human Primary Visual Cortex. *Journal of*

Neuroscience, 29(50), 15721–15726. <https://doi.org/10.1523/JNEUROSCI.4426-09.2009>

- Engineer, C. T., Engineer, N. D., Riley, J. R., Seale, J. D., & Kilgard, M. P. (2015). Pairing Speech Sounds With Vagus Nerve Stimulation Drives Stimulus-specific Cortical Plasticity. *Brain Stimulation*, 8(3), 637–644. <https://doi.org/10.1016/j.brs.2015.01.408>
- Engineer, N. D., Riley, J. R., Seale, J. D., Vrana, W. A., Shetake, J. A., Sudanagunta, S. P., Borland, M. S., & Kilgard, M. P. (2011). Reversing pathological neural activity using targeted plasticity. *Nature*, 470(7332), 101–104. <https://doi.org/10.1038/nature09656>
- Farmer, A. D., Strzelczyk, A., Finisguerra, A., Gourine, A. V., Gharabaghi, A., Hasan, A., Burger, A. M., Jaramillo, A. M., Mertens, A., Majid, A., Verkuil, B., Badran, B. W., Ventura-Bort, C., Gaul, C., Beste, C., Warren, C. M., Quintana, D. S., Hämmerer, D., Freri, E., ... Koenig, J. (2021). International Consensus Based Review and Recommendations for Minimum Reporting Standards in Research on Transcutaneous Vagus Nerve Stimulation (Version 2020). *Frontiers in Human Neuroscience*, 14, 568051. <https://doi.org/10.3389/fnhum.2020.568051>
- Florin-Lechner, S. M., Druhan, J. P., Aston-Jones, G., & Valentino, R. J. (1996). Enhanced norepinephrine release in prefrontal cortex with burst stimulation of the locus coeruleus. *Brain Research*, 742(1–2), 89–97. [https://doi.org/10.1016/S0006-8993\(96\)00967-5](https://doi.org/10.1016/S0006-8993(96)00967-5)
- Frangos, E., Ellrich, J., & Komisaruk, B. R. (2015). Non-invasive Access to the Vagus Nerve Central Projections via Electrical Stimulation of the External Ear: fMRI Evidence in Humans. *Brain Stimulation*, 8(3), 624–636. <https://doi.org/10.1016/j.brs.2014.11.018>
- Giraudier, M., Ventura-Bort, C., & Weymar, M. (2020). Transcutaneous Vagus Nerve Stimulation (tVNS) Improves High-Confidence Recognition Memory but Not Emotional Word Processing. *Frontiers in Psychology*, 11, 1276. <https://doi.org/10.3389/fpsyg.2020.01276>
- Goggins, E., Mitani, S., & Tanaka, S. (2022). Clinical perspectives on vagus nerve stimulation: Present and future. *Clinical Science*, 136(9), 695–709. <https://doi.org/10.1042/CS20210507>
- Hall, C., & Chilcott, R. (2018). Eyeing up the Future of the Pupillary Light Reflex in Neurodiagnostics. *Diagnostics*, 8(1), 19. <https://doi.org/10.3390/diagnostics8010019>
- Holland, N., Robbins, T. W., & Rowe, J. B. (2021). The role of noradrenaline in cognition and cognitive disorders. *Brain*, 144(8), 2243–2256. <https://doi.org/10.1093/brain/awab111>
- Höper, S., Kaess, M., & Koenig, J. (2022). Prefrontal cortex oxygenation and autonomic nervous system activity under transcutaneous auricular vagus nerve stimulation in adolescents. *Autonomic Neuroscience*, 241, 103008. <https://doi.org/10.1016/j.autneu.2022.103008>
- Hulseley, D. R., Hays, S. A., Khodaparast, N., Ruiz, A., Das, P., Rennaker, R. L., & Kilgard, M. P. (2016). Reorganization of Motor Cortex by Vagus Nerve Stimulation Requires Cholinergic Innervation. *Brain Stimulation*, 9(2), 174–181. <https://doi.org/10.1016/j.brs.2015.12.007>

- Hulseley, D. R., Riley, J. R., Loerwald, K. W., Rennaker, R. L., Kilgard, M. P., & Hays, S. A. (2017). Parametric characterization of neural activity in the locus coeruleus in response to vagus nerve stimulation. *Experimental Neurology*, 289, 21–30. <https://doi.org/10.1016/j.expneurol.2016.12.005>
- Hysek, C. M., & Liechti, M. E. (2012). Effects of MDMA alone and after pretreatment with reboxetine, duloxetine, clonidine, carvedilol, and doxazosin on pupillary light reflex. *Psychopharmacology*, 224(3), 363–376. <https://doi.org/10.1007/s00213-012-2761-6>
- Hyvärinen, P., Yrttiaho, S., Lehtimäki, J., Ilmoniemi, R. J., Mäkitie, A., Ylikoski, J., Mäkelä, J. P., & Aarnisalo, A. A. (2015). Transcutaneous Vagus Nerve Stimulation Modulates Tinnitus-Related Beta- and Gamma-Band Activity. *Ear & Hearing*, 36(3), e76–e85. <https://doi.org/10.1097/AUD.0000000000000123>
- Keatch, C., Lambert, E., Kameneva, T., & Woods, W. (2023). Functional Connectivity Analysis of Transcutaneous Vagus Nerve Stimulation (tVNS) using Magnetoencephalography (MEG). *IEEE Transactions on Neural Systems and Rehabilitation Engineering*, 1–1. <https://doi.org/10.1109/TNSRE.2023.3297736>
- Keatch, C., Lambert, E., Woods, W., & Kameneva, T. (2022). Measuring Brain Response to Transcutaneous Vagus Nerve Stimulation (tVNS) using Simultaneous Magnetoencephalography (MEG). *Journal of Neural Engineering*. <https://doi.org/10.1088/1741-2552/ac620c>
- Keute, M., Barth, D., Liebrand, M., Heinze, H.-J., Kraemer, U., & Zaehle, T. (2020). Effects of Transcutaneous Vagus Nerve Stimulation (tVNS) on Conflict-Related Behavioral Performance and Frontal Midline Theta Activity. *Journal of Cognitive Enhancement*, 4(2), 121–130. <https://doi.org/10.1007/s41465-019-00152-5>
- Keute, M., Demirezen, M., Graf, A., Mueller, N. G., & Zaehle, T. (2019). No modulation of pupil size and event-related pupil response by transcutaneous auricular vagus nerve stimulation (taVNS). *Scientific Reports*, 9(1), 11452. <https://doi.org/10.1038/s41598-019-47961-4>
- Keute, M., Wienke, C., Ruhnau, P., & Zaehle, T. (2021). Effects of transcutaneous vagus nerve stimulation (tVNS) on beta and gamma brain oscillations. *Cortex*, 140, 222–231. <https://doi.org/10.1016/j.cortex.2021.04.004>
- Kim, Y., Kadlaskar, G., Keehn, R. M., & Keehn, B. (2022). Measures of tonic and phasic activity of the locus coeruleus—norepinephrine system in children with autism spectrum disorder: An event-related potential and pupillometry study. *Autism Research*, 15(12), 2250–2264. <https://doi.org/10.1002/aur.2820>
- Krahl, S., & Clark, K. (2012). Vagus nerve stimulation for epilepsy: A review of central mechanisms. *Surgical Neurology International*, 3(5), 255. <https://doi.org/10.4103/2152-7806.103015>
- Kühnel, A., Teckentrup, V., Neuser, M. P., Huys, Q. J. M., Burrasch, C., Walter, M., & Kroemer, N. B. (2020). Stimulation of the vagus nerve reduces learning in a go/no-go reinforcement learning task. *European Neuropsychopharmacology*, 35, 17–29. <https://doi.org/10.1016/j.euroneuro.2020.03.023>

- Lehtimäki, J., Hyvärinen, P., Ylikoski, M., Bergholm, M., Mäkelä, J. P., Aarnisalo, A., Pirvola, U., Mäkitie, A., & Ylikoski, J. (2013). Transcutaneous vagus nerve stimulation in tinnitus: A pilot study. *Acta Oto-Laryngologica*, *133*(4), 378–382. <https://doi.org/10.3109/00016489.2012.750736>
- Lewine, J. D., Paulson, K., Bangera, N., & Simon, B. J. (2019). Exploration of the Impact of Brief Noninvasive Vagal Nerve Stimulation on EEG and Event-Related Potentials. *Neuromodulation: Technology at the Neural Interface*, *22*(5), 564–572. <https://doi.org/10.1111/ner.12864>
- Lloyd, B., Wurm, F., de Kleijn, R., & Nieuwenhuis, S. (2023). *Short-term transcutaneous vagus nerve stimulation increases pupil size but does not affect EEG alpha power: A replication* [Preprint]. Neuroscience. <https://doi.org/10.1101/2023.03.08.531479>
- Lorenz, R., Simmons, L. E., Monti, R. P., Arthur, J. L., Limal, S., Laakso, I., Leech, R., & Violante, I. R. (2019). Efficiently searching through large tACS parameter spaces using closed-loop Bayesian optimization. *Brain Stimulation*, *12*(6), 1484–1489. <https://doi.org/10.1016/j.brs.2019.07.003>
- Lu, X., Hong, Z., Tan, Z., Sui, M., Zhuang, Z., Liu, H., Zheng, X., Yan, T., Geng, D., & Jin, D. (2017). Nicotinic Acetylcholine Receptor Alpha7 Subunit Mediates Vagus Nerve Stimulation-Induced Neuroprotection in Acute Permanent Cerebral Ischemia by a7nAchR/JAK2 Pathway. *Medical Science Monitor*, *23*, 6072–6081. <https://doi.org/10.12659/MSM.907628>
- Ludwig, M., Wienke, C., Betts, M. J., Zaehle, T., & Hämmerer, D. (2021). Current challenges in reliably targeting the noradrenergic locus coeruleus using transcutaneous auricular vagus nerve stimulation (taVNS). *Autonomic Neuroscience*, *236*. <https://doi.org/10.1016/j.autneu.2021.102900>
- Marrosu, F., Serra, A., Maleci, A., Puligheddu, M., Biggio, G., & Piga, M. (2003). Correlation between GABAA receptor density and vagus nerve stimulation in individuals with drug-resistant partial epilepsy. *Epilepsy Research*, *55*(1–2), 59–70. [https://doi.org/10.1016/S0920-1211\(03\)00107-4](https://doi.org/10.1016/S0920-1211(03)00107-4)
- Morris, G. L., Gloss, D., Buchhalter, J., Mack, K. J., Nickels, K., & Harden, C. (2013). Evidence-based guideline update: Vagus nerve stimulation for the treatment of epilepsy: Report of the Guideline Development Subcommittee of the American Academy of Neurology. *Neurology*, *81*(16), 1453–1459. <https://doi.org/10.1212/WNL.0b013e3182a393d1>
- Mridha, Z., de Gee, J. W., Shi, Y., Alkashgari, R., Williams, J., Suminski, A., Ward, M. P., Zhang, W., & McGinley, M. J. (2021). Graded recruitment of pupil-linked neuromodulation by parametric stimulation of the vagus nerve. *Nature Communications*, *12*(1), 1539. <https://doi.org/10.1038/s41467-021-21730-2>
- Muthukumaraswamy, S. D., Myers, J. F. M., Wilson, S. J., Nutt, D. J., Lingford-Hughes, A., Singh, K. D., & Hamandi, K. (2013). The effects of elevated endogenous GABA levels on movement-related network oscillations. *NeuroImage*, *66*, 36–41. <https://doi.org/10.1016/j.neuroimage.2012.10.054>

- Näätänen, R., & Picton, T. (1987). The N1 Wave of the Human Electric and Magnetic Response to Sound: A Review and an Analysis of the Component Structure. *Psychophysiology*, *24*(4), 375–425. <https://doi.org/10.1111/j.1469-8986.1987.tb00311.x>
- Neuser, M. P., Teckentrup, V., Kühnel, A., Hallschmid, M., Walter, M., & Kroemer, N. B. (2020). Vagus nerve stimulation boosts the drive to work for rewards. *Nature Communications*, *11*(1), 3555. <https://doi.org/10.1038/s41467-020-17344-9>
- Penry, J. K., & Dean, J. C. (1990). Prevention of Intractable Partial Seizures by Intermittent Vagal Stimulation in Humans: Preliminary Results. *Epilepsia*, *31*(s2), S40–S43. <https://doi.org/10.1111/j.1528-1157.1990.tb05848.x>
- Peuker, E. T., & Filler, T. J. (2002). The nerve supply of the human auricle. *Clinical Anatomy*, *15*(1), 35–37. <https://doi.org/10.1002/ca.1089>
- Rajkowski, J., Kubiak, P., & Aston-Jones, G. (1994). Locus coeruleus activity in monkey: Phasic and tonic changes are associated with altered vigilance. *Brain Research Bulletin*, *35*(5–6), 607–616. [https://doi.org/10.1016/0361-9230\(94\)90175-9](https://doi.org/10.1016/0361-9230(94)90175-9)
- Reimer, J., McGinley, M. J., Liu, Y., Rodenkirch, C., Wang, Q., McCormick, D. A., & Tolia, A. S. (2016). Pupil fluctuations track rapid changes in adrenergic and cholinergic activity in cortex. *Nature Communications*, *7*(1), 13289. <https://doi.org/10.1038/ncomms13289>
- Rembado, I., Song, W., Su, D. K., Levari, A., Shupe, L. E., Perlmutter, S., Fetisov, E., & Zanos, S. (2021). Cortical Responses to Vagus Nerve Stimulation Are Modulated by Brain State in Nonhuman Primates. *Cerebral Cortex*, *31*(12), 5289–5307.
- Rufener, K. S., Wienke, C., Salanje, A., Haghikia, A., & Zaehle, T. (2023). Effects of transcutaneous auricular vagus nerve stimulation paired with tones on electrophysiological markers of auditory perception. *Brain Stimulation*, *16*(4), 982–989. <https://doi.org/10.1016/j.brs.2023.06.006>
- Ruhnau, P., & Zaehle, T. (2021). Transcranial Auricular Vagus Nerve Stimulation (taVNS) and Ear-EEG: Potential for Closed-Loop Portable Non-invasive Brain Stimulation. *Frontiers in Human Neuroscience*, *15*, 699473. <https://doi.org/10.3389/fnhum.2021.699473>
- Samuels, E., & Szabadi, E. (2008a). Functional Neuroanatomy of the Noradrenergic Locus Coeruleus: Its Roles in the Regulation of Arousal and Autonomic Function Part I: Principles of Functional Organisation. *Current Neuropharmacology*, *6*(3), 235–253. <https://doi.org/10.2174/157015908785777229>
- Samuels, E., & Szabadi, E. (2008b). Functional Neuroanatomy of the Noradrenergic Locus Coeruleus: Its Roles in the Regulation of Arousal and Autonomic Function Part II: Physiological and Pharmacological Manipulations and Pathological Alterations of Locus Coeruleus Activity in Humans. *Current Neuropharmacology*, *6*(3), 254–285. <https://doi.org/10.2174/157015908785777193>
- Sara, S. J. (2009). The locus coeruleus and noradrenergic modulation of cognition. *Nature Reviews Neuroscience*, *10*(3), 211–223. <https://doi.org/10.1038/nrn2573>

- Sharon, O., Fahoum, F., & Nir, Y. (2021). Transcutaneous Vagus Nerve Stimulation in Humans Induces Pupil Dilation and Attenuates Alpha Oscillations. *The Journal of Neuroscience*, *41*(2), 320–330. <https://doi.org/10.1523/JNEUROSCI.1361-20.2020>
- Shetake, J. A., Engineer, N. D., Vrana, W. A., Wolf, J. T., & Kilgard, M. P. (2012). Pairing tone trains with vagus nerve stimulation induces temporal plasticity in auditory cortex. *Experimental Neurology*, *233*(1), 342–349. <https://doi.org/10.1016/j.expneurol.2011.10.026>
- Thompson, S. L., O’Leary, G. H., Austelle, C. W., Gruber, E., Kahn, A. T., Manett, A. J., Short, B., & Badran, B. W. (2021). A Review of Parameter Settings for Invasive and Non-invasive Vagus Nerve Stimulation (VNS) Applied in Neurological and Psychiatric Disorders. *Frontiers in Neuroscience*, *15*, 709436. <https://doi.org/10.3389/fnins.2021.709436>
- Urbin, M. A., Lafe, C. W., Simpson, T. W., Wittenberg, G. F., Chandrasekaran, B., & Weber, D. J. (2021). Electrical stimulation of the external ear acutely activates noradrenergic mechanisms in humans. *Brain Stimulation*, *14*(4), 990–1001. <https://doi.org/10.1016/j.brs.2021.06.002>
- Ventureyra, E. C. G. (2000). Transcutaneous vagus nerve stimulation for partial onset seizure therapy. *Child’s Nervous System*, *16*(2), 101–102. <https://doi.org/10.1007/s003810050021>
- Villani, V., Finotti, G., Lernia, D. D., & Tsakiris, M. (2022). Event-related transcutaneous vagus nerve stimulation modulates behaviour and pupillary responses during an auditory oddball task. *Psychoneuroendocrinology*, *140*. <https://doi.org/10.1016/j.psyneuen.2022.105719>
- Wang, Y., Li, L., Li, S., Fang, J., Zhang, J., Wang, J., Zhang, Z., Wang, Y., He, J., Zhang, Y., & Rong, P. (2022). Toward Diverse or Standardized: A Systematic Review Identifying Transcutaneous Stimulation of Auricular Branch of the Vagus Nerve in Nomenclature. *Neuromodulation: Technology at the Neural Interface*, *25*(3), 366–379. <https://doi.org/10.1111/ner.13346>
- Warren, C. M., Tona, K. D., Ouwerkerk, L., van Paridon, J., Poletiek, F., van Steenberg, H., Bosch, J. A., & Nieuwenhuis, S. (2019). The neuromodulatory and hormonal effects of transcutaneous vagus nerve stimulation as evidenced by salivary alpha amylase, salivary cortisol, pupil diameter, and the P3 event-related potential. *Brain Stimulation*, *12*(3), 635–642. <https://doi.org/10.1016/j.brs.2018.12.224>
- Wienke, C., Grueschow, M., Haghikia, A., & Zaehle, T. (2023). Phasic, Event-Related Transcutaneous Auricular Vagus Nerve Stimulation Modifies Behavioral, Pupillary, and Low-Frequency Oscillatory Power Responses. *The Journal of Neuroscience*, *43*(36), 6306–6319. <https://doi.org/10.1523/JNEUROSCI.0452-23.2023>
- Yakunina, N., Kim, S. S., & Nam, E.-C. (2017). Optimization of Transcutaneous Vagus Nerve Stimulation Using Functional MRI. *Neuromodulation: Technology at the Neural Interface*, *20*(3), 290–300. <https://doi.org/10.1111/ner.12541>

- Yap, J. Y. Y., Keatch, C., Lambert, E., Woods, W., Stoddart, P. R., & Kameneva, T. (2020). Critical Review of Transcutaneous Vagus Nerve Stimulation: Challenges for Translation to Clinical Practice. *Frontiers in Neuroscience*, *14*, 284. <https://doi.org/10.3389/fnins.2020.00284>
- Zabara, J. (1985). Peripheral control of hypersynchronous discharge in epilepsy. *Electroencephalography and Clinical Neurophysiology*, *61*(3), S162. [https://doi.org/10.1016/0013-4694\(85\)90626-1](https://doi.org/10.1016/0013-4694(85)90626-1)
- Zabara, J. (1992). Inhibition of Experimental Seizures in Canines by Repetitive Vagal Stimulation. *Epilepsia*, *33*(6), 1005–1012. <https://doi.org/10.1111/j.1528-1157.1992.tb01751.x>
- Zanchetti, A., Wang, S. C., & Moruzzi, G. (1952). The effect of vagal afferent stimulation on the EEG pattern of the cat. *Electroencephalography and Clinical Neurophysiology*, *4*(3), 357–361. [https://doi.org/10.1016/0013-4694\(52\)90064-3](https://doi.org/10.1016/0013-4694(52)90064-3)

3 Appendix: Included peer-reviewed publications

Ludwig, M. *, Wienke, C. *, Betts, M. J., Zaehle, T., & Hämmerer, D. (2021). Current challenges in reliably targeting the noradrenergic locus coeruleus using transcutaneous auricular vagus nerve stimulation (taVNS). *Autonomic Neuroscience*, 236. <https://doi.org/10.1016/j.autneu.2021.102900>

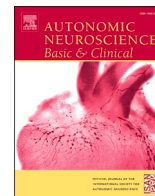
* Shared first authorship

Keute, M., Wienke, C., Ruhnau, P., & Zaehle, T. (2021). Effects of transcutaneous vagus nerve stimulation (tVNS) on beta and gamma brain oscillations. *Cortex*, 140, 222–231. <https://doi.org/10.1016/j.cortex.2021.04.004>

Rufener, K. S. *, Wienke, C. *, Salanje, A., Haghikia, A., & Zaehle, T. (2023). Effects of transcutaneous auricular vagus nerve stimulation paired with tones on electrophysiological markers of auditory perception. *Brain Stimulation*, 16(4), 982–989. <https://doi.org/10.1016/j.brs.2023.06.006>

* Shared first authorship

Wienke, C., Grueschow, M., Haghikia, A., & Zaehle, T. (2023). Phasic, Event-Related Transcutaneous Auricular Vagus Nerve Stimulation Modifies Behavioral, Pupillary, and Low-Frequency Oscillatory Power Responses. *The Journal of Neuroscience*, 43(36), 6306–6319. <https://doi.org/10.1523/JNEUROSCI.0452-23.2023>



Review

Current challenges in reliably targeting the noradrenergic locus coeruleus using transcutaneous auricular vagus nerve stimulation (taVNS)

Mareike Ludwig^{a,f,*}, Christian Wienke^{b,f,1}, Matthew J. Betts^{a,c,f}, Tino Zaehle^{b,f}, Dorothea Hämmerer^{a,d,e,f}

^a Institute for Cognitive Neurology and Dementia Research, Faculty of Medicine, University Hospital Magdeburg, Germany

^b Department of Neurology, Section of Neuropsychology, Otto-v.-Guericke University, Magdeburg, Germany

^c German Center for Neurodegenerative Diseases (DZNE), Otto-von-Guericke University Magdeburg, Magdeburg, Germany

^d Institute of Cognitive Neuroscience, University College London, London, UK

^e Department of Psychology, University of Innsbruck

^f CBBS Center for Behavioral Brain Sciences, Magdeburg, Germany



ARTICLE INFO

Keywords:

Vagus nerve stimulation
Stimulation parameters
Neuromodulation
Noradrenergic system
Locus coeruleus
Neurodegeneration
Cross-species translational approach

ABSTRACT

Transcutaneous auricular vagus nerve stimulation (taVNS), as a non-invasive brain stimulation technique may influence the locus coeruleus-norepinephrine system (LC-NE system) via modulation of the Vagus Nerve (VN) which projects to the LC. Few human studies exist examining the effects of taVNS on the LC-NE system and studies to date assessing the ability of taVNS to target the LC yield heterogeneous results. The aim of this review is to present an overview of the current challenges in assessing effects of taVNS on LC function and how translational approaches spanning animal and human research can help in this regard. A particular emphasis of the review discusses how the effects of taVNS may be influenced by changes in structure and function of the LC-NE system across the human lifespan and in disease.

1. Introduction

The *locus coeruleus* (LC) in the brainstem is one of our main sources of *noradrenaline* (also referred to as norepinephrine, NE) in the brain. It exhibits particular vulnerability in a wide range of neurological and clinical conditions that pose an increasing economic and societal burden. Changes to the LC-NE system in such conditions include an *increase* in NE modulation, e.g., in chronic pain (Llorca-Torrallba et al., 2016), stress and anxiety (Berridge and Waterhouse, 2003; Bremner et al., 1996), but also a *decrease* in NE production and degeneration of NE-producing cells in the LC, e.g., in depression (Bernard et al., 2011), post-traumatic stress disorder (Berridge and Waterhouse, 2003; Pietrzak et al., 2013) and aging (Mather and Harley, 2016). Moreover, for the two most prominent neurodegenerative diseases, Parkinson disease (PD) and Alzheimer disease (AD), LC abnormalities can be observed before typical pathologies in substantia nigra (SN) and transentorhinal/entorhinal cortex respectively, occur (Braak et al., 2011; Braak et al., 2003). A number of these neurodegenerative and psychiatric diseases are currently being treated or investigated to be treated with

pharmacological interventions that also target the noradrenergic system (e.g., sNRIs - selective norepinephrine reuptake inhibitors). However, pharmacological interventions are accompanied with the downside of a lack of anatomical specificity and thus increase the possibility of generating side effects that can have a negative impact on quality of life. Studies in rodents were able to show how to increase LC firing associated with NE release in the hippocampus and cortical target areas over the course of minutes to hours using an invasive vagus nerve stimulation (iVNS) approach (Follesa et al., 2007; Hulsey et al., 2017; Hulsey et al., 2019; Manta et al., 2009). IVNS is used in humans as an adjunctive therapy to treat refractory epilepsy (see Englot et al., 2011 for meta-analysis & Panebianco et al., 2016 for review) as well as depression (see Farmer et al., 2020 for review).

A promising technique to circumvent the caveats of pharmacological or invasive stimulation in humans is transcutaneous auricular vagus nerve stimulation (taVNS) applied mainly to the cymba conchae or, in some studies, to the tragus of the external ear (cf. Fig. 1). Peuker and Filler (2002) showed in an anatomical study that the cymba conchae was innervated solely by the Auricular Branch of the Vagus Nerve (ABVN),

* Corresponding author at: Institute for Cognitive Neurology and Dementia Research, Faculty of Medicine, University Hospital Magdeburg, Germany.

E-mail address: mareike.ludwig@med.ovgu.de (M. Ludwig).

¹ shared first authorship.

whereby the tragus was also innervated by the Great Auricular Nerve and the Auriculotemporal Nerve. The ABVN, together with the remaining nerve fibre bundles of the vagus nerve, reaches the brainstem at the nucleus tractus solitarius (NTS) which has prominent projections to the LC-NE system (cf. Fig. 1), (Butt et al., 2020; Ruffoli et al., 2011). Stimulation at these auricular sites has been shown to activate structures along the vagal afferent pathway in humans (Badran et al., 2018; Yakunina et al., 2017). Therefore taVNS holds great promise as a more anatomically precise and potentially rehabilitating NE therapeutic compared to pharmacological interventions (Collins et al., 2021; Hulsey et al., 2017; Mridha et al., 2021; Sharon et al., 2021). Moreover, it may also offer the possibility for more varied interventions as stimulation interventions are able to modulate local neuronal activity in a particular frequency and for an explicit duration and can thus attempt to mimic naturally occurring firing patterns of the stimulated brain structure (Polanía et al., 2018). Despite these promising properties, current studies using taVNS as a substitute for pharmacological interventions in

depression are plagued by their lack of reliability (Martin and Martín-Sánchez, 2012). To improve the reliability of taVNS interventions, the link between taVNS and the LC-NE system in humans needs to be better understood. This review summarizes the main challenges in this endeavour (see also Fig. 1 for an overview of the main challenges). We draw attention to the still limited understanding of the mechanisms of actions of taVNS and control of mediating factors in humans. Furthermore, we outline how a translational approach might help to understand how interindividual differences in the integrity of the brain, and in particular the LC, might alter taVNS effects.

2. Current outcome measurements of taVNS

The vast majority of taVNS intervention studies in humans lack appropriately validated physiological as well as cognitive outcome measures to monitor temporal and spatial specificity of intervention effects on the LC-NE system. The most commonly used taVNS outcome

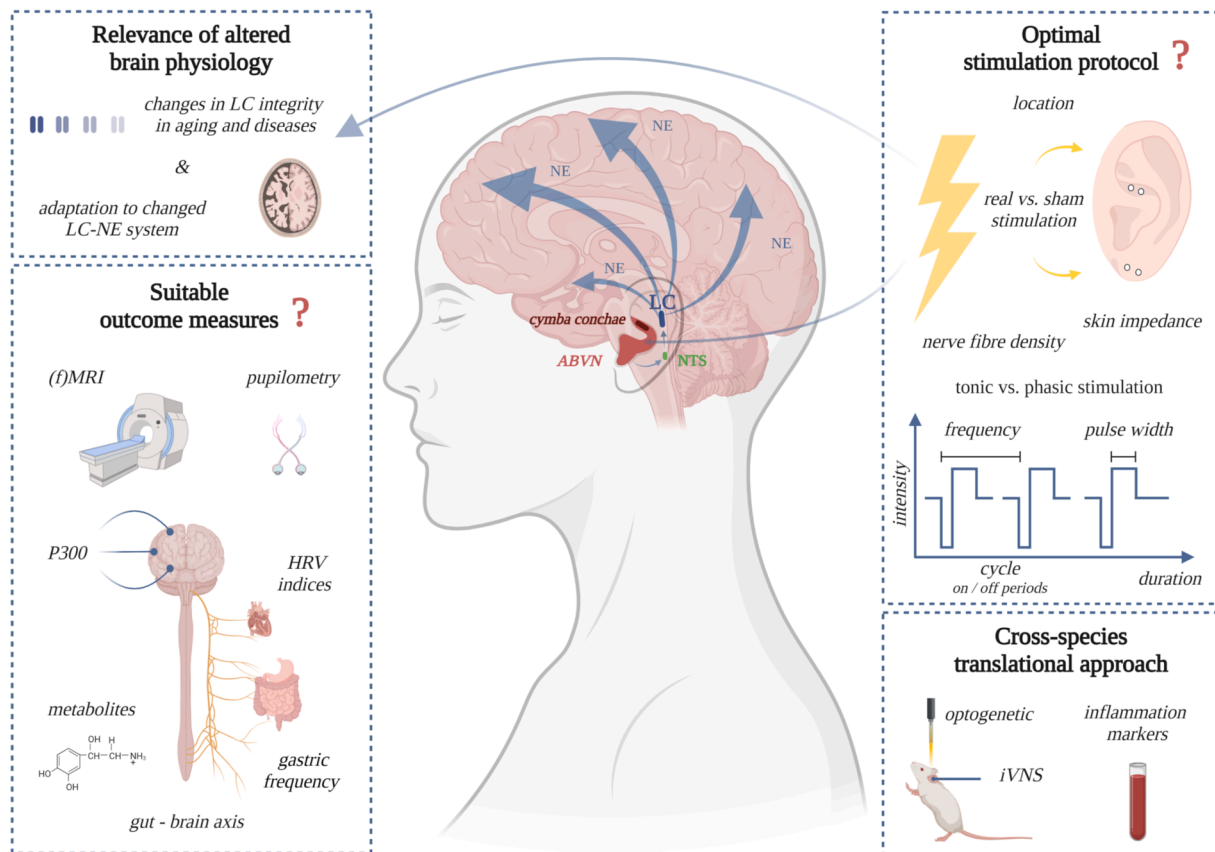


Fig. 1. Challenges in scrutinizing the link between taVNS and the LC-NE System.

Center: TaVNS is applied to regions in the left ear innervated by the ABVN. The stimulation is relayed via the ABVN to the NTS which projects to the LC from where NE is released into various projection areas. Top right: Currently, taVNS in humans is characterized by heterogeneous stimulation protocols. Phasic as well as tonic mono- or biphasic stimulation approaches are based on different stimulation parameters (intensity, frequency, pulse width, cycle, duration), which are tested on different stimulation locations. Most commonly used for real stimulation is cymba conchae and for sham stimulation earlobes (top right: white circles = 2× anode/cathode), which is currently under debate. Interindividual differences in nerve fibre density as well as lack of proper skin cleaning might be a cause for heterogeneous results from previous studies. Bottom right: Cross-species translational approaches can be used to investigate new applications for taVNS in humans and to improve current stimulation methods. Animal research using i/taVNS or optogenetic stimulation can help to improve our understanding of how VNS affects the LC-NE system and how its effects depend on changes in the LC-NE system (see also top left). Bottom left: Suitable outcome measures for taVNS are needed to study taVNS effects in an optimal manner. As of now only indirect measures of LC or noradrenergic function are available such as fMRI, pupillary changes, HRV indices (RMSSD, pNN50), gastric-frequency, P300 and potential NE metabolites. Of these, fMRI offers the most direct way to visualize LC-NE activity. Top left: Alterations in brain physiology, such as the integrity of the LC and adaptation to an altered LC-NE system might account for heterogeneous outcomes and need to be considered especially in clinical populations to adjust the stimulation parameters accordingly. Blue columns indicate the bilateral structure of the LC and the decrease in saturation symbolizes a decline of LC integrity.

Abbreviations: ABVN Auricular Branch of the Vagus Nerve, ERP Event related potential, fMRI functional magnetic resonance imaging, HRV Heart Rate Variability, iVNS invasive Vagus Nerve Stimulation, LC locus coeruleus, LC-NE system locus coeruleus norepinephrinergic system, NE Norepinephrine, NTS nucleus tractus solitarius, taVNS transcutaneous auricular vagus nerve stimulation. (For interpretation of the references to colour in this figure legend, the reader is referred to the web version of this article.)

measures are indirect measures of LC activity (cf. Fig. 1) such as heart rate variability (HRV) indices, pupil dilation, or the P300 event related potential (ERP) which have been discussed in their respective usefulness to indicate LC-NE activation in recent reviews (Burger et al., 2020; Farmer et al., 2020).

Briefly, HRV is a collective term for several indices derived from electrocardiography, whereby the Root Mean Square of Successive Differences (RMSSD) and percentage of consecutive normal sinus RR intervals spaced more than 50 ms apart (pNN50), are thought to reflect vagal activity (see (Burger et al., 2020) for review). However, the extent to which HRV actually reflects vagal nerve engagement is difficult to determine due to the differences in stimulation protocols and HRV indices assessed in previous studies (Burger et al., 2020). For this purpose, Wolf et al. (2021) have developed a Shiny web app that frequently incorporates new results into a Bayesian meta-analysis (termed 'living Bayesian meta-analysis') to investigate the extent to which HRV may be an indirect biomarker for taVNS. Likewise, it is important to critically investigate whether HRV is related to vagal activity at all, as a recent iVNS animal study showed that tonic vagal activity during respiration does not correlate with HRV metrics (Marmarstein et al., 2021).

Pupil dilation can be an easy-to-acquire proxy measure for LC firing. Anatomically, LC projections inhibit the Edinger-Westphal nucleus resulting in a relaxation of the iris sphincter muscle that can be measurable as a change in pupil dilation (Hall and Chilcott, 2018; Samuels and Szabadi, 2008a, 2008b). Functionally, stimulating the LC in monkeys has been shown to result in dilated pupils (Joshi et al., 2016). Still, the link between LC activity and pupil dilation is not exclusive. Other structures such as the hypothalamus or superior colliculus also target the Edinger-Westphal nucleus (Mathôt, 2018), and stimulating in the superior colliculus, for instance, also resulted in increased pupil dilations (Joshi et al., 2016). It is also important to note that not only noradrenergic but also cholinergic axons are involved in dilating the pupil (Reimer et al., 2016).

The P300 ERP, (short P3), occurs around 300 ms after the onset of behaviourally relevant or rare stimuli and especially the P3b subcomponent has been related to parietal noradrenergic pathways involved in decision making and memory (see (Polich, 2007) for a review). Nevertheless, event-related potentials are difficult to source-localize in the brain, especially when it is related to the brainstem structures, so there is currently no conclusive evidence how specifically LC activity and NE release is reflected in P300 ERPs (Farmer et al., 2020). Besides the P3, multiple studies investigated effects of vagus nerve stimulation on cortical oscillations. Results from three studies analysing power in different frequency ranges indicate that invasive and non-invasive VNS might be able to increase cortical arousal. This was observed as a decrease of power in lower frequencies (Bodin et al., 2015; Lewine et al., 2019; Sharon et al., 2021) and an increase of power in higher frequency ranges (Lewine et al., 2019). Of note, only the study from Sharon et al. (2021) used taVNS in a sample of 25 healthy adults. Bodin et al. (2015) used iVNS in 19 epilepsy patients and Lewine et al. (2019) used neck VNS in 8 healthy subjects. However, these results await replication in higher sampled studies. Other studies focused on oscillations related to different aspects of cortical processing. Keute et al. (2019a) observed increased frontal-midline theta power, related to executive function, in trials that elicited go/stop response conflicts during a cued go/no-go change task. In a different study, the authors observed a decrease in power in the theta range (4–8 Hz) over the course of the experiment, but this effect was observed after taVNS as well as after sham stimulation. Additionally, no taVNS effect on motor related beta oscillations or gamma oscillations related to early visual processing could be observed (Keute et al., 2021b). Thus, the use of different cortical oscillations as a proxy for LC-NE activation awaits further investigation in future studies.

Another possibility to evaluate the effect of taVNS would be to examine the concentration of NE and other neurotransmitters and their respective metabolites in blood and cerebrospinal fluid (CSF) following stimulation. The principal metabolite of NE is 3-methoxy-4-

hydroxyphenylglycol (MHPG), which also serves as an indicator of noradrenergic activity (Elsworth et al., 1982; Kanda et al., 1991). In animal models, two weeks of iVNS increased the concentration of NE in prefrontal areas (Manta et al., 2013; Roosevelt et al., 2006). Neurochemical studies in humans, however, are sparse and until now limited to iVNS. Only one study directly assessed NE and MHPG in depressed patients ($N = 21$) implanted with iVNS (Carpenter et al., 2004). No effects on NE and MHPG concentrations were found in CSF taken from lumbar punctures, although an increase in homovanillic acid (HVA), a dopamine metabolite, was observed. However, all subjects were under constant pharmacological therapy, hence the authors could not determine the extent to which the psychotropic medication affected this increase in HVA (Carpenter et al., 2004). As of now more research is needed to determine how CSF metabolites may be used as an indirect biomarker of taVNS. Salivary Alpha-Amylase has also been considered as a proxy for LC-NE activation (e.g., Warren et al., 2019). However, the amount of studies using this proxy is low and their results are inconsistent with regards to how well they reflect an engagement of the LC (see Burger et al., 2020 & Farmer et al., 2020 for detailed reviews).

The VN does not only have a key role in the central nervous system (CNS) and in the autonomic nervous system (ANS), but also in the enteric nervous system (ENS) by signalling from gastrointestinal microbiota to the brain and vice versa (see (Cryan et al., 2019) for review) (see also Section 5). Previous work suggests that the VN may exert anti-inflammatory effects via hypothalamic-pituitary-adrenal (*vagal afferents*) or via cholinergic anti-inflammatory (*vagal efferents*) pathways (e.g., Bonaz et al., 2013, 2017; Tracey, 2002). Furthermore, LC-NE stimulation may also exert anti-inflammatory and neuroprotective effects by increasing the expression of neurotrophic substances such as brain-derived neurotrophic factor (BDNF) (Braun et al., 2014; Furmaga et al., 2012) and by attenuating the release of cytokines such as TNF alpha, IL-1b, IL-6, IL-18 (Borovikova et al., 2000; Meregani et al., 2011; Subramanian et al., 2020). Of note, it is difficult to determine whether differences identified in blood or CSF reflect peripheral or central effects respectively (Molinuevo et al., 2018), so whilst fluid biomarkers may provide a more direct measure of NE levels compared to pupillometry or HRV, the origin of these effects cannot be exclusively determined.

Compared to Pupillometry, ERPs or HRV, *functional magnetic resonance imaging* (fMRI) can be a more direct tool to visualize LC responses. Although fMRI is not a direct measure of, for example, LC firing as it reflects changes in blood flow in the LC area which serves as a proxy for LC activation (e.g., Jacobs et al., 2020; Yi et al., 2021), it is arguably currently our best measure for visualizing LC activation in humans. fMRI studies in combination with taVNS in humans corroborate an involvement of the LC-NE system (see Table 1 for an overview of taVNS-fMRI studies), evident by taVNS-induced functional activation from NTS in LC-NE projection areas such as the amygdala and hippocampus (Sclocco et al., 2019; Yakunina et al., 2017). An overview and recommendations on how to proceed best during combined fMRI and taVNS studies (e.g., imaging resolution 1–2 mm voxel size) have recently been published (see section 'Functional Neuroimaging' (Farmer et al., 2020)). Furthermore, many current studies lack sufficient sample sizes, spatial resolution or postprocessing methods to reliably identify activation in the LC (Yi et al., 2021). Additionally, it should be noted whether the reported increased or decreased functional activation is based purely on real i/taVNS stimulation or on the comparison between real and sham stimulation, with the latter being preferred as a more optimal experimental control.

3. Insufficiently validated stimulation protocols

An important current challenge in evaluating taVNS in human research are the heterogeneous and often poorly-validated stimulation protocols (cf. Fig. 1 – 'Optimal stimulation protocol'). A recent consensus paper provides an overview of this issue (Farmer et al., 2020). The combination of different parameters such as stimulation intensity

Table 1
Studies reporting fMRI activation in LC and its projection areas following taVNS.

Scanner	Author/year	N	Design	Head coil	Structural parameters	fMRI sequence parameters	Smoothing	fMRI results
1.5 T	Dietrich et al., 2008	4 healthy male subjects	50 s ON vs 100 s OFF, 250 μ s, 25 Hz, 4–8mA fMRI for 700 s - four alternating ON and OFF sequences were performed	Not reported	MPRAGE 176 sagittal slices Thickness: 1 mm Matrix: 256 \times 256 FOV: 224 \times 224 mm ²	EPI 36 axial slices TR: 110 ms TE: 60 ms FA: 90° Thickness: 3 mm Matrix: 64 \times 64 pixel FOV: 224 \times 224 mm ²	Not reported	Comparison left tragus vs earlobe stimulation <i>Activation</i> → left LC, thalamus, prefrontal cortex, posterior cingulate gyrus, insula → bilateral postcentral gyrus <i>Deactivations</i> → right nucleus accumbens, cerebella hemisphere
	Kraus et al., 2007	36 healthy subjects in 3 studies Study 1: N = 22 Study 2: N = 8 Study 3: N = 6	30 s ON vs 120 s OFF, 20 μ s, 8 Hz, 4 mA in low condition/5 mA in high condition 130 blocks; 200 in case of alternating low-high stimulation - four alternating ON and OFF sequences were performed - stimulation during blocks 11–20, 41–50, 71–80, 101–110	Not reported	MPRAGE 160 sagittal slices Thickness: 1 mm Matrix: 256 \times 256 FOV: 220 \times 220 mm ² In plane resolution: 0.98 \times 0.98 mm ²	EPI 20 slices TR = 3000 ms TE = 60 ms FA = 90° Thickness: 4 mm Matrix: 128 \times 128 FOV: 220 \times 220 mm ²	Not reported	Comparison anterior wall vs. earlobe stimulation (N = 6) <i>Activation</i> → unspecific patterns <i>Deactivation</i> → paracentral lobe → right parahippocampal gyrus
	Kraus et al., 2013	16 healthy subjects 8 subjects per stimulation location	30 s ON vs 60 s OFF, 20 μ s, 8 Hz, 32.6 V \pm 13.4 V for taVNS, 30.0V \pm 13.5V for sham 130 blocks - four alternating ON and OFF sequences were performed - stimulation during blocks 11–20, 41–50, 71–80, 101–110	Not reported	MPRAGE 160 sagittal slices Thickness: 1 mm Matrix: 256 \times 256 FOV: 220 \times 220 mm ²	EPI 20 slices TR: 3000 ms TE: 60 ms FA: 90° Thickness: 4 mm Matrix: 128 \times 128 FOV: 220 \times 220 mm ²	Not reported	Comparison anterior wall vs. earlobe stimulation (N = 8) <i>Activation</i> → left insula, medial frontal gyrus <i>Deactivation</i> → left parahippocampal gyrus → LC, solitary tract

(continued on next page)

Table 1 (continued)

Scanner	Author/year	N	Design	Head coil	Structural parameters	fMRI sequence parameters	Smoothing	fMRI results
3T	Badran et al., 2018	17 healthy subjects	60 s ON vs 60 s OFF, 500 μ s, 25 Hz, 3.14 mA \pm 0.99 mA for taVNS, 2.43 \pm 1.16 mA for sham	32-channel	In plane resolution: 0.98 \times 0.98 mm ² MPRAGE 208 slices TR:1900 ms TE: 2.26 ms FA: 9°	EPI 47 slices TR: 2800 ms TE: 35 ms FA: 76°	8mm FWHM Gaussian smoothing kernel	Comparison tragus vs earlobe stimulation <u>Increased activation</u> → right caudate → bilateral anterior cingulate, cerebellum → left prefrontal cortex → mid-cingulate
			two scanning sessions for 30 min - 6min each stimulation scan		Voxel size: 1 mm ³	Voxel size: 3.0 mm ³		
	Frangos et al., 2015	12 healthy subjects	Scan 1 as control 2 min rest – 7 min earlobe stimulation – 5 min rest Scan 2 as experimental 2min rest – 7 min left cymba conchae stimulation – 11 min rest 250 μ s, 25 Hz, 0.43 \pm 0.14 mA for taVNS, 0.58 \pm 0.19 mA for sham	12-channel	MPRAGE 176 sagittal slices 1mm isotropic voxels TR: 1900 ms TE: 2.52 ms FA: 9° Matrix: 256 \times 256 FOV: 256 \times 256 mm ² 50% distance factor	EPI 33 axial slices 3mm isotropic voxels TR: 2000 ms TE: 30ms FA: 90° Matrix: 64 \times 64 FOV: 192 \times 192 mm ² Interslice gap: 1.5 mm T2* pulse sequence 43 axial slices	5mm FWHM Gaussian smoothing kernel vs no spatial smoothing	Comparison cymba conchae vs earlobe stimulation <u>Group brainstem analysis</u> → activation of the ipsilateral NTS, STN, LC (contralateral), parabrachial area (contralateral) → bilateral activation in forebrain regions → bilateral deactivations in hypothalamus, hippocampal formation → spatial smoothing (5mm): activation throughout medulla, pons, midbrain, but not regional specific
Garcia et al., 2017	16 migraine patients and 16 healthy controls	360 s stimulation duration, 14 s ON 20 s OFF, 450 μ s, 30H z, 0.85 \pm 1.07 mA – 1.22 \pm 1.33 mA for tvNS, no stimulation during sham Two stimulation scan runs	12-Channel	MPRAGE 176 axial slices TR: 2530 ms TE: 1.64 ms FA: 7°	T2* pulse sequence 43 axial slices TR:2500 ms TE: 30 ms FA: 90° Matrix: 84 \times 84	5mm FWHM Gaussian smoothing kernel	Comparison cymba conchae vs cymba conchae (no current) <u>Increased activation during eRAVANS</u> - NTS - anterior insula, mid-cingulate cortex <u>Post stimulation effects</u> - increased activation in nucleus raphe centralis, LC	

(continued on next page)

Table 1 (continued)

Scanner	Author/year	N	Design	Head coil	Structural parameters	fMRI sequence parameters	Smoothing	fMRI results
			- 11 repetitions with air-puffs			Thickness: 2.62 mm gap: 0.5 mm FOV: 220×220 mm ² Voxel size: 2.62×2.62×3.12 mm ³		
	Peng et al., 2018	24 healthy subjects	30 s ON vs 60 s OFF,	Not reported	Not reported	FSPGR NEX = 1	6mm FWHM Gaussian	Comparison cymba conchae vs. earlobe stimulation (N = 16)
			250 μs, 20 Hz, between 4 and 8 mA			TR: 6.6ms TE: 2.8ms	smoothing kernel	Activation: → bilateral amygdala, prefrontal cortex → left caudate, posterior cingulum cortex, parahippocampal gyrus, putamen
			fMRI for 420 s - baseline for 60 s			FA: 60°		
			- four alternating stimulation ON and OFF sequences were performed			Thickness: 1mm		
						Matrix: 256×256 FOV: 16cm/image		
	Sclocco et al., 2020	30 healthy subjects	Five 8.5-min duration fMRI scan runs	64 -channel	MPRAGE 176 axial slices	EPI multi-band factor 575 axial slices		Comparison cymba conchae vs. no current
			1× sham stimulation run 4× active RAVANS scans using different frequencies at 2 Hz (7.18 ± 0.95 mA),			2 mm isotropic voxel		<i>Greater activation for 100 Hz RAVANS vs. sham</i> - bilateral LC, dorsal and medial raphe nuclei,
			10 Hz (6.46 ± 1.30 mA), 25 Hz (5.93 ± 1.21 mA), 100 Hz (5.57 ± 1.18 mA)		TR: 2530 ms TE1/TE2/TE3/TE4: 1.69/3.55/5.41/7.27 ms FA: 7°	TR: 1250 ms TE: 33 ms		<i>Greater activation for 2 Hz RAVANS vs. sham</i> - right LC, dorsal raphe nuclei <i>Greater activation for 100 Hz RAVANS vs.</i> <i>Greater activation for 2 Hz vs.</i>

(continued on next page)

Table 1 (continued)

Scanner	Author/year	N	Design	Head coil	Structural parameters	fMRI sequence parameters	Smoothing	fMRI results
			300 μ s, 1.5 sec phasic bursts			Thickness: 2 mm		10 Hz and 25 Hz - right LC, dorsal raphe nuclei a) 10 Hz RAVANS: right LC b) 25 Hz RAVANS: right LC, dorsal raphe nuclei sig. correlation between 2 and 100 Hz - right LC, dorsal raphe nuclei
	Yakunina et al., 2017	37 healthy subjects	30 s ON vs 60 s OFF, 500 μ s, 25 Hz, 0.77 \pm 0.42 mA at inner tragus, 0.81 \pm 0.48 mA at ear canal, 0.91 \pm 0.47 mA at cymba, and 0.81 \pm 0.38 mA for sham at cymba, and 0.81 \pm 0.38 mA for sham - repeated for four times in a run - each subject eight 6-min fMRI runs with up to 90 s rest in between runs	32-Channel SENSE (Philips)	FOV: 256 \times 256 mm ² T1 coronal 3D TR: 9.8 ms TE: 4.8 ms FA: 8 $^{\circ}$ Thickness: 1.0 mm Matrix: 256 \times 256 \times 195 FOV: 220 \times 220 mm ² Voxel size: 0.94 \times 0.94 mm MPRAGE	FOV: 220 \times 220 mm ² EPI 30 oblique coronal slices TR: 2000 ms TE: 35 ms FA: 90 $^{\circ}$ Matrix: 80 \times 80 FOV: 220 \times 220 mm ² Voxel size: 2.75 \times 2.75 mm EPI 31 slices, 150 phases	8mm FWHM Gaussian smoothing kernel vs no spatial smoothing	Comparison cymba conchae vs. earlobe stimulation Activation → unsmoothed data: bilateral LC and NTS
	Zhang et al., 2019	29 migraine patients	200 μ s, 1 Hz, 1.5–3 mA - each scan consisted of six 20 - s ON conditions separated by 20- or 30-s 'OFF' periods - 5 min real or sham taVNS fMRI scan - 8 min continuous real or sham taVNS without fMRI	24-channel	TR: 1900 ms TE: 2.27 ms FA: 9 $^{\circ}$ Thickness: 1.0 mm Matrix: 256 \times 256	TR: 2000 ms TE: 30 ms Thickness: 3.5 mm Matrix: 64 \times 64	6mm FWHM Gaussian smoothing kernel	Comparison cymba conchae vs. tail of the helix stimulation Deactivation based on ROI analysis →in the bilateral LC

(continued on next page)

Table 1 (continued)

Scanner	Author/year	N	Design	Head coil	Structural parameters	fMRI sequence parameters	Smoother	fMRI results
7T	Sclocco et al., 2019	16 healthy subjects	Four 8-min duration fMRI scan runs 1 s 'ON', 450 μ s, 25 Hz, 1.6 \pm 2.3 mA (eRAVANS) 1.7 \pm 2.4 mA (iRAVANS) for taVNS, 1.4 \pm 1.1 mA for sham - passive control scan - two active stimulation scans - one active control scan run	32-channel	FOV: 256 \times 256 mm ²	FOV: 224 \times 224 mm ² EPI multi-band factor 2 38 coronal slices 1.2mm isotropic voxel size TR: 0.99 s TE: 23 ms FA: 58° FOV: 192 \times 192 mm ² band width: 1562 Hz pix ⁻¹ echo spacing: 0.76 ms, R = 4 in-plane (GRAPPA)	smoothing kernel smoothing kernel	Comparison cymba conchae vs. earlobe stimulation Greater activation for eRAVANS - LC, dorsal and medial raphe nuclei

(mA), stimulation frequency (Hz), pulse width (μ s) and duty cycle (stimulation on / stimulation off) provide a large parameter space from which researchers have to choose optimal stimulation protocols with for the most part unknown efficacy in humans. Moreover, many taVNS studies in humans use commercially available and certified devices with predefined stimulation parameters, e.g., a stimulation frequency of 25 Hz, pulse width between 200-300 μ s and a duty cycle of 30 s on and 30 s off (Yap et al., 2020). Researchers are then only able to adjust the stimulation intensity to their individual needs (e.g., Bauer et al., 2016; Beste et al., 2016; Borges et al., 2019; Ferstl et al., 2021; Frangos et al., 2015; Warren et al., 2019). This already limits possible study designs, where often a more flexible manipulation of parameters is desirable. Indeed, 30 s stimulation with 25 Hz has been shown to increase LC firing and NE release in iVNS studies with rats (Dorr and Debonnel, 2006; Manta et al., 2009, 2013). Pulse width and the off-period in these studies however differed from the parameters pre-set in many taVNS devices. Using predefined stimulation parameters may simplify comparisons between human studies, however it is difficult to compare effects with animal studies where parameters often vary (Colzato and Beste, 2020).

Regarding the stimulation intensity, iVNS in rats has shown a dose-dependent relationship with higher intensities leading to increased LC firing and NE release. Driven activity in the LC increased monotonically with the tested stimulation intensities from 0.2 mA to 2.5 mA (Hulsey et al., 2017). However, a higher LC firing rate does not always appear to be beneficial. Animal studies on cortical plasticity using iVNS in rats suggest that the relationship between stimulation intensity and stimulation effects may not always increase monotonically. Plasticity was more pronounced at moderate intensities around 0.8 mA whilst at higher stimulation intensities (1.2–1.6 mA), iVNS disrupted cortical plasticity and behavioral benefits (Borland et al., 2016; Morrison et al., 2021; Souza et al., 2021). Currently, human studies which systematically investigate the effect of different stimulation intensities for taVNS are lacking. In human taVNS studies, two different approaches are used: (i) using a fixed stimulation intensity across all subjects and (ii) individual adjustment of intensity. In the second case, researchers can choose to stimulate below or above the individual perceptual threshold. Whilst the first approach assures uniform stimulation parameters across participants, the latter method gives the advantage of avoiding uncomfortable or even painful stimulation. Both options (fixed and individualized intensities) are viable given that the current intensity is high enough to activate myelinated A-fibres, which contribute a large part of the ABVN (Safi et al., 2016). From a theoretical point of view, it seems reasonable that stimulation intensities for taVNS should not fall below 0.75 mA to recruit A-fibres of the ABVN. Using computational models, Helmers and colleagues estimated stimulation intensities between 0.75 and 1.75 mA are sufficient to cause vagal activation with pulse widths between 200 and 500 μ s. However, their model was restricted to the cervical VN and based on the histological examination of the VN from only one subject (Helmers et al., 2012). In practice, 'moderate', non-invasive stimulation intensities with regard to taVNS effect are likely to be higher, since skin impedance and properties of subcutaneous tissues affect the current flow (Keller and Kuhn, 2009). Inadequate skin cleaning and degreasing before stimulation can easily increase impedance at the skin level and thus may reduce the current that reaches the nerve fibres (Badran et al., 2019; Burger et al., 2020).

The most commonly applied frequency in human studies at present is 25 Hz (see Table 2 in (Farmer et al., 2020)), but conclusive evidence about the effectiveness of this frequency in humans is lacking. The effects of varying frequency (0, 7.5, 15, 30, 60, 120 Hz) keeping the other parameters constant, were shown with iVNS in rats (Hulsey et al., 2017). Specifically, they showed that higher stimulation frequencies lead to greater maximal discharge rates over a shorter duration. Varying the iVNS frequency thus influenced the timing but not the total amount of LC activity (Hulsey et al., 2017). A first more systematic approach in human studies based on perceptual thresholds was reported by Sclocco et al. (2020). They were able to show that perceptual ratings of

stimulation intensity did not differ between conditions when higher stimulation intensities were combined with lower frequencies (7.18 ± 0.95 mA (2 Hz) > 6.46 ± 1.30 mA (10 Hz) > 5.93 ± 1.21 mA (25 Hz) > 5.57 ± 1.18 mA (100 Hz)) and interestingly the perceptual rating did not differ between the conditions (Sclocco et al., 2020). Moreover, a wider cluster of fMRI activation in respiratory-gated taVNS (RAVANS) at 100 Hz was found in serotonergic (dorsal (DR) and median (MR) raphe nuclei) and noradrenergic (LC) nuclei, whilst lower 2 Hz RAVANS also lead to DR and right LC activation (Sclocco et al., 2020). These results also illuminate that high responders to 2 Hz RAVANS were also high responders to 100 Hz RAVANS and that due to the differentially perceived sensory stimulation the influence of sensory pathways on LC activations cannot be excluded (Sclocco et al., 2020). Based on these results, a high stimulation frequency (e.g. 25 Hz) should be tested in comparison to lower frequencies (e.g. 10, 15 Hz) in taVNS studies, keeping the other stimulation parameters constant, in order to be able to give conclusive evidence regarding the influence of stimulation frequency on the LC-NE system.

Besides stimulation intensity and frequency, the *pulse width* also affects iVNS efficacy in a dose-dependent manner. In rodent studies using iVNS, higher pulse width lead to increased LC firing rates (0, 30, 100, 500 μ s (Hulsey et al., 2017)), pupil dilation (100, 200, 400 or 800 μ s (Mridha et al., 2021)) and behavioral as well cortical arousal states (100, 500 or 800 μ s (Collins et al., 2021)). In human taVNS studies, pulse width typically varies between 200 and 1000 μ s (Redgrave et al., 2018) and needs to be further systematically investigated. Likewise, the relevance of changes in stimulus cycle requires further investigation in both animal and human research. A current trend towards investigating the effects of phasic (Sharon et al., 2021), event-related stimulation rather than tonic stimulation with particular stimulus cycles is interesting in this regard (summarized below in Section 3). Badran et al. (2019) were able to show that the perceptual threshold decreases with increased pulse width (real stimulation at tragus, $N = 15$), which suggests that parameter manipulations should be assessed in the context of manipulations of other parameters. However, at this point it is unclear how perceived intensity correlates with taVNS outcome measures.

Considering all stimulation parameters, it is evident that their optimal settings and interdependency is insufficiently studied in humans. The lack of studies systematically investigating stimulation parameters in humans is compounded by a frequent use of insufficiently validated outcome measures (see Section 1). Moreover, it is currently unclear to what extent perceptual ratings of stimulation intensity relate to stimulation effects on the VN, and result in additional LC engagement via sensory pathways. Another often neglected aspect, which Wolf et al. (2021) rigorously discussed based on neurobiological pathways, is the *stimulation side* of the ear, i.e., left vs. right (e.g., stronger HRV indices for right sided taVNS reported by De Couck et al. (2017)). In this regard, animal research suggests that the right nodose ganglia (NG) have better access to dopaminergic structures such as the SN (Han et al., 2018) and stimulation of the left ear in humans has a stronger effect on invigoration when food reward is involved (Neuser et al., 2020). These results suggest lateralisation effects and motivate further systematic studies in this respect. Currently, however, it seems likely that the stimulation side has no systematic impact on taVNS effects as measured based on HRV indices (Keute et al., 2021a) or mood changes (Ferstl et al., 2021).

One outstanding and non-trivial question remains, namely the systematic testing of the location for real vs. *sham stimulation*. Electrical stimulation above the sensory threshold induces an easily recognizable somatosensory percept that could explain potential stimulation effects. Thus, a proper sham stimulation is necessary to assure that observed effects are based on LC stimulation and not merely on the somatosensory perception of the stimulation (Keute et al., 2018). Most study designs are based on the results of Peuker and Filler (2002) and even if Yakunina et al. (2017) already tested various locations for real stimulation using a taVNS-fMRI approach, sham stimulation locations in humans are not systematically tested yet. Typically, sham stimulation is applied to the

left ear lobe (Burger et al., 2020; Butt et al., 2020) since it is considered to be relatively free of ABVN fibres (Peuker and Filler, 2002). However, this location has been challenged as an appropriate target for sham stimulation because of the inhomogeneous density of sympathetic nerves in the human ear (Borges et al., 2021; Cakmak, 2019; Rangon, 2018). Cakmak et al. (2018) recommend upper parts of the ear instead of the earlobe for sham stimulation, since they observed that perivascular, sympathetic neurotransmitters are denser in the upper rather than lower auricular areas adjacent to the cymba concha for real stimulation. A previous study with patients suffering from PD ($N = 14$) showed that stimulation of the anti-tragus muscle zone located at the top of the ear lobe led to improved motor functions (Cakmak et al., 2017). Another proposed control method is to use real taVNS sites but without stimulation (Garcia et al., 2017) or with a drastically reduced stimulation frequency (e.g., 1 Hz) (Bauer et al., 2016). However, these approaches are rarely ever used and still need to be validated. Especially stimulation with 1 Hz at intensities above the perceptual threshold is easily recognized as different from and thus no longer indistinguishable from 'real' taVNS (Colzato and Beste, 2020). These results show that more research is needed to delineate proper targets for active sham stimulation. Stimulation protocols that differ in (subjective) intensity or stimulation patterns between real and sham control have to further consider placebo or expectancy-related confounds when comparing real and sham stimulation (Farmer et al., 2020). As of now, there is no sham stimulation that fulfils the criteria proposed by Butt et al. (2020), i.e., no innervation of ABVN fibres while being indistinguishable from taVNS.

4. Potential of phasic stimulation to illuminate the link between taVNS and LC-NE activation

LC neurons are thought to generally display two distinct firing modes with different discharge patterns and NE releasing properties (Aston-Jones and Cohen, 2005; Berridge and Waterhouse, 2003; Florin-Lechner et al., 1996): (i) a *tonic activity mode* (long-lasting, constant activity with 0.5–5 Hz) and (ii) a *phasic activity mode* (short bursts of activity with 10–20 Hz) (Aston-Jones and Bloom, 1981; Aston-Jones and Cohen, 2005; Clayton et al., 2004). A study in rats suggests that higher levels of NE release can be achieved by *phasic stimulation* compared to tonic stimulation (Florin-Lechner et al., 1996). Moreover, animal studies show that *phasic bursts* of NE release (through experimental interventions like electric foot shocks) support memory encoding by fostering LTPs (long term potentiation) in hippocampal projection areas (Luo et al., 2015) and are able to support inhibitory control in prefrontal areas by increasing the signal to noise ratio (Aston-Jones and Cohen, 2005; Berridge and Waterhouse, 2003). Pupil dilation has emerged as an increasingly used indirect measure of *phasic LC activity* (see Section 1) in human and animal studies (Gilzenrat et al., 2010; Murphy et al., 2014). Both, animal and human research has already shown that an increased pupil dilation is associated with *phasic LC activation*, although there is no exclusive link between LC firing and pupil dilation (Aston-Jones and Cohen, 2005; Eckstein et al., 2017; Joshi et al., 2016; Murphy et al., 2014; Samuels and Szabadi, 2008a).

Animal research has explored the influence of different stimulation parameters on the LC-NE system more systematically, in particular the effects of phasic stimulation. For instance a recent iVNS study in monkeys showed that phasic bursts of more than 30–50 Hz lead to stronger vagus evoked potentials compared with low frequency bursts of 5 Hz (Rembado et al., 2021). Hulsey et al. (2017) verified that short bursts of 0.5 s of iVNS drives phasic LC activity even at 0.2 mA and that increased VNS amplitude leads to increased LC firing. This relationship is consistent with recent findings by Mridha et al. (2021) who adjusted various stimulation parameters (amplitude, frequency, pulse width) in a study in mice and observed the strongest effects of VNS on pupil dilation, at 0.9 mA, 20 Hz and 800 μ s with short bursts of 10 s (Mridha et al., 2021). Collins et al. (2021) confirmed a dose dependent effect of VNS on the LC-NE system, whereby a higher stimulation intensity and longer

stimulation duration (0.8 mA and 5 s instead of 0.5 s of short bursts) induced larger pupil dilation. Furthermore, [Mridha et al. \(2021\)](#) found that VNS stimulation intensity was correlated with the extent of cholinergic axon activation. This specific timing response of cortical activation due to VNS was also addressed by [Collins et al. \(2021\)](#), showing that after VNS onset, both NE and ACh cortical activation was observed, followed by whisking and locomotion approx. 1 s thereafter as well as pupil dilation about 1.5 s afterwards in awake as well as anesthetized rats. Additionally, [Hulseley et al. \(2019\)](#) also showed an involvement of the motor cortex during IVNS stimulation (0.8 mA, short bursts of 0.5 s). Effects of phasic iVNS on stimulus-specific plasticity were also observed in rat auditory cortex (see [Section 5](#)), where previously induced tinnitus pathology could be eliminated with a short burst of 0.5 s of iVNS at 0.8 mA (N. D. [Engineer et al., 2011](#)).

In *human research*, [Sharon et al. \(2021\)](#) were able to show a robust pupil dilation based on short bursts of 3.4 s taVNS (2.20 ± 0.24 mA). Similar short bursts of 4 s taVNS (2 mA) ([Keute et al., 2021a](#)) or 1 s taVNS ([Sclocco et al., 2019](#)) in humans, resulted in changes in HR and HRV indices ([Keute et al., 2021a](#)) as well as changed HRV indices during the exhalation phase of the respiratory cycle (eRAVANS) ([Sclocco et al., 2019](#)). Moreover, the LC activation observed by [Sclocco et al. \(2020\)](#) already reported in [Section 2](#), was also based on short bursts, in this case 1.5 s taVNS. However, it should be noted that [Keute et al. \(2021a, 2021b\)](#) and [Sclocco et al. \(2020, 2019\)](#) did not choose an active sham control stimulation location (no current at all) in comparison to [Sharon et al. \(2021\)](#) (see [Section 2](#) for sham-controlled designs). In summary, phasic stimulation approaches might be more useful than tonic approaches when investigating the direct effects of different stimulation parameters and can prove a useful tool for understanding how i/taVNS affects the LC-NE system. Studies with longer stimulation bursts found no immediate effects of taVNS, neither with respect to pupil dilation (e.g., 60 s of taVNS ([Keute et al., 2019a, 2019b](#))) or HRV indices (e.g., 30 s of taVNS ([Borges et al., 2019](#); [De Couck et al., 2017](#)), see ([Burger et al., 2020](#)) for review). Moreover, as the majority of findings reporting optimal stimulation parameters were from animal studies focusing on phasic or burst-like stimulations, phasic stimulation approaches may be more preferable for determining whether these optimal stimulation parameters translate to comparable taVNS stimulation effects in humans.

5. Potential factors influencing stimulation effects between individuals

Apart from open questions in the stimulation protocols and outcome measures, interindividual differences in ABVN properties and the status of the LC-NE system itself may influence taVNS effects (cf. [Fig. 1](#) – ‘Relevance of altered brain physiology’). This is mainly relevant when studying clinical subpopulations which are often the target for taVNS interventions. Regarding the ABVN, only one study so far, by [Safi et al. \(2016\)](#), counted the amount of myelinated nerve fibres in the ABVN and observed considerable variability between subjects (for review see ([Yap et al., 2020](#))). It should be noted here, that the subjects had different histories of medical conditions, so healthy populations might show lower variability ([Safi et al., 2016](#)). Moreover, the density of nerve fibres of the cavum conchae (recess auricle), which is part of the ABVN, varies as well ([Bermejo et al., 2017](#)). This variability might already play an important role in explaining why some individuals benefit from taVNS whilst others do not ([Butt et al., 2020](#)). Moreover, many of the conditions where taVNS can be usefully applied will involve a decline or alteration in LC-NE function. For instance in AD and PD, alterations in LC function may occur before clinical symptoms manifest ([Braak et al., 2003, 2011](#)). For AD, post-mortem studies have shown that, although the number of NE neurons is reduced, certain NE metabolites were not. This was taken as evidence for some compensatory upregulation in NE production in reaction to the loss of LC-NE neurons by which the remaining LC neurons increase their firing rate ([Herrmann et al., 2004](#)).

Furthermore, there is evidence that, at least in early stages of LC decline, increased adrenoceptor density in hippocampus and amygdala might compensate for reduced LC-NE signalling ([Andrés-Benito et al., 2017](#); [Szot et al., 2006](#)). This means that adaptive mechanisms in the brain aimed at compensating altered LC function may influence the effects of externally applied stimulation by, e.g., increasing the response of individual LC neurons or the sensitivity of target areas through increased receptor levels. Similarly, a post-mortem study examining the expression of signalling genes and growth factors revealed a decline in LC function in individuals suffering from depression ([Bernard et al., 2011](#)), which might underlie the use of sNRIs in the treatment of depression ([Moret and Briley, 2011](#)). A meta-analysis has shown that the effects of depression treatment, one of the main areas of i/taVNS application, were only apparent after controlling for depression severity, which revealed stronger effects in more severely affected individuals ([Martin and Martín-Sánchez, 2012](#)). Correspondingly, [Ferstl et al. \(2021\)](#) were able to show that lower baseline levels of positive mood in healthy subjects were associated with greater taVNS (30 s on/off stimulation cycle) induced improvements in motivation. At present, it is unknown whether clinical and cognitive assessments of disease severity are associated with greater LC-NE system decline. Nonetheless, existing studies suggest variability in taVNS effects are also observed in cognitively normal populations as well. Stimulation studies should thus focus more on taking into account interindividual differences in the integrity of the stimulated LC-NE system when interpreting taVNS effects to reduce unreliable and heterogeneous results. Reduced LC integrity has been observed in several clinical populations such as PD and AD as well as major depression (see ([Liu et al., 2017](#)) for an extensive review). Using this approach, interindividual differences in LC integrity can however also be observed in older healthy adults ([Betts et al., 2017](#); [Hämmerer et al., 2018](#); [Liu et al., 2019](#)). Interindividual differences in LC integrity in humans can be determined in terms of signal intensity using neuromelanin-sensitive MRI ([Betts et al., 2019](#)), a technique developed in 2006 ([Sasaki et al., 2006](#)). A combination of ultra-high-field MRI and histological analyses on post-mortem brain tissues confirmed that the localization of the neuromelanin contrast in MRI corresponds to NE-neurons in the LC ([Keren et al., 2015](#)). Related to this, advances in our understanding of the relevance of an altered functionality of the LC-NE system can motivate different interventional avenues with different types of stimulation approaches, which have been as of yet insufficiently explored. Specifically, high-frequency stimulation might carry potential for inhibiting overcompensated (overactive) LC neurons which are thought to contribute to chronic pain ([Bernard et al., 2011](#)) and aggressive behavior in conditions of declining LC-NE integrity possibly related to excessive LC activity ([Liu et al., 2018](#)). However, the interactions among brain areas when investigating different stimulation protocols will also have to be considered. For instance, high-frequency (100 Hz) optogenetic burst stimulation of basolateral amygdala neurons was recently reported to drive excitatory neurons in the medial prefrontal cortex into a blocked state with reduced activity ([Klavriv et al., 2017](#)). In another rat model, it was shown that an overactivation of the LC - BLA pathway provoked pain and that blocking this pathway led to a reduction in pain-induced anxiety ([Llorca-Torralba et al., 2019](#)). Therefore, high-frequency stimulation might carry potential for inhibiting overcompensated (overactive) LC neurons which are thought to contribute to chronic pain. Similarly, aggressive behavior in conditions of declining LC-NE integrity is possibly related to excessive LC activity ([Liu et al., 2018](#)). Due to a long-standing lack of appropriate imaging measures for the LC-NE system and a still developing understanding of the role of the LC-NE system in higher cognitive functions ([Sara and Bouret, 2012](#)), current commercially available taVNS devices might not take full advantage of the therapeutic potential of taVNS interventions in humans.

6. Potential of translational cross-species approaches to illuminate the link between taVNS and LC-NE activation

Before a new therapy or treatment is applied to humans, they are usually tested in animal models. The potential of iVNS to treat epilepsy, for instance, was first demonstrated in canine models (Zabara, 1985, 1992) before it was investigated in the first human trials (Penry and Dean, 1990). Animal research is now helping us to further our knowledge about the functional mechanisms of iVNS and provides new hypotheses for potential applications of taVNS in humans (cf. Fig. 1 – ‘Cross-species translational approach’). One example for this, among others, is the evolution from studies investigating NE-related plasticity in the primary auditory cortex (A1) of rats towards the development of potential, non-invasive tinnitus interventions in humans. Tinnitus, the perception of sounds without corresponding stimuli, is thought to be based largely on maladaptive A1 map reorganizations leading to an increased number of neurons responding to certain frequencies (Eggermont, 2015; Eggermont and Roberts, 2015; N. D. Engineer et al., 2011; Wu et al., 2016). In recent years, i/taVNS approaches were investigated as adjunctive treatment options for tinnitus due to its potentially neuromodulating effect (Stegeman et al., 2021). Early work investigating NE effects on auditory cortical plasticity used ionophoretic infusion of NE directly into rat auditory cortex paired with tone stimuli and observed frequency specific modulation in neuronal tuning curves (Manunta and Edeline, 2004). In a subsequent study, also in rats, direct, phasic stimulation of the LC paired with pure tones altered response characteristics of A1 neurons, corroborating the role of the LC-NE system for neural plasticity. Of note, frequency-specific increases in spike rates were observed already after 100 pairings, persisting up to 15 min after stimulation (Edeline et al., 2011). These observations were then used to generate hypotheses that iVNS in rats could yield similar results. Indeed, pairing pure tones with iVNS (performed 300 times a day for 20 days) increased the number of recording sites that preferably responded to the paired frequency compared with an unpaired control group (N. D. Engineer et al., 2011). Similar results were observed when speech sounds were used as stimuli (C. T. Engineer et al., 2015), which is in line with increased temporal flexibility of A1 neurons due to VNS-tone pairing (Shetake et al., 2012). These results generated new ideas to use iVNS and potentially taVNS to modulate cortical plasticity in a targeted manner in therapeutic settings to treat tinnitus. N. D. Engineer et al. (2011) used iVNS to reverse tinnitus in a rat model. Stimulation was applied as phasic bursts of 0.5 s, beginning 150 ms before tone onset and these pairings were repeated 300 times a day for 18 days. In rats receiving iVNS-tone pairings, behavioral correlates of tinnitus were eliminated after the therapy, whereas animals from the three control groups (iVNS without tones, tones without iVNS or no therapy) showed consistent impairments. Three weeks after the therapy, neural recordings from A1 revealed that pathological changes in the treated group but not in the control groups returned to normal levels (N. D. Engineer et al., 2011). Following these results, pilot studies in humans with implanted VNS electrodes emerged, using iVNS-tone pairing paradigms to treat tinnitus (De Ridder et al., 2014 ($N = 10$); Tyler et al., 2017 ($N = 30$); Vanneste et al., 2017 ($N = 18$)). Random tones were presented together with 0.5 s phasic (Tyler et al., 2017; Vanneste et al., 2017) or 30 s tonic (De Ridder et al., 2014) iVNS in order to reduce pathological, neuroplastic changes in auditory cortex regions. Subjects reported a reduction in subjective tinnitus symptoms (Tyler et al., 2017; Vanneste et al., 2017). Likewise, electrophysiological recordings performed before and after the therapy revealed that iVNS-tone pairing reduced gamma band activity (30–44 Hz) in left auditory cortex and phase coherence between auditory cortex and other brain areas associated with the tinnitus perception including the cingulate cortex (Vanneste et al., 2017). Hypersynchronous activity in the gamma band of the auditory cortex is an electrophysiological marker of tinnitus (Langguth et al., 2013; Weisz et al., 2007) while the cingulate cortex is associated with its affective components (e.g., distress) (Vanneste et al., 2010). In

parallel, researchers aimed to establish taVNS as a non-invasive procedure to circumvent the invasiveness and high costs of iVNS. Lehtimäki et al. (2013) used a tailored sound therapy (ST) combined with continuously applied taVNS (25 Hz, 45–60 min) at the left tragus. Additional subjects ($N = 8$) were presented with pure tones centred at their tinnitus frequency while their brain activity was recorded via magnetencephalography (MEG) either during taVNS or no stimulation. The ST group not only showed decreases in subjective tinnitus symptoms after ST paired with taVNS but also a mood improvement while the MEG group showed a reduced amplitude of the N1m during taVNS (Lehtimäki et al., 2013). The N1m, the magnetic equivalent of the N1 ERP, reflects early auditory processing in A1 (Näätänen and Picton, 1987) and an increased N1m amplitude has been observed in many tinnitus patients, indicating hyperactivity in the A1 (Lehtimäki et al., 2013). A major drawback of this study, however, is that both results could have been obtained based on ST alone (e.g., Pantev et al., 2012). Hyvärinen et al. (2015) recorded brain activity via MEG while presenting tinnitus patients ($N = 7$) with tones matched to their individual tinnitus frequency either during continuous taVNS (25 Hz) on the left tragus or no stimulation. Additional control subjects ($N = 8$) without tinnitus were presented with 1 kHz tones and sham-stimulation at the left earlobe. They showed that taVNS in tinnitus patients' modulated tone evoked synchronicity in the beta- and gamma-band (Hyvärinen et al., 2015). Hypersynchronous activity in the auditory beta range has also been observed in patients suffering from tinnitus and auditory hallucinations (Vanneste et al., 2013). Yet, it is imperative to notify that these results have to be interpreted with caution as highlighted in detail by two recent reviews (Stegeman et al., 2021; Yakunina and Nam, 2021). Both, studies that used taVNS alone as well as studies that used taVNS in combination with ST, have severe methodological flaws. They lack sufficient sample sizes and appropriate blinding, are not designed as randomized controlled trials and results and methods are often reported with low quality (Stegeman et al., 2021). Furthermore, they rely on the assumption that cortical reorganization in the tonotopic map of A1 is a major cause for tinnitus, which is highly debated (Yakunina and Nam, 2021). With these caveats in mind, no clear statement for the effectiveness of taVNS in the treatment of tinnitus and more research using randomized controlled trials is needed (Stegeman et al., 2021; Yakunina and Nam, 2021). Nevertheless, animal research is still valuable to further delineate the exact cortical and neuronal causes of tinnitus and potential ways to reverse these. If properly conducted (i.e., sham controlled, blinded, sufficiently powered), human studies can then use non-invasive electrophysiological markers to improve the usefulness of taVNS in the remedy of tinnitus.

Apart from the auditory system, Hulsey et al. (2019) showed an involvement of the motor cortex during iVNS indicating stimulus-specific cortical plasticity of iVNS. Specifically, iVNS in rats paired with proximal forelimb movements increased the cortical representation of these movements (Hulsey et al., 2019). Similar, iVNS in rats paired with rehabilitative training after spinal cord injury improved forelimb strength compared to rehabilitative training without iVNS (Darrow et al., 2020). In line with the cortical plasticity potential of iVNS, Capone et al. (2017) were able to demonstrate that taVNS at the inner side of the tragus (2.0–4.5 mean mA, 20 Hz, 300 μ s, 30 s every 5th min for 60 min) combined with robotic rehabilitation can improve arm functionality in patients with ischemic ($N = 5$) or haemorrhagic ($N = 2$) chronic stroke. However, this study also has a weakness in power, as only 7 subjects received real stimulation and 5 subjects (ischemic: $N = 3$) sham stimulation. As mentioned above, there is currently an increasing interest in understanding how taVNS might affect the gut-brain axis. Animal as well as human studies indicate an i/ta VNS induced reduction of food intake accompanied by weight loss and reduction of gastric frequency via vagal afferents (for review see (Farmer et al., 2020)). Additionally, Gil et al. (2009) were able to show not only that long-term iVNS with a low stimulation frequency (0.05 Hz), but also by applying a higher stimulation frequency (10 Hz, 10 ms, 200 mV, 12 h per day for 42 days)

(Gil et al., 2011) can lead to reduced food intake and body weight in rats on a high-fat diet. Similarly, at 1 Hz, stimulation of the afferent fibres was shown to reduce food intake in rats by influencing the response to stomach peristalsis within 100 days (Yao et al., 2018). Gil et al. (2011) further observed neuronal responses in NTS, decreased levels of leptin and increased levels of ghrelin after iVNS in rats on a high-fat diet. Both hormones are important because leptin contributes to inhibiting food intake and ghrelin to stimulating appetite (see (Klok et al., 2007) for review). An imbalance of this hormone release can promote obesity (Cryan et al., 2019), which is associated with health problems not only in animals but also in humans. Teckentrup et al. (2020) investigated the potential role of taVNS on gastric frequency in healthy adults ($N = 21$). Specifically, it was shown that afferent stimulation (25 Hz, 30 s on/off stimulation cycle) had an effect on metabolic efferents and resulted in reduced myoelectric frequency, but did not affect resting energy expenditure (Teckentrup et al., 2020). This effect might be driven by dopamine release in the brainstem (Teckentrup et al., 2020) which highlights once again that the VN is involved in the regulation of the activity of a variety of brain structures and internal organs. Yet, the extent to which taVNS can really contribute positively as an additional treatment option for obesity still needs to be investigated in more detail. In the future, translational approaches could try to establish iVNS and taVNS in the same animal models using outcome measures that have been shown to be indicative of LC-NE activity in both animals and humans. Different parameter combinations could then be systematically investigated in their respective effectiveness and compared between iVNS and taVNS. If based on this, an effect of similar magnitude can be shown in animals, one could show (i) to what extent the parameters for iVNS differ from taVNS in the animal itself and (ii) in comparison to common taVNS parameters used in humans. Thus, it would then also be possible to adapt the stimulation parameters used in animal research more specifically for taVNS in humans.

7. Summary and conclusion

A dysregulation of the LC-NE system characterizes a wide range of clinical and neurological conditions, including depression, chronic pain, post-traumatic stress disorder, neurodegenerative diseases, as well as cognitive decline in aging (Betts et al., 2019; Hämmerer et al., 2018; Liu et al., 2017). Compared to pharmacological therapies, taVNS has the potential for a more anatomically and functionally targeted intervention which can provide a valuable tool if properly validated. Here we reviewed the current challenges in evaluating the effectiveness of taVNS in reaching the LC-NE system in humans and outline experimental approaches that may help to overcome them. Challenges in assessing the effects of taVNS on the LC-NE system in humans (cf. Fig. 1) include most importantly difficulties in (i) identifying adequate biomarkers that index taVNS efficacy on the level of an engagement of the LC-NE system as well as (ii) identifying optimal stimulation protocols.

We outline how both of these shortcomings can be overcome by moving towards phasic i/taVNS protocols as well as investigating i/taVNS effects in cross-species translational approaches. In comparison to tonic stimulation interventions, phasic stimulations have the advantage of allowing for an immediate and repeated assessment of stimulation effects on the LC-NE system. Moreover, the ability to elicit LC firing and NE release by phasic or burst-like interventions has been well validated in animal studies that investigate NE and LC function using event-related interventions such as foot shocks or direct stimulation interventions to the LC (Chen and Sara, 2007). Indeed, phasic i/taVNS has been shown to modulate LC-NE activity in animal studies (Collins et al., 2021; Hulsey et al., 2017, 2019; Mridha et al., 2021) as well as human studies (Keute et al., 2019a; Sclocco et al., 2019, 2020; Sharon et al., 2021). In contrast, human taVNS studies using tonic stimulation (e.g. Borges et al., 2019; De Couck et al., 2017; Keute et al., 2019a, 2019b) have not always yielded reliable effects on the LC-NE system.

Secondly, cross-species translational research is of great importance

to increase our understanding of how taVNS in humans affects the LC-NE system. Considerable knowledge regarding optimal stimulation parameters (e.g., Hulsey et al., 2017) or outcome measures (e.g., Collins et al., 2021; Mridha et al., 2021) has already been gained from iVNS in rodents. Such results can form the starting points for testing similar effects using taVNS in humans. TaVNS has emerged as a potential treatment option for tinnitus via modulating cortical plasticity in A1. However, results from human studies are few and inconclusive at best due to methodological shortcomings. Additional studies that are better controlled (e.g., sham controlled, randomized, balanced and properly blinded designs) with sufficient power are required to delineate how VNS findings in rodents can be translated to further understand how taVNS can be used as a reliable intervention for human tinnitus. Similarly, first approaches that show how i/taVNS can influence the rehabilitation of motor areas in the brain or regulate gastric frequency as well as weight loss and food intake await a more thorough validation in humans. In particular, fMRI offers great potential as an outcome measure as it provides the advantage that taVNS induced changes can be observed in the LC more directly with high spatial acuity compared to more peripheral outcome measures of LC activity such as pupillometry or HRV. Additional electrophysiological recordings with high temporal resolution such as EEG could then provide information about the timing of these effects. Not only the different stimulation sites (left vs. right ear) and locations (real vs. sham stimulation), but also stimulation parameters and their influence on the LC-NE system could be addressed using taVNS-fMRI. In addition, taVNS-fMRI might also help identify how the interaction of different stimulation parameters influences LC activation. At present, we do not know how the different stimulation parameters have to be combined in order to optimise taVNS effects on the LC-NE system.

Future stimulation devices used for basic research, individual at-home treatments as well as to study different clinical conditions should thus have the potential to let practitioners manipulate all stimulation parameters such as intensity, frequency, pulse width and duty cycle to adjust to their individual needs. Although taVNS can be assumed to stimulate VN and LC via the ABVN, the involvement of sensory pathways cannot be completely excluded due to for instance somatosensory reactions to the sensation of being stimulated. Studies assessing the painfulness or discomfort of taVNS applications should consider these as covariates when assessing interindividual differences. It remains to be systematically investigated to what extent an engagement of the LC via sensory stimulation effects, complicates the assessment of differences between real and sham stimulation.

A further reason for the heterogeneous results of taVNS interventions in humans, might be interindividual variability in the LC-NE system and the ABVN. The integrity of the LC is especially important when taVNS is considered as adjunctive treatment in clinical populations that may be affected by reduced NE modulation such as depression or neurodegenerative diseases. However, some evidence points towards an adaptation in the LC-NE system in response to a reduced NE supply in form of an upregulated NE release of the remaining LC neurons or an increase in NE receptors in target areas (Andrés-Benito et al., 2017; Herrmann et al., 2004; Szot et al., 2006). Such changes in the impact of NE release would then have to be taken into account when externally modulating NE release via taVNS. It is therefore important to add measures that allow to characterize interindividual differences in the LC-NE system in particular in the evaluation of taVNS in clinical populations. Measures such as neuromelanin-sensitive MRI sequences which help to assess the role of LC integrity can for instance prove relevance in this regard. Neuromelanin-sensitive MRI has already provided insight about the interindividual variability in LC integrity in healthy, older adults (Betts et al., 2017; Hämmerer et al., 2017; Liu et al., 2017). Additional measures that inform about interindividual differences in LC-NE function or responsiveness might then ultimately also inform the choice of individualized stimulation parameters. Stimulation parameters derived from studies with healthy subjects may prove less effective when applied

- exploratory retrospective study. *Sci. Rep.* 7 (1), 1–11. <https://doi.org/10.1038/s41598-017-17750-y>.
- Warren, C.M., Tona, K.D., Ouwerkerk, L., van Paridon, J., Poletiek, F., van Steenbergen, H., Nieuwenhuis, S., 2019. The neuromodulatory and hormonal effects of transcutaneous vagus nerve stimulation as evidenced by salivary alpha amylase, salivary cortisol, pupil diameter, and the P3 event-related potential. *Brain Stimul.* 12 (3), 635–642. <https://doi.org/10.1016/j.brs.2018.12.224>.
- Weisz, N., Müller, S., Schlee, W., Dohrmann, K., Hartmann, T., Elbert, T., 2007. The neural code of auditory phantom perception. *J. Neurosci.* 27 (6), 1479–1484. <https://doi.org/10.1523/JNEUROSCI.3711-06.2007>.
- Wolf, V., Kühnel, A., Teckentrup, V., Koenig, J., Kroemer, N.B., 2021. Does Non-invasive Vagus Nerve Stimulation Affect Heart Rate Variability? A Living and Interactive Bayesian Meta-analysis. *BioRxiv*. <https://doi.org/10.1101/2021.01.18.426704>.
- Wu, C., Stefanescu, R.A., Martel, D.T., Shore, S.E., 2016. Tinnitus: maladaptive auditory–somatosensory plasticity. *Hear. Res.* 334 (12), 20–29. <https://doi.org/10.1016/j.heares.2015.06.005>.
- Yakunina, N., Nam, E.-C., 2021. Direct and transcutaneous vagus nerve stimulation for treatment of tinnitus: a scoping review. *Front. Neurosci.* 15 (May) <https://doi.org/10.3389/fnins.2021.680590>.
- Yakunina, N., Kim, S.S., Nam, E.-C., 2017. In: Optimization of Transcutaneous Vagus Nerve Stimulation Using Functional MRI. *Neuromodulation: Technology at the Neural Interface*, 20(3), pp. 290–300. <https://doi.org/10.1111/ner.12541>.
- Yao, G., Kang, L., Li, J., Long, Y., Wei, H., Ferreira, C.A., Wang, X., 2018. Effective weight control via an implanted self-powered vagus nerve stimulation device. *Nat. Commun.* 9 (1), 1–10. <https://doi.org/10.1038/s41467-018-07764-z>.
- Yap, J.Y.Y., Keatch, C., Lambert, E., Woods, W., Stoddart, P.R., Kameneva, T., 2020. Critical review of transcutaneous vagus nerve stimulation: challenges for translation to clinical practice. *Front. Neurosci.* 14 (April) <https://doi.org/10.3389/fnins.2020.00284>.
- Yi, Y.-J., Lüsebrink, F., Maaß, A., Ziegler, G., Yakupov, R., Kreißl, M.C., Betts, M., Speck, O., Düzel, E., Hämmerer, D., 2021. It is the *Locus Coeruleus!* Or... is it? : A proposition for analyses and reporting standards for structural and functional magnetic resonance imaging of the noradrenergic *Locus Coeruleus* (S. 2021.10.01.462807). <https://doi.org/10.1101/2021.10.01.462807>.
- Zabara, J., 1985. Peripheral control of hypersynchronous discharges in epilepsy. Retrieved from *Electroencephalogr. Clin. Neurophysiol.* 61, 5162. <https://ci.nii.ac.jp/naid/10009203636/en/>.
- Zabara, J., 1992. Inhibition of experimental seizures in canines by repetitive vagal stimulation. *Epilepsia* 33 (6), 1005–1012. <https://doi.org/10.1111/j.1528-1157.1992.tb01751.x>.
- Zhang, Y., Liu, J., Li, H., Yan, Z., Liu, X., Cao, J., Park, J., Wilson, G., Liu, B., Kong, J., 2019. Transcutaneous auricular vagus nerve stimulation at 1 Hz modulates locus coeruleus activity and resting state functional connectivity in patients with migraine: an fMRI study. *NeuroImage: Clinical* 24, 101971. <https://doi.org/10.1016/j.nicl.2019.101971>.



Registered Report

Effects of transcutaneous vagus nerve stimulation (tVNS) on beta and gamma brain oscillations



Marius Keute^{a,c,*}, Christian Wienke^{a,b}, Philipp Ruhnau^{a,b} and Tino Zaehle^{a,b}

^a Department of Neurology, Otto-von Guericke-University, Magdeburg, Germany

^b Center for Behavioral Brain Sciences, Otto-von-Guericke University, Magdeburg

^c Institute for Neuromodulation and Neurotechnology, University of Tübingen, Tübingen, Germany

ARTICLE INFO

Article history:

Protocol received: 10 December, 2018

Protocol accepted: 23 July, 2019

Received 18 February 2021

Reviewed 25 March 2021

Revised 5 April 2021

Accepted 12 April 2021

Action editor Chris Chambers

Published online 24 April 2021

Keywords:

tVNS

MEG

Movement beta

Visual gamma

Biomarker

ABSTRACT

Physiological and behavioral effects induced through transcutaneous vagus nerve stimulation (tVNS) are under scrutiny in a growing number of studies, yet its mechanisms of action remain poorly understood. One candidate mechanism is a modulation of γ -aminobutyric acid (GABA) transmission through tVNS. Two recent behavioral studies suggest that such a GABAergic effect might occur in a lateralized fashion, i.e., the GABA modulation might be stronger in the left than in the right brain hemisphere after tVNS applied to the left ear. Using magnetoencephalography (MEG), we tested for GABA-associated modulations in resting and event-related brain oscillations and for a lateralization of those effects in a sample of 41 healthy young adults. Our data provide substantial evidence against all hypotheses, i.e., we neither find effects of tVNS on oscillatory power nor a lateralization of effects.

© 2021 Elsevier Ltd. All rights reserved.

1. Introduction

Transcutaneous vagus nerve stimulation (tVNS) is a non-invasive brain stimulation technique that has received increasing attention in recent years. It has been introduced as a non-invasive alternative to direct or invasive vagus nerve

stimulation (iVNS) (Ventureyra, 2000). Clinically, it is effective as an adjunct therapy for pharmacoresistant epilepsy (Bauer et al., 2016; He et al., 2013; Stefan et al., 2012) and depression (Fang et al., 2016; Trevizol et al., 2015). Furthermore, it has been suggested as a prospective treatment for a variety of conditions, including chronic headache (Barbanti et al., 2015; Magis, Gérard, & Schoenen, 2013, p. P198), tinnitus (Lehtimäki

* Corresponding author. Department of Neurology, Otto-von Guericke-University, Magdeburg, Germany.

E-mail address: marius.keute@gmail.com (M. Keute).

<https://doi.org/10.1016/j.cortex.2021.04.004>

0010-9452/© 2021 Elsevier Ltd. All rights reserved.

et al., 2013), post-operative cognitive dysfunction (Xiong et al., 2009), cerebral ischemia (Lu et al., 2017), and Alzheimer's disease (Kaczmarczyk, Tejera, Simon, & Heneka, 2018). (see Fig. 4)

So far, the mechanisms of action of tVNS are not fully understood, and an improved understanding of these mechanisms will be highly relevant and necessary for future research, highlighting how patients can benefit from tVNS as well as for therapy development and improvement. It is consistently found that the locus coeruleus-norepinephrine (LC-NE) system is activated through both iVNS and tVNS. This activation is mediated by the nucleus of the solitary tract (NTS), the principal brain projection area of the afferent branches of the vagus nerve (Ruffoli et al., 2011). LC activation is considered the core mechanism of tVNS (Assenza et al., 2017; Badran et al., 2018; Raedt et al., 2011; Ventura-Bort et al., 2018; Warren et al., 2019). One of several other candidate mechanisms of action is an increase in γ -aminobutyric acid (GABA) transmission in the brain (Ruffoli et al., 2011; Walker, Easton, & Gale, 1999; Woodbury & Woodbury, 1991), mediated through activation of the NTS and LC (Berridge & Waterhouse, 2003; Toussay, Basu, Lacoste, & Hamel, 2013). The research literature on GABAergic neuromodulation by tVNS is sparse, compared to the amount of studies investigating effects of tVNS on LC-NE activity. Given that GABA transmission has a role in the pathophysiology of epilepsy (Baulac et al., 2001), depression (Möhler, 2012), tinnitus (Brozoski, Spires, & Bauer, 2007), and other neurological and psychiatric conditions, it is of high relevance to better understand GABAergic actions of tVNS in order to predict and understand its therapeutic effects.

In support of a GABAergic mechanism of tVNS, it has been found that GABA_A receptor density was increased in patients after receiving long-term iVNS (Marrosu et al., 2003). Moreover, GABA concentration in the cerebrospinal fluid of patients receiving iVNS was increased (Ben-Menachem et al., 1995; Carpenter et al., 2004). The number of studies specifically investigating the relationship between tVNS and GABA transmission, however, is limited. Short-term (~1 h) tVNS in healthy subjects modulated cortical excitability (Capone et al., 2015) as well as automatic motor inhibition (Keute, Ruhnu, Heinze, & Zaehle, 2018), both of which are highly correlated to GABA concentration in the motor cortex as measured by magnetic resonance spectroscopy (Boy et al., 2010; Stagg et al., 2011).

Interestingly, both studies (Capone et al., 2015; Keute et al., 2018) suggest a possible lateralization of the tVNS effect, in that GABA-associated parameters were modulated in the right, but not in the left brain hemisphere. Similarly, effects of iVNS on the electroencephalogram (EEG) spectrum have been found that were stronger in the right hemisphere (Marrosu et al., 2005). Since both iVNS and tVNS are almost exclusively administered to the left ear/vagus nerve, these findings are compatible with a selective or stronger GABAergic effect of t-/iVNS in the contralateral hemisphere. Even though we are not aware of any anatomical or physiological evidence that could account for a lateralization of tVNS effects, the potential

occurrence of such a lateralization in three independent studies warrants further investigation.

Brain oscillations as measured by EEG or magnetoencephalography (MEG) often have specific relationships to local GABA concentrations and can therefore be used as biomarkers: Pharmacological increases of systemic GABA levels are consistently associated to increases in beta power at rest (Greenblatt et al., 1989; Hall, Barnes, Furlong, Seri, & Hillebrand, 2010; Nutt et al., 2015; van Lier, Drinkenburg, van Eeten, & Coenen, 2004). Furthermore, GABA concentration in the motor cortex is related to peri-movement beta and gamma power modulations (Gaetz, Edgar, Wang, & Roberts, 2011; Muthukumaraswamy et al., 2013), and GABA concentration in the visual cortex is related to gamma power responses to visual stimulation (R. A. E. Edden, Muthukumaraswamy, Freeman, & Singh, 2009; Muthukumaraswamy, Edden, Jones, Swettenham, & Singh, 2009).

This study will use MEG to capture brain oscillations associated to GABA transmission. Using brain oscillations as a marker for GABA has several advantages: the combination of resting and event-related oscillations outlined above has a very specific relationship to GABA. MEG allows to record from the whole brain simultaneously at a good temporal resolution, and to spatially reconstruct sources of specific signals in the brain, which will be helpful to capture a possible lateralization of tVNS effects.

In fact, a recent study found that cervical tVNS increased beta and gamma power and decreased theta and alpha power (Lewine, Paulson, Bangera, & Simon, 2018). Moreover, invasive stimulation of the nucleus of the solitary tract (NTS) in cats increased beta power (Martínez-Vargas, Valdés-Cruz, Magdaleno-Madrigal, Fernández-Mas, &). The NTS is one of the neural targets of vagus nerve stimulation (Clancy, Deuchars, & Deuchars, 2013).

We hypothesize that tVNS will increase GABA concentration, leading to GABA-associated MEG alterations. Specifically, our first set of hypotheses relate to overall GABAergic modulation through tVNS:

- H₁: global resting-state beta power is increased during tVNS compared to sham.
- H_{2A}: peri-movement beta desynchronization (PMBD) in the motor cortex is stronger during tVNS compared to sham.
- H_{2B}: post-movement beta rebound (PMBR) in the motor cortex is weaker during tVNS compared to sham.
- H₃: gamma power response to visual stimulation in the visual cortex is stronger during tVNS.

Furthermore, we hypothesize that the effects from H₁ and H₂ are lateralized, i.e., stronger in the brain hemisphere contralateral to the stimulation.

- H₄: The tVNS effect on resting-state beta power will be stronger in the right (contralateral) hemisphere.
- H_{5A}: The tVNS effect on PMBD will be stronger in the right (contralateral) hemisphere for left-hand responses compared to PMBD in the left motor cortex for right-hand responses.

H_{5B} : The tVNS effect on PMBR will be stronger in the right (contralateral) hemisphere for left-hand responses compared to PMBR in the left motor cortex for right-hand responses.

2. Methods

2.1. General procedure

Upon arrival, written informed consent was obtained from each participant. Participants were reimbursed with money (8 €/hr) or course credit. Head landmarks and head shape were digitized using a Polhemus Fastrak digitizer (Polhemus, VT, USA). The stimulation electrodes were attached (see below), and the participant was seated inside the MEG device. The following procedure is sketched in Fig. 1: A 3-min baseline MEG measurement was carried out, with the instruction for the participant to relax, not to think about anything in particular, keep the eyes open and blink, cough, and move only during stimulation, as far as possible. Subsequently, electrical stimulation was administered for 30 min with a 60s ON/60s OFF cycle, during which the participant had no specific instruction. After pre-stimulation, two blocks of resting MEG were obtained, each with a duration of 3 min, with 1 min of stimulation between both blocks. All resting and on-task MEG recordings were carried out while the electrical stimulation is turned off to avoid contamination of the data with stimulation artifacts. After the resting blocks, two blocks (180s each) of the motor task and two blocks (180 sec each) of visual stimulation were carried out, with 60s of stimulation between all blocks. The order of the tasks was counterbalanced across participants, but kept constant within each participant (i.e., in the sham and tVNS session). The procedure was identical for sham and tVNS sessions, with the only difference being the stimulation site (cymba conchae/tVNS vs scapha/sham). All experimental procedures were carried out in accordance with the declaration of Helsinki and have been approved by the ethics committee of the medical faculty at the University of Magdeburg.

2.2. Participants

The experiment was carried out with 41 healthy young participants (29 females). Mean age was 23.8 years (SD 3.4, range 19–30). Each participant underwent sham and tVNS stimulation in pseudo-randomized order on separate days. Sham and tVNS measurements for each participant were scheduled at least 48 h apart and at the same daytime (± 1 h). All participants were free from any current or past neurological or psychiatric diseases and regular drug intake (both medical and recreational, except for oral contraceptives). They had normal or corrected-to-normal vision and were eligible for tVNS, MEG and MRI (in particular, no cardiac pacemakers or metal implants in or close to the head).

2.3. Motor task

Peri-movement beta power was assessed using a cued finger movement task. Participants were instructed to press a button

with their left or right index finger, according to the direction of an arrow displayed centrally on the screen (displayed in black on a grey background, width 1° , height .5 degree of visual angle). During each 180 sec block, 24 left-pointing and 24 right-pointing arrows were presented in pseudo-randomized order, with stimulus durations of 200 msec and a randomly jittered inter-stimulus interval between 3 and 3.5 sec. A red fixation point was visible on the center of the screen throughout the task to prevent eye movements.

2.4. Visual stimulation

Visual stimuli were stationary, vertical circular gratings with a spatial frequency of 3 cycles per degree and maximum contrast. Throughout the experiment, a central fixation dot was visible. The screen background had the average luminance of the gratings. Stimuli were presented centrally on the screen and subtended 2 degrees of visual angle. In each 180 sec block, 48 gratings were presented for 1 sec, followed by a jittered inter-stimulus interval between 2 and 2.5 sec. This stimulus design is similar to the one used by Muthukumaraswamy et al. (2009).

2.5. Electrical stimulation

tVNS was administered to the cymba conchae, sham stimulation to the scapha of the left ear. Two medical Ag/AgCl stimulation electrodes (4×4 mm) were mounted on a piece of silicone at a center-to-center distance of 1 cm. The electrodes were attached to the ear using a small amount of adhesive electrode cream (Natus Neurology, www.natus.com) and medical adhesive tape, if necessary. Direct current pulses were delivered using a medical stimulation device (Digitimer DS7, www.digitimer.com). Current intensity was set to 1 mA, delivered in 200 μ s pulses at 25 Hz. Stimulation was administered in blocks of 60 sec, each followed by a 30 sec break (during pre-task stimulation) or by a 180 sec MEG recording block. These parameters are within the range of standard parameters used in other tVNS studies (Badran et al., 2018; Frangos, Ellrich, & Komisaruk, 2015).

2.6. MEG measurement and analysis

MEG was recorded from 306 sensors (102 magnetometers and 204 planar gradiometers) from 102 head positions using a Neuromag Triux device (Elekta AB¹) at a sampling rate of 1000 Hz and an online band-pass filter (.01–330 Hz). Offline data analysis was carried out using the FieldTrip toolbox (Oostenveld, Fries, Maris, & Schoffelen, 2011) in Matlab 2018 (MathWorks²). Bad sensors (high noise level or flat) were identified by visual inspection, removed from the data and, for data visualization only, reconstructed using spline interpolation. Severely artifact-laden epochs were excluded from further analysis, based on visual inspection. Ocular and heart beat related artifacts were removed by means of independent component analysis (ICA). Data were visually inspected again, and segments with remaining gross artifacts were excluded.

¹ www.elekta.com.

² www.mathworks.com.

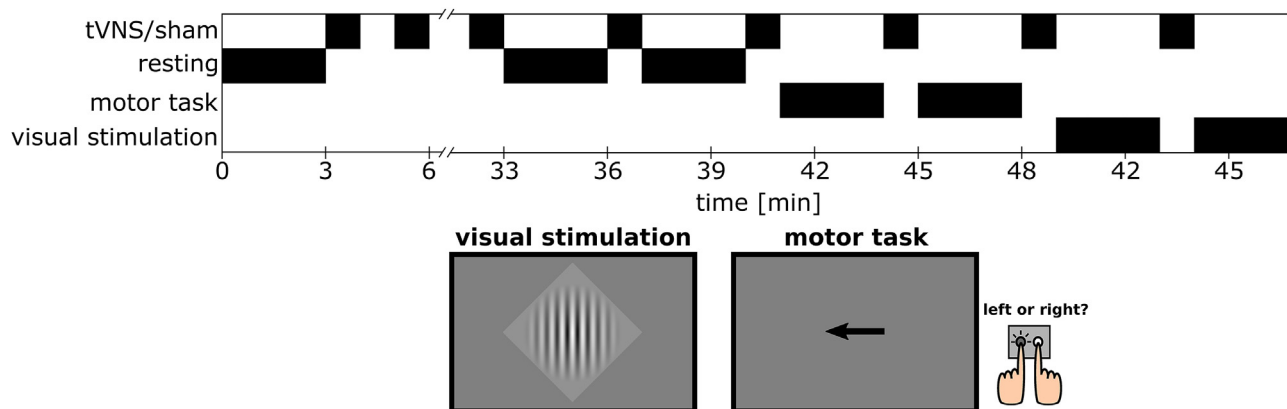


Fig. 1 – Experimental procedure. The order of the motor task and visual stimulation were counterbalanced across participants. Panels below: Illustration of experimental stimuli (not true to scale).

Participants were excluded from further analyses if more than half of the epochs in the motor task or more than half of the visual stimulation epochs or half of the resting-state recording time have to be excluded, or if they have no clear PMBD, PMBR, or visual gamma response, based on visual inspection and running t-tests against baseline, in one or both sessions. We excluded three participants from analysis of the motor task data, and five participants from analysis of the visual stimulation data.

Subsequently, MEG data were transformed to source space using linearly constrained minimum variance (LCMV) beamforming, resulting in source level epochs (Lithari, Sánchez-García, Ruhnu, & Weisz, 2016; Neuling et al., 2015). Briefly, individual structural magnetic resonance images where obtainable were aligned to the MEG space with the information from the head shapes. In case the individual MRI was not available we used the template MRI available in the Fieldtrip toolbox and morphed it to the individual head shapes using affine transformation. Then an equally spaced 1 cm grid in MNI space was warped to the individual brain volume. Using this MNI space grid (~3000 voxels) allowed for direct statistical comparisons of activity across participants. The aligned brain volumes were further used to create single-sphere head models and lead field matrices (Nolte, 2003). Together with the head model, the lead field matrix and the average covariance matrix beamformer filters for each grid point were calculated. These filters were subsequently multiplied with the sensor level epochs resulting in source level epochs.

A time-frequency analysis of source level data was carried out using Morlet wavelets. Center frequencies were logarithmically spaced between 1 and 64 Hz in steps of .125 octaves at a frequency resolution $f/\sigma_f = 6$, moving along the signal in steps of 50 msec. Resulting power estimates were baseline-normalized and converted to dB [$10 \cdot \log_{10}(\text{Power}/\text{Power}_{\text{baseline}})$]. For the resting-state measurement, the 3 min measurement prior to electrical stimulation served as baseline. For the motor task, pre-movement beta desynchronization (PMBD) and post-movement beta rebound (PMBR)

were assessed by subtracting \log_{10} -transformed source-space power in the contralateral motor cortex (virtual sensor at MNI coordinates $[-48, -8, 50]$ and $[48, -8, 50]$ ³ for left and right primary motor cortex, respectively) across the beta band (15–30 Hz) and over a time window between $-1.25 - .5$ sec relative to the button press (for PMBD) or between 1 and 1.75 sec (for PMBR) from time-averaged log-power over the entire trial ($-1.25 - 1.75$ sec). For the visual stimulation, we used a baseline of $-1 - 0$ sec relative to stimulus onset and compared it to the presentation time of the stimuli (0–1 sec). For analysis of visual stimulation data, we created virtual sensors at MNI coordinates $[-2, -80, 34]$, $[-28, -96, -6]$ and $[28, -96, -6]$ for central, left, and right primary visual cortex, respectively, and analyzed gamma power averaged across the three virtual sensors. For the analysis of resting and movement-related beta power, we averaged the baseline-corrected log-power values over beta frequencies (15–30 Hz), for the analysis of gamma power, we averaged over gamma frequencies (30–60 Hz). For event-related data from the motor task and visual stimulation, we additionally averaged over time bins and trials. To test for lateralization of tvNS effects, we computed lateralization indices as differences between resting beta log-power in the left and right hemisphere, and between PMBD and PMBR to left- and right-hand movements in the contralateral motor cortex, respectively. We calculated all lateralization indices such that hypotheses H_4 , H_{5A} and H_{5B} predict higher values for tvNS compared to sham (i.e., subtracting right hemisphere values from left hemisphere values for PMBD and PMBR, and vice versa for resting beta power).⁴

Resulting session-wise values for resting beta power, PMBD, PMBR, visual gamma response, and lateralization indices were compared between sham and tvNS sessions by

³ The MNI coordinates for the virtual sensors were not included in the stage 1 protocol. They were specified for increased transparency.

⁴ We further specified calculation of lat. indices compared to the stage 1 protocol.

means of paired-sample one tailed Bayesian t-tests using R and the BayesFactor package (Morey, Rouder, & Jamil, 2015). Based on previous literature, we expected \log_{10} -transformed spectral power values to have approximately normal distributions (Kiebel, Tallon-Baudry, & Friston, 2005), rendering the use of t-tests appropriate.⁵

2.7. Design analysis and interpretation plan

A recent study, though in a small sample, found that cervical tVNS increased beta and gamma power and decreased theta and alpha power (Lewine et al., 2018). This study reports, for the comparison between baseline-normalized beta power in the tVNS versus sham condition, a t-value of 2.64, which, given a sample size of 8 subjects in a within-subjects design, corresponds to an effect size of $d_z \sim .93$. Effects of similar magnitude have been found for peri-movement beta oscillations 3 h after administration of 15 mg tiagabine ($d_z \sim .81$, Muthukumaraswamy et al., 2013), and for alpha power following transcranial alternating current stimulation ($d_z \sim .86$, Zaehle, Rach, & Herrmann, 2010). Given a possible publication bias, we had a more conservative expectation to find effect sizes $d_z \sim .5$ for all our hypotheses. A simulation-based Bayes factor design analysis (Schönbrodt & Wagenmakers, 2018) found that given $d_z = .5$ and $n = 40$, Bayes factors conclusively favored the working hypothesis ($BF > 6$) 76.5% of the time for the simulated data. If necessary, sample size would have been increased until Bayes factors clearly favor either the null or working hypothesis for all hypotheses, up to a total sample size of 60 participants (120 experimental sessions), which we consider the maximum number of participants that is technically and economically feasible.

All hypotheses were tested by paired-sample Bayesian t-tests, as described above. The specific variables of interest for each hypothesis can be found in Table 1. If all of hypotheses H_1 – H_3 were confirmed, we would interpret this as a confirmation for an overall increase in GABAergic activity induced through tVNS. Conversely, if all respective null hypotheses were confirmed, we would conclude that tVNS has no effect on GABAergic activity in healthy individuals. If only some of the hypotheses were confirmed, we would conclude that tVNS has regionally or functionally selective effects on GABAergic activity. The strength of this conclusion would depend on whether or not tests for the non-confirmed hypotheses would have conclusive results (in favor of the respective null hypotheses).

Likewise, confirmation of hypotheses H_4 – H_5 would lead us to the conclusion that GABAergic modulation through tVNS occurs in a lateralized fashion, and a partial confirmation to the conclusion that lateralization is functionally specific.

This study was pre-registered with the Open Science Framework. The original proposal, including a design analysis and pilot data, can be found at <https://osf.io/xn47t/>.

⁵ In the stage 1 protocol, we had stated that we would use Gaussian priors for the t-tests. We were unaware, however, that the Bayesian t-test method has pre-defined (Jeffreys/Cauchy) priors, so that we were not at liberty to define our own. We have corrected this error.

Table 1 – Overview of variables to be tested for each hypothesis.

	Hypothesis	Variable of interest
H1	global resting-state beta power is increased during tVNS compared to sham.	Global beta power
H2A	peri-movement beta desynchronization (PMBD) in the motor cortex is stronger during tVNS compared to sham.	PMBD (averaged over left- and right-hand responses, from the contralateral motor cortices)
H2B	post-movement beta rebound (PMBR) in the motor cortex is weaker during tVNS compared to sham.	PMBR (averaged over left- and right-hand responses, from the contralateral motor cortices)
H3	gamma power response to visual stimulation in the visual cortex is stronger during tVNS.	Gamma power response from the visual cortex
H4	The tVNS effect on resting-state beta power will be stronger in the right (contralateral) hemisphere.	Lateralization index for global beta power
H5A	The tVNS effect on PMBD will be stronger in the right (contralateral) hemisphere for left-hand responses compared to PMBD in the left motor cortex for right-hand responses.	Lateralization index for PMBD
H5B	The tVNS effect on PMBR will be stronger in the right (contralateral) hemisphere for left-hand responses compared to PMBR in the left motor cortex for right-hand responses.	Lateralization index for PMBR

The Matlab and R code used for data analysis will be made available on Github (<https://github.com/mkeute/tVNS-oscillations>). MEG data will be made available on Harvard Dataverse (<https://doi.org/10.7910/DVN/OD0SU0>).

3. Results

Resting spectral power in the theta band (~8 Hz) and in the high beta band (~25 Hz) was reduced pre-to-post-stimulation, across sham and tVNS sessions (Confidence interval does not overlap zero, see Fig. 2B). Mean beta power was numerically lower in tVNS compared to sham sessions, contrary to our hypothesis. Accordingly, we found substantial evidence against H_1 ($t_{40} = -1.98$, $BF_{01} = 16.4$). Furthermore, lateralization of beta power, i.e., power difference between left- and right-hemisphere sensors, was numerically lower in tVNS sessions, therefore, we found substantial evidence against H_4 ($t_{40} = -.60$, $BF_{01} = 8.6$).

Mean PMBD across response hands was $-.37$ dB in tVNS as well as sham sessions (see Fig. 3). We found substantial evidence against H_{2A} ($t_{37} = .24$, $BF_{01} = 6.8$). Furthermore, we found no effect of tVNS on PMBD lateralization, i.e., substantial evidence against H_{5A} ($t_{37} = -.53$, $BF_{01} = 8.2$).

Mean PMBR across response hands was $.38$ dB in tVNS and $.36$ dB in sham sessions. We found substantial evidence against H_{2B} ($t_{37} = .24$, $BF_{01} = 8.7$). Furthermore, we found no effect of tVNS on PMBR lateralization, i.e., substantial evidence against H_{5B} ($t_{37} = -.68$, $BF_{01} = 8.9$).

Mean gamma response was $.1$ dB in tVNS as well as sham sessions (see Fig. 4). We found substantial evidence against H_3 ($t_{35} = -.42$, $BF_{01} = 7.6$).

4. Discussion

In this study, our goal was to better understand the cortical dynamics induced by tVNS. Even though the neuromodulatory effects of VNS have been shown by a range of animal studies, especially with respect to the locus coeruleus and NE

transmission, and, to a lesser extent, inhibitory GABAergic transmission, the human VNS literature has remained rather inconsistent. For instance, no robust effect of tVNS on non-invasive markers of NEergic neuromodulation (e.g., pupil dilation; Keute, Demirezen, Graf, Mueller, & Zaehle, 2019; Warren et al., 2019; Burger, Van der Does, Brosschot, & Verkuil, 2020; Sharon, Fahoum, & Nir, 2021) and peripheral vagus-associated activation (e.g., heart rate variability; Clancy et al., 2014; De Couck et al., 2017; Borges, Laborde, & Raab, 2019) has been shown, even though the anatomical and physiological underpinnings of VNS would predict such effects. In our study, we tested for effects of tVNS on oscillatory markers for cortical GABAergic activity. We hypothesized that tVNS would impact resting beta power, movement-related beta power deflections, and visual gamma responses. Furthermore, based on tentative evidence from previous studies, we predicted the beta effects to be lateralized, i.e., stronger in the contralateral hemisphere relative to the stimulated ear. Our data provide substantial evidence against all hypotheses: we found that tVNS did not modulate the beta and gamma power markers, nor was there a lateralized effect of tVNS.

To the best of our knowledge, only one previous study has examined effects of non-invasive (cervical) VNS on spectral power of brain oscillations at rest across several frequency bands (Lewine et al., 2018). This study reported diminished theta and alpha power as well as increased beta and gamma power at selected EEG electrodes, both compared to sham and baseline. With respect to the theta band, our data show some compatibility with these findings in that we found resting theta power to be diminished pre-to-post-stimulation, albeit not between tVNS and sham. However, none of the other findings are in line with our data, which may be partially accounted for by methodical differences between both studies (cervical vs auricular stimulation; EEG vs MEG; resting power from single electrodes vs global resting power).

Besides oscillatory power at rest, we investigated characteristic oscillations of the active primary motor and primary visual cortex at source level. We predicted specific, GABA-associated changes in beta and gamma power deflections by tVNS, respectively, but did not find any.

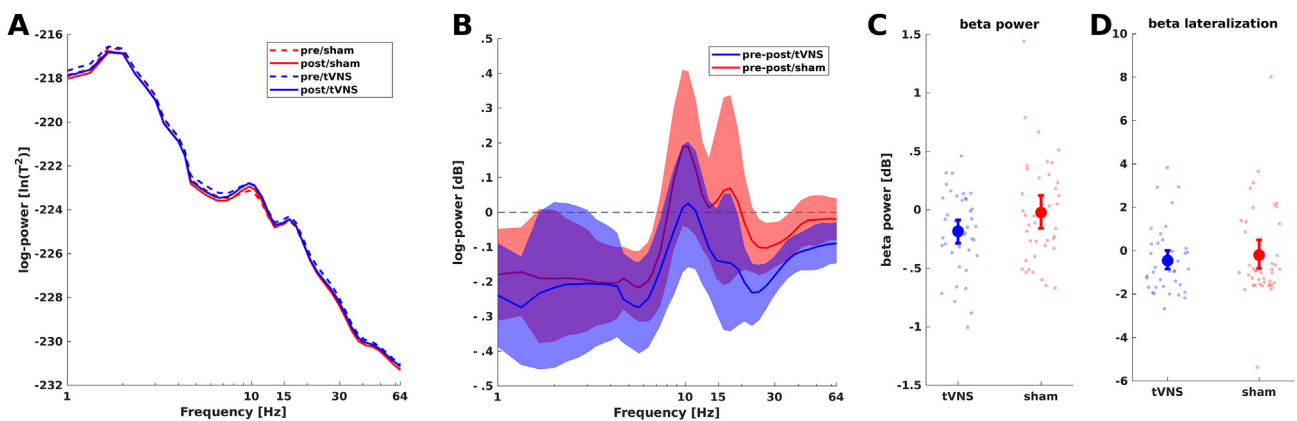


Fig. 2 – A: Log-transformed mean resting spectra pre- and post-sham/tVNS stimulation. Spectra were calculated for each sensor and averaged across sensors and subjects. B: Difference between pre- and post-stimulation spectra with bootstrapped 95% CI. C: Subject-wise pre-post beta power (15–30 Hz) power difference. D: Beta power lateralization.

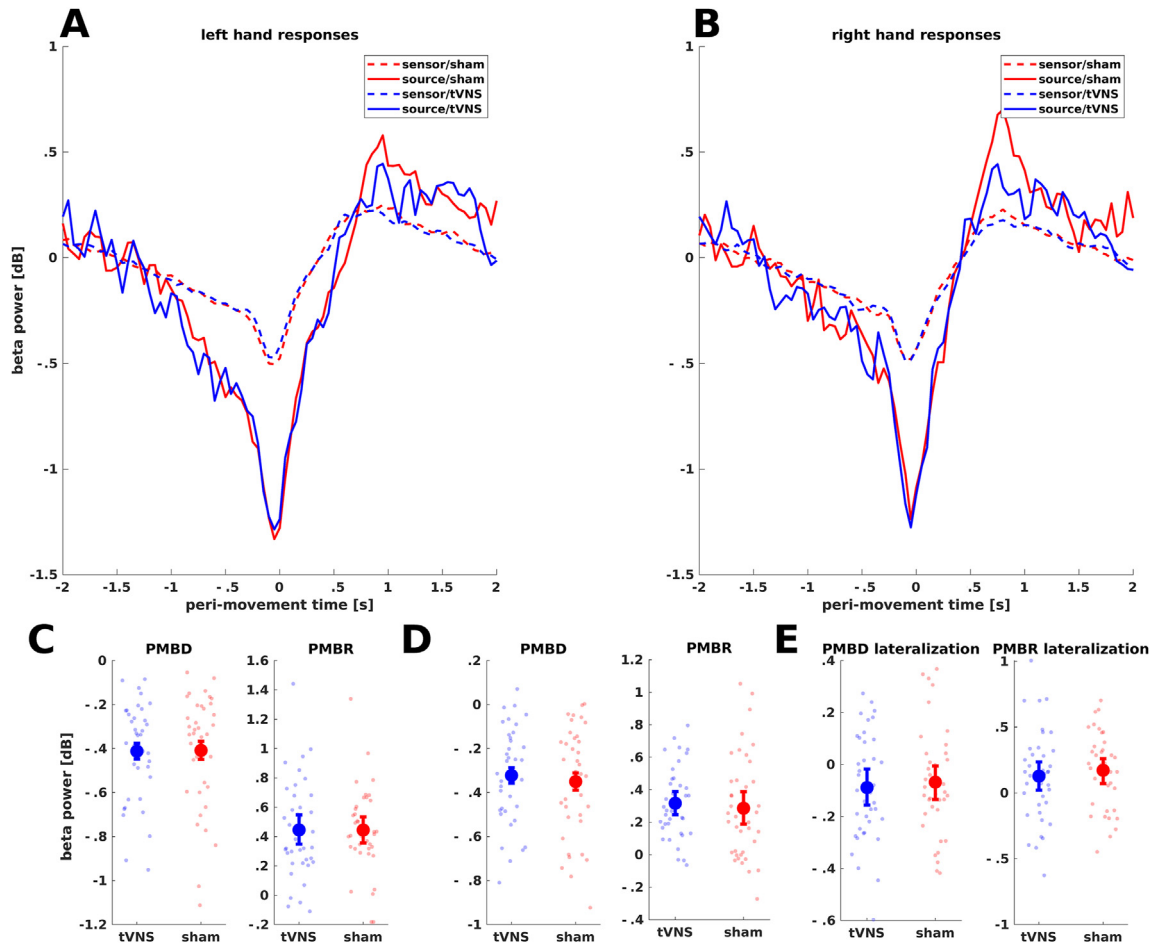


Fig. 3 – A: Time course of beta power around left-hand responses in the motor task. Dashed lines: Power averaged across all sensors; solid lines: Power from virtual sensor in the contralateral primary motor cortex. For visualization, data were baseline corrected to a period from -2 to -1 sec. B: Same for right-hand responses. C: Subject-wise extracted PMBD and PMBR values for left-hand responses, baseline-corrected for the time windows specified in the Methods section, and bootstrapped 95% CI. D: Same for right-hand responses. E: PMBD and PMBR lateralization with bootstrapped 95% CI.

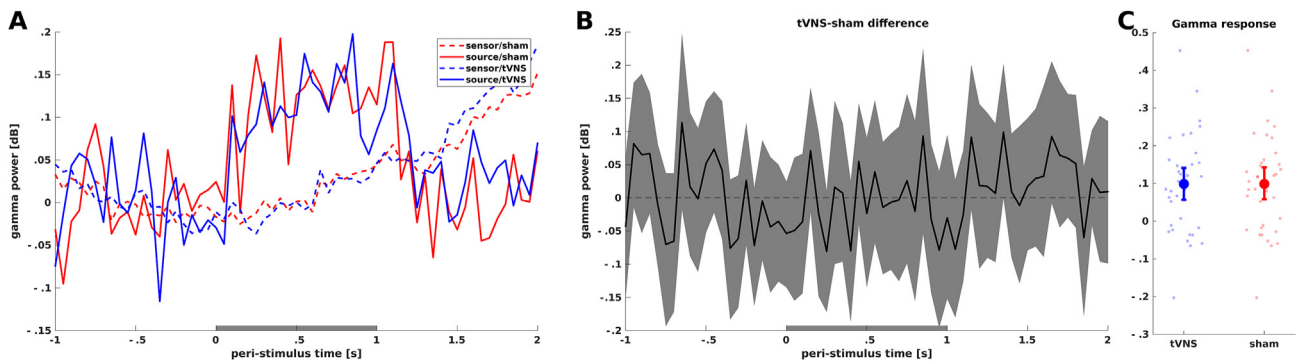


Fig. 4 – A: Time course of gamma power around visual stimulation. Dashed lines: Power averaged across all sensors; solid lines: Power from virtual sensors in the primary visual cortex. Grey horizontal bar indicates time of stimulus presentation. B: tVNS-sham difference with bootstrapped 95% CI. C: Subject-wise mean gamma response during stimulus presentation.

Overall, our findings do not support any short-term effect of tVNS on GABAergic cortical activity in healthy subjects. Previous studies had reported increases in extrasynaptic GABA concentration and GABA receptor density following invasive VNS in epilepsy patients (Ben-Menachem et al., 1995; Marrosu et al., 2003). Our findings suggest that these changes probably reflect a neuroplastic adaptation triggered by long-term VNS rather than a fast upregulation of cortical GABA levels following VNS treatment onset. Furthermore, the role of GABA transmission in epileptogenesis is more complex than could be described in terms of ‘too much’ or ‘not enough’: the postsynaptic effect of GABAergic interneurons is partially reversed in epileptic brains, i.e., excitatory rather than inhibitory, so that an increase in GABA transmission, without further synaptic reorganization, could even promote, rather than alleviate, seizures (Kaila, Ruusuvuori, Seja, Voipio, & Puskarjov, 2014). In light of this, it appears plausible that VNS helps the epileptic brain initiate a specific, plastic process to revert pathological GABA signaling, rather than just acting by a global GABA increase.

On the other hand, two previous studies (Capone et al., 2015; Keute et al., 2018) reported behavioral and electrophysiological effects of tVNS that could be accounted for by a modulation in GABA transmission in the motor cortex. Both studies also provided tentative evidence for a lateralized tVNS effect, but did not formally test for such an effect. Neither the GABAergic mechanism nor the lateralized effect was confirmed by the present study. Importantly, the assumed GABAergic mechanisms of both studies had opposite signs (Keute et al., 2018 was more compatible with a GABA decrease; Capone et al., 2015 was more compatible with a GABA increase), so it appears likely that other, possibly GABA-unrelated mechanisms underlie the findings of both studies. Furthermore, our findings do not confirm any lateralization of effects. Of note, stimulation parameters in both previous studies differed from those in the present study. Specifically, in the previous studies, a higher stimulation intensity (8 mA) was used, and stimulation was intermittent rather than continuous. Therefore, comparability between the studies might be limited, even though there is no apparent reason to expect a systematic bias with respect to GABAergic neuro-modulatory effects.

It is currently one of the central challenges in VNS research to understand why treatment responses are so variable between studies, subjects, and within subjects, and to identify short-term biomarkers that allow for a reliable prediction of long-term treatment response and titration of stimulation parameters. GABA-associated brain oscillations appeared to be a promising marker, especially because of the GABAergic mediation of anti-epileptic VNS effects (Ben-Menachem et al., 1995; Marrosu et al., 2003), but this prediction did not hold true. This is not to say, however, that readouts from ongoing MEG or EEG are altogether unsuitable as VNS biomarkers. A growing number of studies have shown behavioral, cognitive and neurological VNS effects, and it appears likely that these effects are systematically reflected in altered brain activity patterns. This might require using more involved methods, e.g., connectivity or network metrics, as some first studies have done to predict long-term clinical outcomes of invasive VNS (Babajani-Feremi, Noorizadeh, Mudigoudar, & Wheless,

2018; Mithani et al., 2019). It is important to note that in order to qualify as a predictive biomarker, a physiological readout would not only have to be systematically changed by the stimulation, but the readout (or its change) would also need to be reliably correlated to a clinical, physiological, or behavioral outcome of the stimulation (Burger, D’Agostini, Verkuil, & Van Diest, 2020; Keute, Machetanz, Berelidze, Guggenberger, & Gharabaghi, 2021). Furthermore, specific patterns of brain oscillations in clinical populations will have to be taken into account, as they might interact with oscillatory VNS markers (cf. Marrosu et al., 2005). Overall, we are confident that predictive markers will also be identifiable for short-term tVNS, and we encourage the use of our data, which will be made available for download, for further exploration.

Declaration of competing interest

All authors declare no conflict of interest.

Author contributions

MK designed research, analyzed data and wrote the manuscript. CW collected data and reviewed the manuscript. PR designed research, analyzed data and reviewed the manuscript. TZ designed research, supervised the study, and reviewed the manuscript.

Open practices

The study in this article earned Open Data, Open Materials and Preregistered badges for transparent practices. Data and materials for this study can be found at <https://github.com/mkeute/tVNS-oscillations> and <https://doi.org/10.7910/DVN/OD0SU0>.

Acknowledgements

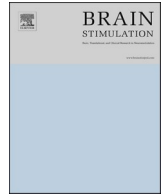
This study was supported by the federal state of Saxony-Anhalt and the European Regional Development Fund in the Center for Behavioral Brain Sciences (CBBS, ZS/2016/04/78113).

REFERENCES

- Assenza, G., Campana, C., Colicchio, G., Tombini, M., Assenza, F., Di Pino, G., et al. (2017, July 1). Transcutaneous and invasive vagal nerve stimulations engage the same neural pathways: In-vivo human evidence. *Brain Stimulation*, 10, 853–854. <https://doi.org/10.1016/j.brs.2017.03.005>
- Babajani-Feremi, A., Noorizadeh, N., Mudigoudar, B., & Wheless, J. W. (2018). Predicting seizure outcome of vagus nerve stimulation using MEG-based network topology. *NeuroImage: Clinical*, 19, 990–999.
- Badran, B. W., Dowdle, L. T., Mithoefer, O. J., LaBate, N. T., Coatsworth, J., Brown, J. C., et al. (2018). Neurophysiologic effects of transcutaneous auricular vagus nerve stimulation

- (taVNS) via electrical stimulation of the tragus: A concurrent taVNS/fMRI study and review. *Brain Stimulation*. <https://doi.org/10.1016/j.brs.2017.12.009>
- Barbanti, P., Grazi, L., Egeo, G., Padovan, A. M., Liebler, E., & Bussone, G. (2015). Non-invasive vagus nerve stimulation for acute treatment of high-frequency and chronic migraine: An open-label study. *The Journal of Headache and Pain*, 16(1), 61.
- Bauer, S., Baier, H., Baumgartner, C., Bohlmann, K., Fauser, S., Graf, W., et al. (2016). Transcutaneous vagus nerve stimulation (tVNS) for treatment of drug-resistant epilepsy: A randomized, double-blind clinical trial (cMPsE02). *Brain Stimulation*, 9(3), 356–363.
- Baulac, S., Huberfeld, G., Gourfinkel-An, I., Mitropoulou, G., Beranger, A., Prud'homme, J.-F., et al. (2001). First genetic evidence of GABA A receptor dysfunction in epilepsy: A mutation in the $\gamma 2$ -subunit gene. *Nature Genetics*, 28(1), 46.
- Ben-Menachem, E., Hamberger, A., Hedner, T., Hammond, E. J., Uthman, B. M., Slater, J., et al. (1995). Effects of vagus nerve stimulation on amino acids and other metabolites in the CSF of patients with partial seizures. *Epilepsy Research*, 20(3), 221–227. [https://doi.org/10.1016/0920-1211\(94\)00083-9](https://doi.org/10.1016/0920-1211(94)00083-9)
- Berridge, C. W., & Waterhouse, B. D. (2003). The locus coeruleus-noradrenergic system: Modulation of behavioral state and state-dependent cognitive processes. *Brain Research Reviews*, 42(1), 33–84. [https://doi.org/10.1016/S0165-0173\(03\)00143-7](https://doi.org/10.1016/S0165-0173(03)00143-7)
- Borges, U., Laborde, S., & Raab, M. (2019). Influence of transcutaneous vagus nerve stimulation on cardiac vagal activity: Not different from sham stimulation and no effect of stimulation intensity. *Plos One*, 14(10), Article e0223848.
- Boy, F., Evans, C. J., Edden, R. A. E., Singh, K. D., Husain, M., & Sumner, P. (2010). Individual differences in subconscious motor control predicted by GABA concentration in SMA. *Current Biology*, 20(19), 1779–1785. <https://doi.org/10.1016/j.cub.2010.09.003>
- Brozoski, T. J., Spires, T. J. D., & Bauer, C. A. (2007). Vigabatrin, a GABA transaminase inhibitor, reversibly eliminates tinnitus in an animal model. *Journal of the Association for Research in Otolaryngology: JARO*, 8(1), 105–118.
- Burger, A. M., D'Agostini, M., Verkuil, B., & Van Diest, I. (2020a). Moving beyond belief: A narrative review of potential biomarkers for transcutaneous vagus nerve stimulation. *Psychophysiology*, 57(6), Article e13571.
- Burger, A. M., Van der Does, W., Brosschot, J. F., & Verkuil, B. (2020b). From ear to eye? No effect of transcutaneous vagus nerve stimulation on human pupil dilation: A report of three studies. *Biological psychology*, 152, 107863.
- Capone, F., Assenza, G., Di Pino, G., Musumeci, G., Ranieri, F., Florio, L., et al. (2015). The effect of transcutaneous vagus nerve stimulation on cortical excitability. *Journal of Neural Transmission*, 122(5), 679–685. <https://doi.org/10.1007/s00702-014-1299-7>
- Carpenter, L. L., Moreno, F. A., Kling, M. A., Anderson, G. M., Regenold, W. T., Labiner, D. M., et al. (2004). Effect of vagus nerve stimulation on cerebrospinal fluid monoamine metabolites, norepinephrine, and gamma-aminobutyric acid concentrations in depressed patients. *Biological Psychiatry*, 56(6), 418–426. <https://doi.org/10.1016/j.biopsych.2004.06.025>
- Clancy, J. A., Deuchars, S. A., & Deuchars, J. (2013). The wonders of the Wanderer. *Experimental Physiology*, 98(1), 38–45. <https://doi.org/10.1113/expphysiol.2012.064543>
- Clancy, J. A., Mary, D. A., Witte, K. K., Greenwood, J. P., Deuchars, S. A., & Deuchars, J. (2014). Non-invasive vagus nerve stimulation in healthy humans reduces sympathetic nerve activity. *Brain stimulation*, 7(6), 871–877.
- De Couck, M., Cserjesi, R., Caers, R., Zijlstra, W. P., Widjaja, D., Wolf, N., & Gidron, Y. (2017). Effects of short and prolonged transcutaneous vagus nerve stimulation on heart rate variability in healthy subjects. *Autonomic Neuroscience*, 203, 88–96.
- Edden, R. A. E., Muthukumaraswamy, S. D., Freeman, T. C. A., & Singh, K. D. (2009). Orientation discrimination performance is predicted by GABA concentration and gamma oscillation frequency in human primary visual cortex. *Journal of Neuroscience*, 29(50), 15721–15726. <https://doi.org/10.1523/JNEUROSCI.4426-09.2009>
- Fang, J., Rong, P., Hong, Y., Fan, Y., Liu, J., Wang, H., et al. (2016). Transcutaneous vagus nerve stimulation modulates default mode network in major depressive disorder. *Biological Psychiatry*, 79(4), 266–273. <https://doi.org/10.1016/j.biopsych.2015.03.025>
- Frangos, E., Ellrich, J., & Komisaruk, B. R. (2015). Non-invasive access to the vagus nerve central projections via electrical stimulation of the external ear: fMRI evidence in humans. *Brain Stimulation*, 8(3). <https://doi.org/10.1016/j.brs.2014.11.018>
- Gaetz, W., Edgar, J. C., Wang, D. J., & Roberts, T. P. L. (2011). Relating MEG measured motor cortical oscillations to resting γ -aminobutyric acid (GABA) concentration. *Neuroimage*, 55(2), 616–621.
- Greenblatt, D. J., Ehrenberg, B. L., Gunderman, J., Locniskar, A., Scavone, J. M., Harmatz, J. S., et al. (1989). Pharmacokinetic and electroencephalographic study of intravenous diazepam, midazolam, and placebo. *Clinical Pharmacology and Therapeutics*, 45(4), 356–365.
- Hall, S. D., Barnes, G. R., Furlong, P. L., Seri, S., & Hillebrand, A. (2010). Neuronal network pharmacodynamics of GABAergic modulation in the human cortex determined using pharmacomagnetoencephalography. 594 pp. 581–594). <https://doi.org/10.1002/hbm.20889> (December 2008).
- He, W., Jing, X.-H., Zhu, B., Zhu, X.-L., Li, L., Bai, W.-Z., et al. (2013). The auriculo-vagal afferent pathway and its role in seizure suppression in rats. *BMC Neuroscience*, 14, 1. <https://doi.org/10.1186/1471-2202-14-85>
- Kaczmarczyk, R., Tejera, D., Simon, B. J., & Heneka, M. T. (2018). Microglia modulation through external vagus nerve stimulation in a murine model of Alzheimer's disease. *Journal of Neurochemistry*, 146(1), 76–85.
- Kaila, K., Ruusuvoori, E., Seja, P., Voipio, J., & Puskarjov, M. (2014). GABA actions and ionic plasticity in epilepsy. *Current opinion in neurobiology*, 26, 34–41.
- Keute, M., Demirezen, M., Graf, A., Mueller, N. G., & Zaehle, T. (2019). No modulation of pupil size and event-related pupil response by transcutaneous auricular vagus nerve stimulation (taVNS). *Scientific reports*, 9(1), 1–10.
- Keute, M., Machetanz, K., Berelidze, L., Guggenberger, R., & Gharabaghi, A. (2021). Neuro-cardiac coupling predicts transcutaneous auricular vagus nerve stimulation effects. *Brain stimulation*, 14(2), 209–216.
- Keute, M., Ruhnau, P., Heinze, H.-J., & Zaehle, T. (2018). Behavioral and electrophysiological evidence for GABAergic modulation through transcutaneous vagus nerve stimulation. *Clinical Neurophysiology*, 129(9).
- Kiebel, S. J., Tallon-Baudry, C., & Friston, K. J. (2005). Parametric analysis of oscillatory activity as measured with EEG/MEG. *Human Brain Mapping*, 26(3), 170–177.
- Lehtimäki, J., Hyvärinen, P., Ylikoski, M., Bergholm, M., Mäkelä, J. P., Aarnisalo, A., et al. (2013). Transcutaneous vagus nerve stimulation in tinnitus: A pilot study. *Acta Otolaryngologica*, 133(February), 378–382. <https://doi.org/10.3109/00016489.2012.750736>
- Lewine, J. D., Paulson, K., Banger, N., & Simon, B. J. (2018). Exploration of the impact of brief noninvasive vagal nerve stimulation on EEG and event-related potentials. *Neuromodulation: Technology at the Neural Interface*, 22(5).

- Lithari, C., Sánchez-García, C., Ruhнау, P., & Weisz, N. (2016). Large-scale network-level processes during entrainment. *Brain Research*, 1635, 143–152.
- Lu, X., Hong, Z., Tan, Z., Sui, M., Zhuang, Z., Liu, H., et al. (2017). Nicotinic acetylcholine receptor alpha7 subunit mediates vagus nerve stimulation-induced neuroprotection in acute permanent cerebral ischemia by a7nAChR/JAK2 pathway. *Medical Science Monitor: International Medical Journal of Experimental and Clinical Research*, 23, 6072.
- Magis, D., Gérard, P., & Schoenen, J. (2013). Transcutaneous vagus nerve stimulation (tVNS) for headache prophylaxis: Initial experience. *The Journal of Headache and Pain*, 14(S1), P198.
- Marrosu, F., Santoni, F., Puligheddu, M., Barberini, L., Maleci, A., Ennas, F., et al. (2005). Increase in 20–50 Hz (gamma frequencies) power spectrum and synchronization after chronic vagal nerve stimulation. *Clinical Neurophysiology*, 116(9), 2026–2036.
- Marrosu, F., Serra, A., Maleci, A., Puligheddu, M., Biggio, G., & Piga, M. (2003). Correlation between GABAA receptor density and vagus nerve stimulation in individuals with drug-resistant partial epilepsy. *Epilepsy Research*, 55(1–2), 59–70. [https://doi.org/10.1016/S0920-1211\(03\)00107-4](https://doi.org/10.1016/S0920-1211(03)00107-4)
- Martínez-Vargas, D., Valdés-Cruz, A., Magdaleno-Madriral, V., Fernández-Mas, R., & Almazán-Alvarado, S. (2017). Effect of electrical stimulation of the nucleus of the solitary tract on electroencephalographic spectral power and the sleep–wake cycle in freely moving cats. *Brain Stimulation*, 10(1), 116–125.
- Mithani, K., Mikhail, M., Morgan, B. R., Wong, S., Weil, A. G., Deschenes, S., & Ibrahim, G. M. (2019). Connectomic profiling identifies responders to vagus nerve stimulation. *Annals of neurology*, 86(5), 743–753.
- Möhler, H. (2012). The GABA system in anxiety and depression and its therapeutic potential. *Neuropharmacology*, 62(1), 42–53.
- Morey, R. D., Rouder, J. N., & Jamil, T. (2015). BayesFactor: Computation of Bayes factors for common designs. *R Package*, 9, 2014. Version 0.9.
- Muthukumaraswamy, S. D., Edden, R. A. E., Jones, D. K., Swettenham, J. B., & Singh, K. D. (2009). Resting GABA concentration predicts peak gamma frequency and fMRI amplitude in response to visual stimulation in humans. *Proceedings of the National Academy of Sciences*, 106(20), 8356–8361.
- Muthukumaraswamy, S. D., Myers, J. F. M., Wilson, S. J., Nutt, D. J., Lingford-Hughes, A., Singh, K. D., et al. (2013). The effects of elevated endogenous GABA levels on movement-related network oscillations. *Neuroimage*, 66, 36–41.
- Neuling, T., Ruhнау, P., Fusca, M., Demarchi, G., Herrmann, C. S., & Weisz, N. (2015). Shed light on the black box: Using MEG to recover brain activity during tACS. *Brain Stimulation: Basic, Translational, and Clinical Research in Neuromodulation*, 8(2), 381–382.
- Nolte, G. (2003). The magnetic lead field theorem in the quasi-static approximation and its use for magnetoencephalography forward calculation in realistic volume conductors. *Physics in Medicine and Biology*, 48(22), 3637.
- Nutt, D., Wilson, S., Lingford-Hughes, A., Myers, J., Papadopoulos, A., & Muthukumaraswamy, S. (2015). Differences between magnetoencephalographic (MEG) spectral profiles of drugs acting on GABA at synaptic and extrasynaptic sites: A study in healthy volunteers. *Neuropharmacology*, 88, 155–163.
- Oostenveld, R., Fries, P., Maris, E., & Schoffelen, J.-M. (2011). FieldTrip: Open source software for advanced analysis of MEG, EEG, and invasive electrophysiological data. *Computational Intelligence and Neuroscience*, 2011, 1.
- Raedt, R., Clinckers, R., Mollet, L., Vonck, K., El Tahry, R., Wyckhuys, T., et al. (2011). Increased hippocampal noradrenaline is a biomarker for efficacy of vagus nerve stimulation in a limbic seizure model. *Journal of Neurochemistry*, 117(3), 461–469. <https://doi.org/10.1111/j.1471-4159.2011.07214.x>
- Ruffoli, R., Giorgi, F. S., Pizzanelli, C., Murri, L., Paparelli, A., & Fornai, F. (2011). The chemical neuroanatomy of vagus nerve stimulation. *Journal of Chemical Neuroanatomy*, 42(4), 288–296. <https://doi.org/10.1016/j.jchemneu.2010.12.002>
- Schönbrodt, F. D., & Wagenmakers, E.-J. (2018). Bayes factor design analysis: Planning for compelling evidence. *Psychonomic Bulletin & Review*, 25(1), 128–142.
- Sharon, O., Fahoum, F., & Nir, Y. (2021). Transcutaneous vagus nerve stimulation in humans induces pupil dilation and attenuates alpha oscillations. *Journal of Neuroscience*, 41(2), 320–330.
- Stagg, C. J., Bestmann, S., Constantinescu, A. O., Moreno Moreno, L., Allman, C., Mekle, R., et al. (2011). Relationship between physiological measures of excitability and levels of glutamate and GABA in the human motor cortex. *The Journal of Physiology*, 589(23), 5845–5855. <https://doi.org/10.1113/jphysiol.2011.216978>
- Stefan, H., Kreiselmeyer, G., Kerling, F., Kurzbuch, K., Rauch, C., Heers, M., et al. (2012). Transcutaneous vagus nerve stimulation (t-VNS) in pharmacoresistant epilepsies: A proof of concept trial. *Epilepsia*, 53(7), e115–e118.
- Toussay, X., Basu, K., Lacoste, B., & Hamel, E. (2013). Locus coeruleus stimulation recruits a broad cortical neuronal network and increases cortical perfusion. *Journal of Neuroscience*, 33(8), 3390–3401.
- Trevizol, A. P., Taiar, I., Barros, M. D., Liquidatto, B., Cordeiro, Q., & Shiozawa, P. (2015). Transcutaneous vagus nerve stimulation (tVNS) protocol for the treatment of major depressive disorder: A case study assessing the auricular branch of the vagus nerve. *Epilepsy & Behavior*, 53, 166–167.
- van Lier, H., Drinkenburg, W. H. I. M., van Eeten, Y. J. W., & Coenen, A. M. L. (2004). Effects of diazepam and zolpidem on EEG beta frequencies are behavior-specific in rats. *Neuropharmacology*, 47(2), 163–174.
- Ventura-Bort, C., Wirkner, J., Genheimer, H., Wendt, J., Hamm, A. O., & Weymar, M. (2018). Effects of transcutaneous vagus nerve stimulation (tVNS) on the P300 and alpha-amylase level: A pilot study. *Frontiers in Human Neuroscience*, 12. <https://doi.org/10.3389/fnhum.2018.00202>
- Ventureyra, E. C. (2000). Transcutaneous vagus nerve stimulation for partial onset seizure therapy. A new concept. *Child's Nervous System : ChNS : Official Journal of the International Society for Pediatric Neurosurgery*, 16(2), 101–102. <https://doi.org/10.1007/s003810050021>
- Walker, B. R., Easton, A., & Gale, K. (1999). Regulation of limbic motor seizures by GABA and glutamate transmission in nucleus tractus solitarius. *Epilepsia*, 40(8), 1051–1057.
- Warren, C. M., Tona, K. D., Ouwerkerk, L., Van Paridon, J., Poletiek, F., van Steenberghe, H., et al. (2019). The neuromodulatory and hormonal effects of transcutaneous vagus nerve stimulation as evidenced by salivary alpha amylase, salivary cortisol, pupil diameter, and the P3 event-related potential. *Brain Stimulation*, 12(3), 635–642.
- Woodbury, J. W., & Woodbury, D. M. (1991). Vagal stimulation reduces the severity of maximal electroshock seizures in intact rats: Use of a cuff electrode for stimulating and recording. *Pacing and Clinical Electrophysiology*, 14(1), 94–107.
- Xiong, J., Xue, F. S., Liu, J. H., Xu, Y. C., Liao, X., Zhang, Y. M., et al. (2009). Transcutaneous vagus nerve stimulation may attenuate postoperative cognitive dysfunction in elderly patients. *Medical Hypotheses*, 73(6), 938–941.
- Zaehle, T., Rach, S., & Herrmann, C. S. (2010). Transcranial alternating current stimulation enhances individual alpha activity in human EEG. *Plos One*, 5(11), Article e13766. <https://doi.org/10.1371/journal.pone.0013766>



Effects of transcutaneous auricular vagus nerve stimulation paired with tones on electrophysiological markers of auditory perception

Katharina S. Rufener^{a,c,*}, Christian Wienke^{b,1}, Alena Salanje^b, Aiden Haghikia^{b,c,d}, Tino Zaehle^{b,c}

^a Department of Child and Adolescent Psychiatry and Psychotherapy, Otto-von-Guericke-University Magdeburg, Germany

^b Department of Neurology, Otto-von-Guericke-University Magdeburg, Germany

^c Center for Behavioral Brain Sciences (CBBS), Otto-von-Guericke-University Magdeburg, Germany

^d German Center for Neurodegenerative Diseases (DZNE) Magdeburg, Germany

ARTICLE INFO

Keywords:

Transcutaneous vagus nerve stimulation
Auditory cortex
Tone pairing

ABSTRACT

Background: Transcutaneous auricular vagus nerve stimulation (taVNS) has been introduced as a non-invasive alternative to invasive vagus nerve stimulation (iVNS). While iVNS paired with tones has been highlighted as a potential effective therapy for the treatment of auditory disorders such as tinnitus, there is still scarce data available confirming the efficacy of non-invasive taVNS. Here, we assessed the effect of taVNS paired with acoustic stimuli on sensory-related electrophysiological responses.

Methods: A total of 22 healthy participants were investigated with a taVNS tone-pairing paradigm using a within-subjects design. In a single session pure tones paired with either active taVNS or sham taVNS were repeatedly presented. Novel tones without electrical stimulation served as control condition. Auditory event related potentials and auditory cortex oscillations were compared before and after the tone pairing procedure between stimulation conditions.

Results: From pre to post pairing, we observed a decrease in the N1 amplitude and in theta power to tones paired with sham taVNS while these electrophysiological measures remained stable for tones paired with active taVNS a pattern mirroring auditory sensory processing of novel, unpaired control tones.

Conclusion: Our results demonstrate the efficacy of a short-term application of non-invasive taVNS to modulate auditory processing in healthy individuals and, thereby, have potential implications for interventions in auditory processing deficits.

1. Introduction

Electrical stimulation of the vagus nerve applied in pharmacoresistant epilepsy and depression has been demonstrated to reduce the disease-related symptoms [1]. Although the precise neurophysiological mechanisms underlying these therapeutic effects are still not fully understood, it is suggested that vagus nerve stimulation (VNS) acts via afferent projections to the nucleus of the solitary tract from which there are projections to subcortical structures including the nucleus basalis, the locus coeruleus, and the dorsal raphe nuclei [2]. Thereby, VNS affects excitatory neurotransmitter systems related to these subcortical structures and, finally, the release of mainly norepinephrine and serotonin to various brain structures including the thalamus, the cerebellum,

and the neocortex [3,4]. Additionally, VNS may also activate inhibitory mechanisms via gamma-aminobutyric acid (GABA) release [5,6]. Since the availability of neurotransmitters in the neocortex is critical in sensory perception and cognition VNS has also been shown to affect behavior in the animal model [7] and in human patients [8–11]. The main drawback of VNS is, however, its inherently invasive nature as well as the risks and costs associated with the necessary surgical implantation [12,13].

Transcutaneous auricular vagus nerve stimulation (taVNS) has been introduced as a non-invasive alternative to VNS [14,15]. TaVNS applies electrical pulses to the auricular branch of the vagus nerve via electrodes placed at the outer ear, i.e. the cymba concha or the tragus [4,16]. Functional magnetic resonance imaging (fMRI) has demonstrated that

* Corresponding author. Department of Child and Adolescent Psychiatry and Psychotherapy, Otto-von-Guericke-University Magdeburg, Germany.

E-mail address: katharina.rufener@med.ovgu.de (K.S. Rufener).

¹ These authors contributed equally to the publication.

taVNS can stimulate the “classical” central vagal projections in humans [15] and that taVNS-evoked effects on perception and cognition are most likely caused by increased norepinephrine-availability in the neocortex [17]. However, despite its sparse, easy, and straight forward characteristic there is only scarce evidence on the efficacy of taVNS to modulate sensory perception in human subjects, and, accordingly, its efficacy is still under debate.

An established paradigm to assess the impact of a neuromodulator on functional properties of sensory cortex areas relies on the temporal coupling of a sensory stimulus and a neuromodulator [18]. In rodents, pairing acoustic stimuli with VNS resulted in structural and functional changes in the auditory system and, on the behavioral level, in related sensory perception [12,13,19–22]. In order to shed more light on the efficacy of taVNS in healthy human participants we here investigated its effect on objective electrophysiological markers of auditory sensory perception, i.e. the N1 amplitude. In concrete, we adapted a VNS tone-pairing paradigm established in the animal research [19] but using non-invasive taVNS and examined the changes in auditory event-related potentials from pre tone-pairing to post tone-pairing with active taVNS or sham taVNS. In addition, we assessed taVNS-induced changes in oscillatory activity. Since previous work reported a decrease in the auditory N1 amplitude after repetitive stimulus presentation [23,24] we hypothesized that the N1 amplitude and the power in oscillatory activity in the auditory cortex will decrease to tones paired with sham taVNS from pre tone-pairing to post tone-pairing. Based on previous work performed in the animal model demonstrating that pairing a pure tone with VNS is sufficient to generate frequency-specific changes in cortical map organization in the auditory cortex [19–21] we furthermore hypothesized that pairing tones with active taVNS would differentially modulate the N1 amplitude and oscillatory activity as compared to sham taVNS.

2. Material and methods

2.1. Participants

For this study 22 healthy participants (10 female) at the age of 19–30 years (M : 23.91, SD : 3.04) were recruited via advertisements at the Otto-von-Guericke University Magdeburg. Sample size was determined based on previous studies assessing the effect of transauricular vagus nerve stimulation in humans [25–27]. All participants were native German speakers with normal or corrected-to-normal vision. Further inclusion criteria were: age 18–30 years, normal hearing performance. Exclusion criteria were: a history of neurologic and psychiatric disorders, brain surgery, CNS-influencing medication, pregnancy, history of migraine or epilepsy, metal pieces in the body (e.g., shunts, pacemaker), and active implants in the ear (e.g., cochlear implant). After information about the study procedure, participants gave their written informed consent. Participants received a monetary reimbursement (€ 8 per hour.). The study was approved by the local ethics committee of the Medical Faculty, University of Magdeburg and was conducted in accordance with the Declaration of Helsinki.

2.2. Experimental procedure

The current study represents a single-blinded, sham-controlled within-subject design. The order in which sham taVNS and active taVNS was applied was randomized between participants. Fig. 1 gives an overview of the experimental procedure. The experiment consisted of a baseline block followed by a stimulation block and an evaluation block. All participants completed all three blocks consecutively.

In the baseline block (pre tone-pairing) brain responses to pure tones were measured. We presented 60 tones with a frequency of 500 Hz, 60 tones with a frequency of 5000 Hz, and 60 tones with random frequencies chosen between 1000 and 4000 Hz (*control tones*) in randomized order at an interstimulus interval (ISI) of 2500 ± 75 ms. In order to assure that participants remained focused and actively listened to the

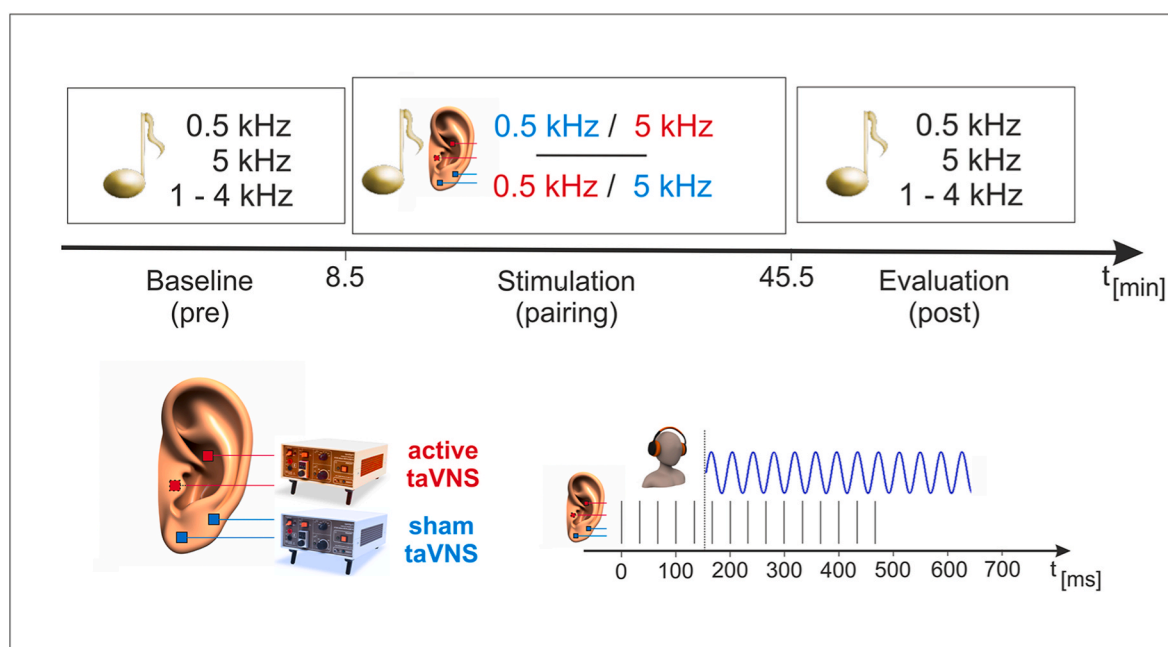


Fig. 1. Experimental procedure. Upper row: Initial brain responses to pure tones were assessed in a baseline measurement (pre). Subsequently, these pure tones were paired with either active taVNS or sham taVNS. In the evaluation block (post) brain responses were again measured to quantify stimulation specific effects of the pairing procedure. Lower row, left: Electrode positions used for taVNS (red rectangles) and sham stimulation (blue rectangles). Note that each participant received both the taVNS-pairing and the sham-pairing procedure within a single session. Lower row, right: The electrical stimulation consisted of 15 pulses (200 μ s) delivered at 30 Hz. The pulse series started 150 ms prior to the onset of the to-be paired pure tone (dashed line). (For interpretation of the references to color in this figure legend, the reader is referred to the Web version of this article.)

tones, they had to respond to intermittently presented white noise target tones ($n = 24$) by pressing a button with their right index finger (auditory vigilance task). The baseline block took about 8.5 min.

In the stimulation block, 500 Hz and 5000 Hz pure tones were paired with active taVNS and sham taVNS. The assignment of the tones to the stimulation condition was counterbalanced between participants so that in 50% of participants the 500 Hz tones were paired with active taVNS while the 5000 Hz tones were paired with sham taVNS, and vice versa. 222 tone pairings were performed (111 tones paired with active taVNS, 111 tones paired with sham taVNS). Note that tones paired with sham taVNS and tones paired with active taVNS were presented in randomized order (i.e. not in a block design that would result in carry over effects) with an ISI of $8000 \text{ ms} \pm 125 \text{ ms}$ while the participants watched a silent movie. The stimulation block took about 37 min. The subsequent evaluation block (post tone-pairing) was identical to the baseline block.

All acoustic stimuli had a duration of 500 ms including a 5 ms rise/fall and were presented at 65 dB SPL binaurally via headphones (Sennheiser HD 65 TV). Stimulus presentation as well as control of the electrical stimulation (see below) was achieved using the Presentation software, Version 18.1 (Neurobehavioral Systems, Inc., Berkeley, CA, <https://www.neurobs.com/>). The total duration of the experiment was about 60 min.

2.3. taVNS parameters and tone pairing procedure

We used two Digitimer Constant Current Stimulators DS7A (Welwyn Garden City, UK) to apply active taVNS and sham taVNS. For active taVNS, two 0.5 cm^2 Ag/AgCl-electrodes (Neuroline 700) were fixated at the cymba conchae region and medial of the tragus at the entry of the meatus of the left ear (Fig. 1) using a small amount of conductive and adhesive paste (Grass EC2). Sham taVNS was achieved by placing two additional electrodes at the left ear lobe, which is free of vagal fibers [3, 20] and verified not to activate cortical and brain stem regions [21]. We used monophasic square wave pulses with a duration of 200 μs . The frequency was set to 30 Hz as it allowed us to apply an integer number of pulses (i.e. 15) in a 500 ms time window. The stimulation intensity was set to 4 mA. The electrical stimulation in the active taVNS and the sham taVNS condition started 150 ms before tone onset [21,28] (Fig. 1, bottom). Participants were blinded to the hypothesized differential mechanisms of the electrodes. Debriefing after performing the last block revealed that participants were not able to correctly indicate which electrode served as active taVNS and sham taVNS.

2.4. Electroencephalogram (EEG)

During the baseline and the evaluation blocks, we continuously recorded EEG data with a sampling rate of 1000 Hz using 25 Ag/AgCl-electrodes equally distributed over the scalp. We used a BrainAmp DC-amplifier (BrainVision Recorder 1.21, Brainproducts, Munich, Germany). The reference electrode was positioned on the right mastoid, the ground electrode at position AFz. To monitor eye movements, one electrode was positioned lateral and one below the right eye. The further electrodes were placed at Fp1, Fp2, F7, F3, Fz, F4, F8, FC5, FC6, T7, C3, Cz, C4, T8, Tp9, CP5, CP6, Tp10, P7, P3, Pz, P4, P8, O1, O2 and at the left mastoid according to the international 10–20 system of electrode placement. The impedance of all electrodes was kept below 10 k Ω .

2.5. Data analysis

Data preprocessing and analyses were performed using Matlab R2018b (MATLAB and Statistics Toolbox release, 2018, The Mathworks Inc., Natick, Massachusetts, US) and custom made scripts using the Fieldtrip toolbox [29]. Offline, continuous EEG data were high pass filtered at 1 Hz and low pass filtered at 60 Hz. A band stop filter between 48.5 and 51.5 Hz was used to remove line noise. Bidirectional IIR Butterworth filters were used. The filtered EEG time series were then cut

into epochs from $\pm 2 \text{ s}$ relative to sound onset. Epochs were visually inspected and trials containing gross artifacts (e.g., electrode saturation, extensive muscle contractions) were removed before applying an independent component analysis (logistic infomax algorithm). For each subject 4–7 components reflecting eye blinks, eye movements, cardiac artifacts or stimulation artifacts were removed. Epochs were then re-referenced to the linked mastoids. A second visual inspection was performed in which trials exceeding $\pm 100 \mu\text{V}$ as well as remaining artifacts were removed.

Subsequently, in order to investigate taVNS-induced effects on electrophysiological brain response patterns, event related potentials (ERPs) at electrode Cz were computed for each of the three stimulation conditions (active taVNS, sham taVNS, control condition) and for both the baseline and the evaluation block, separately. ERPs were baseline corrected relative to the 100 ms before tone onset. We extracted the mean component amplitudes as they are less susceptible to noise and latency variability [30]. We therefore computed the individual ERP averaged across all six conditions (active taVNS, sham taVNS, control condition, separate for baseline and evaluation block). Based on this waveform, we determined the local peak for the P50 (maximum positive amplitude value between 0 and 100 ms), the N1 (maximum negative amplitude value between 50 and 150 ms), and the P2 (maximum positive amplitude value between 150 and 250 ms). Peak latencies were then used to define an individual time window for each component (peak latency $\pm 5 \text{ ms}$ for the P50; peak latency $\pm 25 \text{ ms}$ for the N1 and the P2). Individual P50, N1 and P2 amplitudes were then quantified as mean amplitude in the respective time windows for each of the six conditions. Additionally, time-frequency representations (TFRs) of the six conditions were obtained using complex Morlet wavelets between 2 and 45 Hz in 1 Hz steps in 25 ms bins from -2 to 2s. Wavelet cycles increased linearly from 3 cycles at 2 Hz to a maximum of 7 cycles at 40 Hz. Wavelet analysis was applied to the single trials before averaging to obtain total power. For the TFR data, a baseline correction using decibel transformation was performed for the time window from -500 ms to -200 ms before tone onset, since the time-frequency decomposition can leak trial related activity into the pre-trial period due to temporal smoothing [31]. Finally, source reconstruction of the N1 ERP was performed using linearly constrained minimum variance (LCMV) beamforming [25]. Beamforming was performed using the standard boundary element forward model and the MNI brain template [32], both implemented in Fieldtrip (see Ref. [31] for a detailed description of forward model construction). EEG electrodes were aligned with the head model before the lead field matrix was computed for each grid point (resolution: 1 cm). The regularization factor lambda was set to 15%. The covariance matrix was computed from -500 to 500 ms. For each stimulation condition (active taVNS, sham taVNS, control condition) a common spatial filter was computed using the combined data from pre tone-pairing and post tone-pairing. This filter was then applied to the pre tone-pairing and post tone-pairing ERPs, separately. Dipole moments around individual N1 peaks $\pm 25 \text{ ms}$ were averaged [28] before relative activity changes of brain activity was computed by subtracting the post tone-pairing activation from the pre tone-pairing activation and dividing by the post tone-pairing activation: $\frac{\text{source}(\text{pre}) - \text{source}(\text{post})}{\text{source}(\text{post})}$.

We used the Automated Anatomical Labeling (AAL) atlas [33] to define left and right Heschl's Gyrus, i.e. the primary auditory cortex (A1) as region of interest (ROI). Average values of the relative activity difference (pre-to-post) were extracted from this ROI for each subject for further analysis.

2.6. Statistical analyses

Statistical analyses were conducted using R 4.1.1 (R Core Team 2021) and R Studio 2021.9.0.351 (Rstudio Team 2021). To ensure that participants paid adequate attention to the acoustic stimuli, we employed non-parametric Wilcoxon test to compare accuracy in the

auditory vigilance task between the baseline block and the evaluation block.

In order to assess effects of taVNS tone-pairing on brain responses, linear mixed models (LMMs) were used to analyze ERPs and source amplitudes. LMMs were fitted using the *lme4*-package [34]. Statistical significance of predictors and their interaction was determined using the ANOVA-function from the *car*-package [35], which calculates the Wald chi-square statistic for each predictor. *Stimulation* (active taVNS, sham taVNS, control) and *block* (baseline, evaluation) and their interaction were treated as fixed effects. The random effect structures contained random intercepts and slopes for *stimulation* and *block* across subjects. In case of a significant interaction we performed pre-to-post comparisons for each stimulation condition (active taVNS, sham taVNS, control tones) separately using Bonferroni corrected Wilcoxon tests. Additionally, subject-wise differences between baseline (pre tone-pairing) and evaluation block (post tone-pairing) were computed for each stimulation condition separately. These differences were then compared between the stimulation conditions. Finally, we controlled for potential differences in the baseline block using separate LMMs.

For the TFR analysis, pre-to-post tone-pairing differences were assessed using non-parametric cluster based permutation testing as implemented in Fieldtrip [29]. Across all electrodes, power values from pre tone-pairing and post tone-pairing were compared using a two-tailed dependent sample *t*-test for each of the three stimulation conditions (active taVNS, sham taVNS, control condition) separately. The relevant time window was set from –200 to 500 ms relative to tone onset. A Monte Carlo approach using cluster-based statistics was used to determine statistical significance and control for multiple comparisons. Test statistic was the maximal sum per cluster, 5000 randomizations were used and the significance level was set to $\alpha = 5\%$. In case the cluster based permutation testing revealed differences between pre tone-pairing and post tone-pairing for one condition, average pre-to-post tone-pairing power differences for each stimulation condition from this time-frequency-electrode constellation were extracted for each subject for further analysis.

3. Results

3.1. Results of the auditory vigilance task

Participants paid sufficient and stable attention to the stimuli throughout the experiment: Response accuracy for detecting the white noise stimuli was 99.05% in the baseline block and 99.62% in the evaluation block ($V = 8.0$, $p = 0.3$).

3.2. Results of the scalp N1 amplitude

The N1 amplitudes significantly decreased from the baseline block to the evaluation block ($\chi^2_{(1)} = 10.745$, $p = 0.001$). Furthermore, N1 amplitudes were significantly modulated by the factor *stimulation* ($\chi^2_{(2)} = 15.768$, $p < 0.001$) driven by a significant *stimulation* \times *block* interaction ($\chi^2_{(2)} = 13.110$, $p = 0.001$). Analyzing the N1 amplitudes for each stimulation condition separately revealed a significant reduction of the N1 amplitude to tones paired with sham taVNS from baseline (M: -7.95 μV , SD: 3.72) to evaluation (M: -5.41 μV , SD: 2.93, $V = 26$, $p_{\text{corr}} = 0.002$, Fig. 2A, blue), while N1 amplitudes to tones paired with active taVNS showed no significant difference from baseline (M: -7.49 μV , SD: 3.94) to evaluation (M: -6.48 μV , SD: 3.51, $V = 92.0$, $p_{\text{corr}} = 0.827$, Fig. 2A, red). Similarly, no significant pre-to-post change was found for control tones (baseline: M: -8.14 μV , SD: 3.10; evaluation: M: -7.51 μV , SD: 2.84, $V = 103.0$, $p_{\text{corr}} = 1$, Fig. 2A, green).

Furthermore, the decrease in the N1 amplitude from pre tone-pairing to post tone-pairing was stronger in the sham taVNS condition (M: -2.54 , SD: 2.94, Fig. 3A, blue) compared to the active taVNS condition (M: -1.01 , SD: 2.49; $V = 46.0$, $p_{\text{corr}} = 0.022$, Fig. 3A, red) and compared to the control tones (M: -0.62 , SD: 1.97; $V = 208.0$, $p_{\text{corr}} = 0.02$, Fig. 3A, green). No significant difference was observed between N1 amplitude differences to tones paired with active taVNS and to control tones ($V = 132.0$, $p_{\text{corr}} = 1$). Thus, the differences from baseline to evaluation (i.e. from pre tone-pairing to post tone-pairing) were significantly modulated by the factor *stimulation*. Finally, no difference in the baseline N1 amplitudes were found between the stimulation conditions ($\chi^2_{(2)} = 0.72$, $p = 0.7$). In sum, pairing tones with active taVNS systematically affected the electrophysiological responses of the auditory system: The reduction of the N1 amplitude in response to tones paired with active taVNS was

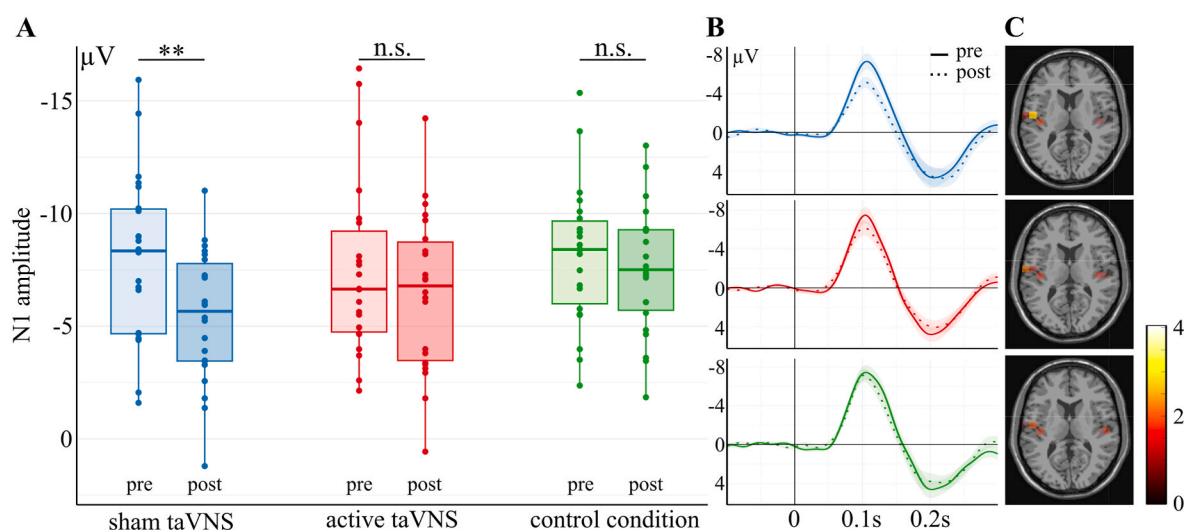


Fig. 2. Stimulation-specific changes on the N1 amplitude. A) Boxplots showing the observed changes in N1 amplitude from pre tone-pairing (light colors) to post tone-pairing procedure (darker colors) for the three stimulation conditions, separately. B) Event related potentials (ERP) in the pre (solid lines) and the post block (dashed lines) depicted separately for the sham taVNS- condition (blue lines), the active taVNS condition (red lines), and the control condition (green lines). C) Relative changes in A1-activity from pre to post tone-pairing for sham taVNS (upper panel), active taVNS (middle panel), and the control condition (lower panel). Dots represent the subjects individual data. Error bars indicate standard deviation, Asterisks indicate statistically significant differences. (For interpretation of the references to color in this figure legend, the reader is referred to the Web version of this article.)

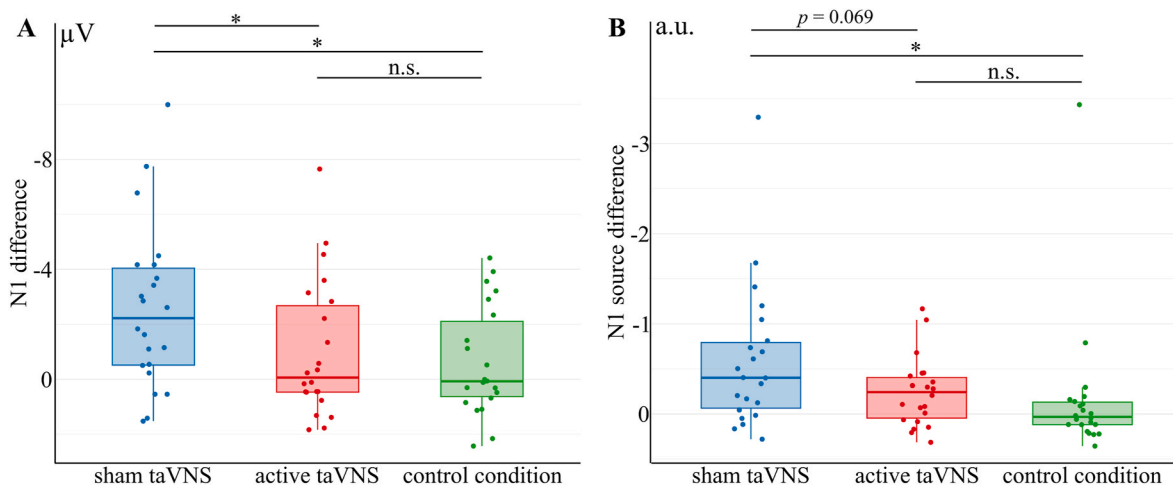


Fig. 3. N1 amplitude differences from baseline to evaluation. Pre-to-post pairing changes on the N1 amplitude recorded at the Cz-electrode (A) and in the primary auditory cortex ROI (B). Blue boxplots represent data from the sham taVNS condition, red boxplots from the active taVNS condition, and green boxplots from the control condition without any electrical stimulation. Dots represent the subjects individual data. Error bars indicate standard deviation. Asterisks indicate statistically significant differences, numbers represent the corrected p-values. (For interpretation of the references to color in this figure legend, the reader is referred to the Web version of this article.)

markedly attenuated compared to tones paired with sham taVNS and this attenuated pre-to-post reduction was comparable to the N1 amplitude reduction in response to novel control tones.

3.3. Results of the scalp P50 and P2 amplitude

Neither the LMM for the P50 amplitude nor for the P2 amplitude revealed a significant main effect or interaction (all $p > 0.1$).

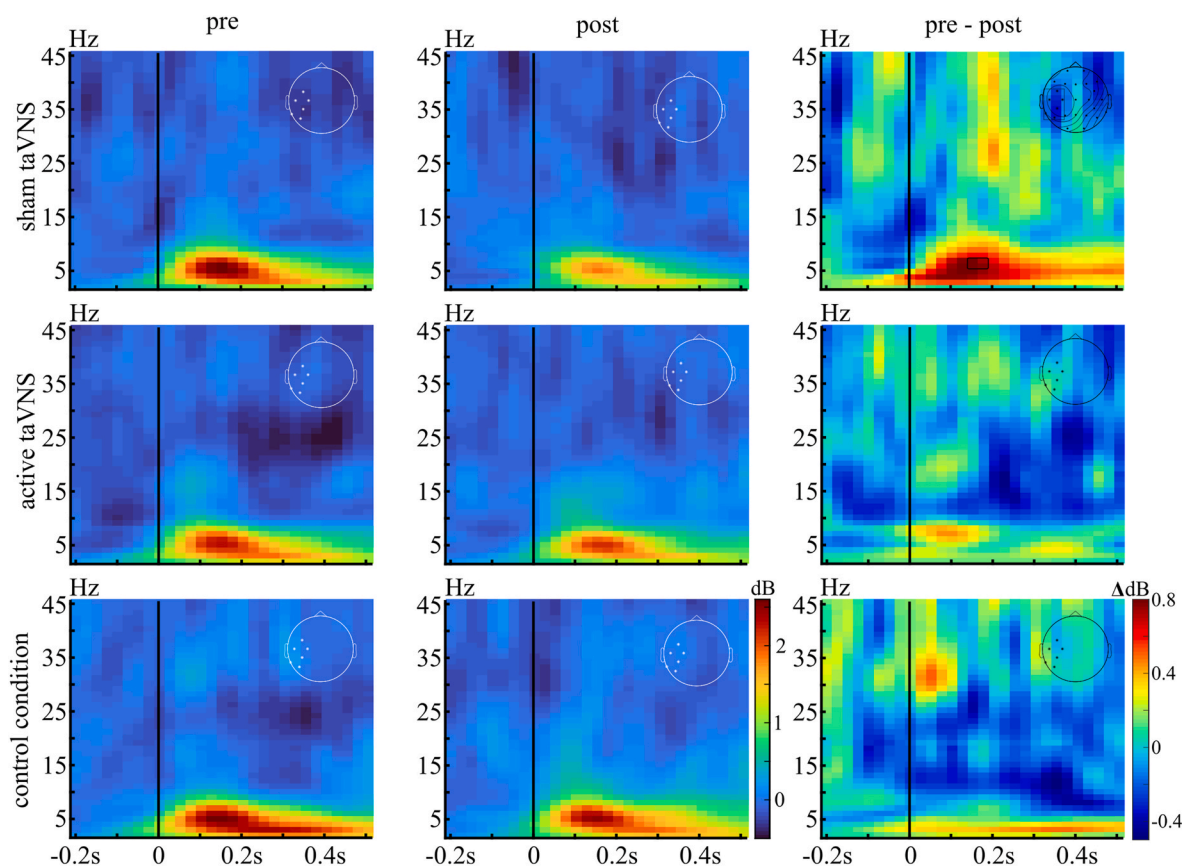


Fig. 4. taVNS-induced changes on TFR-data. In the sham taVNS condition (upper row), a significant electrodes cluster located over temporo-parietal areas was found in the theta range (6–7 Hz) peaking at about 150–200 ms after tone onset: Here, power changes from pre-to-post pairing were significantly stronger in the sham taVNS condition compared to the control condition (lower row). A numerical difference was evident between sham taVNS and active taVNS (middle row).

3.4. Results of the N1 in the auditory cortex ROI

Relative changes in the N1 amplitude from baseline to evaluation revealed activity peaks in bilateral A1-regions (Fig. 3C). The ROI analysis on N1-source activity revealed no significant main effect of the factors *stimulation* ($\chi^2_{(2)} = 0.041, p = 0.98$) or *block* ($\chi^2_{(2)} = 3.33, p = 0.07$) but a significant *stimulation* \times *block* interaction ($\chi^2_{(2)} = 11.25, p = 0.004$). Analogous to the N1 amplitudes, analysis of N1-source data for each stimulation condition separately showed a statistical trend towards a reduction of the N1-source activity to tones paired with sham taVNS from baseline (M: 0.66, SD: 0.27) to evaluation (M: 0.56, SD: 0.29, $V = 196.0, p_{corr} = 0.069$), while the N1-source activity to tones paired with active taVNS showed no significant difference from baseline (M: 0.65, SD: 0.33) to evaluation (M: 0.58, SD: 0.24, $V = 186.0, p_{corr} = 0.16$). Similarly, no significant pre-to-post change was found to control tones (baseline: M: 0.61, SD: 0.28; evaluation: M: 0.63, SD: 0.29, $V = 109.0, p_{corr} = 1$). Furthermore, the pre-to-post pairing decrease in the N1-source activity to tones paired with sham taVNS (M: 0.59, SD: 0.79, Fig. 3B, blue) was stronger compared to tones paired with active taVNS (M: 0.24, SD: 0.38; $V = 197.0, p_{corr} = 0.069$, Fig. 3B, red) as well as compared to the control tones (M: 0.15, SD: 0.77; $V = 38.0, p_{corr} = 0.013$, Fig. 3B, green). No significant difference was observed between pre-to-post changes in N1-source activity to tones paired with active taVNS and to control tones ($V = 59.0, p_{corr} = 0.089$). Finally, no difference in the baseline N1-source activity was evident between the stimulation conditions ($\chi^2_{(2)} = 2.01, p = 0.37$).

3.5. Results of the TFR-data

Statistical analysis of the TFR-data revealed a significant electrode cluster ($p_{cluster} = 0.018$) of six temporo-parietal electrodes over the left hemisphere (Fig. 4, upper right panel, black rectangle). Pairing tones with sham taVNS led to a significant power reduction specifically in the theta band (6–7 Hz) peaking around 150–200 ms after onset of the pure tones. This change in the theta power was significantly stronger in the sham taVNS condition (M: 0.76, SD: 1.02, Fig. 4, upper row) compared to the control condition (M: 0.15, SD: 0.89; $t_{(21)} = -2.3, p_{corr} = 0.048$, Fig. 4, lower row). A numerical difference was evident between sham taVNS and active taVNS (M: 0.18, SD: 0.79). Here, however, statistical analysis failed to reach significance after correcting for multiple comparisons ($t_{(21)} = -2.0, p_{corr} = 0.087$; p uncorrected = 0.029). No significant difference in theta power was found between active taVNS and the control condition ($t_{(21)} = 0.16, p_{corr} = 1$). Results from the TFR-analysis thus mirror the findings from the N1-data.

4. Discussion

Studies in the animal model have shown that pairing (invasive) VNS with acoustic stimuli over extended time periods can elicit plasticity in sound coding of the primary auditory cortex [19,20,36,37]. Building on this, we investigated short-term effects of non-invasive taVNS on electrophysiological markers of auditory sensory processing. We applied a tone-pairing paradigm in which healthy adult participants were presented with acoustic stimuli paired with either active taVNS or sham taVNS and compared stimulation-specific changes. As expected, we found that the N1 amplitude and theta power decreased after repeatedly pairing tones with sham taVNS. Importantly, these electrophysiological measures remained stable for tones paired with active taVNS, a finding that mirrored the auditory sensory processing of the novel, unpaired control tones. These results indicate that also a short-term application of non-invasive taVNS can have significant effects on auditory processing in healthy individuals.

In the present study we observed that N1 amplitudes to tones paired with sham taVNS decreased after repetitive presentation, a typical finding generally interpreted as sensory adaptation [23,24]. Importantly, the N1 amplitude to tones paired with active taVNS remained

stable after repetitive stimulus presentation. The auditory N1-component, which is generated in the primary and secondary auditory cortex region [38–40], is probably one of the most often investigated auditory ERPs in humans. Typically, a decrease in the N1 amplitude is found when physically identical stimuli are repeatedly presented. This pattern has been discussed as the consequence of sensory adaptation due to refractoriness and/or latent inhibition [24,41,42]. Interestingly, after presenting tones repetitively at high frequency and short interstimulus intervals, increased N1 amplitudes were found and interpreted as a consequence of long-term potentiation (LTP)-driven learning and cortical plasticity [43,44]. Besides the repeated occurrence of external sensory stimuli, LTP-driven cortical plasticity requires activation of the norepinephrine (NE) system [45–48]. In the rodent auditory system, disruption of NE supply caused a lack of plasticity [21–23] whereas relative short periods of increased NE supply improved long lasting neuroplastic changes [49]. A similar pattern as to the N1 was found in oscillatory brain activity: Theta power to tones paired with active taVNS remained stable from baseline to post-pairing while it decreased to tones paired with sham taVNS. Theta oscillations are typically observed during learning [50–52] and are associated with LTP and experience-dependent neural plasticity as well [53–55].

There is compelling evidence that direct neuromodulation of the noradrenergic and cholinergic path can drive plasticity in the auditory cortex. In their seminal work on auditory plasticity, Kilgard et al. (2002) [56] demonstrated that electrical stimulation of the cholinergic nucleus basalis paired with sensory stimulation drives plasticity in the auditory cortex that mimics neuroplastic changes induced by perceptual learning. In the animal model, tone-pairing with invasive stimulation of the nucleus basalis resulted in cortical map reorganization of the auditory cortex that was specific to the frequencies of the paired tones [57]. Also in the animal model, the pairing of sounds with invasive VNS has been demonstrated to reverse tinnitus-related cortical maladaptation [19]. In humans, invasive VNS paired with tones adjusted to the individual tinnitus frequency improved tinnitus-related symptoms [12,58]. For non-invasive taVNS, however, there is yet no data available on its efficacy in combination with a tone pairing procedure in tinnitus patients (see Refs. [59,60]).

Results of the present study extend these previous findings in that we report taVNS-effects already after a single tone-pairing session and, most importantly, via non-invasively stimulating vagus nerve projections. Previous research in humans has shown that taVNS activates cerebral afferents of the vagal pathway [14,61]. In addition, behavioral and electrophysiological effects on auditory sensory processing have been measured as a consequence of taVNS [62,63]. Since taVNS-induced effects on the availability of neurotransmitters is not limited to the auditory cortex but occur in the entire neocortex [3,7,64–66] our findings have implications for sensory processing in other cortical areas and modalities. Awaiting data from studies pairing e.g. visual or tactile stimuli with taVNS, we suggest in the meantime that results of the present study can be replicated in other modalities and cortical sites.

In order to verify that our effects were actually caused by taVNS our study design included two control conditions: The co-occurrence of pure tones and sham taVNS applied to the ear lobe as well as pure tones of varying frequencies without any electrical stimulation. While the aim of the former condition was to control for potential sensory effects of the electrical stimulation, the latter targeted on mere habituation effects due to the repetitive exposure to the identical stimulus. Because the stimulation intensity was above the subject's perceptual threshold, a sham taVNS (control) condition in which identical electrical pulses as in the verum taVNS condition were applied but to an area without any vagal projects was inevitable to allow for a successful blinding of the participants. Moreover, in that we used such an active sham taVNS condition, effects caused by e.g. anticipating the pulse trains or potential unspecific modulations of attention due to sensory perception of the electrical stimulation can be excluded.

A limitation of our work is that no conclusions on the temporal

stability of the observed effects can be drawn because our study design did not include a follow-up measurement. In the animal model, however, using invasive stimulation of the vagus nerve together with a tone pairing procedure over 20 days led to long-term effects up to three weeks [19]. Since we found stimulation specific electrophysiological changes already after a single session, it seems likely that the repetitive administration of (non-invasive) taVNS and a tone pairing paradigm can also evoke longer lasting effects. However, future studies will shed more light on this important aspect.

Furthermore, our study design did not include measures such as e.g. accuracy in the detection or discrimination of acoustic stimuli that would allow drawing conclusions on the behavioral consequences of a taVNS tone-pairing procedure. Thus, although the results of the present work emphasize that taVNS can influence sensory processing in the auditory cortex, future studies are needed to investigate the behavioral impact of this intervention to, ultimately, pave the way on the applicability of taVNS in the clinical setting.

Finally, we used the same stimulation intensity for active taVNS and sham taVNS to avoid potential confounding effects. Therefore, we cannot fully rule out the fact that the stimulation conditions were differently perceived by the participants and that this might have contributed to the reported stimulation-specific effects.

5. Conclusion

Together, our results demonstrate that short-term periods of non-invasive taVNS can have significant effects on auditory processing in healthy individuals: Pairing acoustic stimuli with taVNS systematically affected electrophysiological markers of auditory processing. Thereby, we provide first evidence on the efficacy of taVNS to modulate sensory perception in the *in vivo* human auditory cortex. Our findings provide evidence that non-invasive, peripheral neuromodulation may be a useful tool to enhance and restore sensory processing. Perspectively, taVNS paired with sensory stimulation may allow to compensate for sensory processing deficits by modulating neuroplasticity and related changes in cortical structures.

Author contributions

KSR: planned the study, analyzed the data, wrote the original draft. CW: analyzed the data, wrote the original draft. AS: collected the data, analyzed the data. AH: provided materials/reagents. TZ: planned the study, wrote the original draft, and provided materials/reagents. All authors participated in interpreting the results, writing the manuscript and approved the final version.

Declaration of competing interest

The authors declare that they have no known competing financial interests or personal relationships that could have appeared to influence the work reported in this paper.

Acknowledgements



This work was funded by the Leibniz Association (SAS-2015-LIN-LWC) and by the federal state of Saxony-Anhalt and the European Regional Development Fund (ERDF) in the Center for Behavioral Brain Sciences (CBBS, ZS/2016/04/78113).

References

- [1] Johnson RL, Wilson CG. A review of vagus nerve stimulation as a therapeutic intervention. *JIR* 2018;11:203–13.
- [2] Butt MF, Albusoda A, Farmer AD, Aziz Q. The anatomical basis for transcutaneous auricular vagus nerve stimulation. *J Anat* 2020;236(4):588–611.
- [3] Ruffoli R, Giorgi FS, Pizzanelli C, Murri L, Paparelli A, Fornai F. The chemical neuroanatomy of vagus nerve stimulation. *J Chem Neuroanat* 2011;42(4):288–96.
- [4] Badran BW, Brown JC, Dowdle LT, Mithoefer OJ, LaBate NT, Coatsworth J, et al. Tragus or cymba conchae? Investigating the anatomical foundation of transcutaneous auricular vagus nerve stimulation (taVNS). *Brain Stimul* 2018;11(4):947–8.
- [5] Ben-Menachem E, Hamberger A, Hedner T, Hammond EJ, Uthman BM, Slater J, et al. Effects of vagus nerve stimulation on amino acids and other metabolites in the CSF of patients with partial seizures. *Epilepsy Res* 1995;20(3):221–7.
- [6] Marrosu F, Serra A, Maleci A, Puligheddu M, Biggio G, Piga M. Correlation between GABAA receptor density and vagus nerve stimulation in individuals with drug-resistant partial epilepsy. *Epilepsy Res* 2003;55(1–2):59–70.
- [7] Collins L, Boddington L, Steffan PJ, McCormick D. Vagus nerve stimulation induces widespread cortical and behavioral activation. *Curr Biol* 2021;31(10):2088–2098. e3.
- [8] Schevernels H, van Bochove ME, De Taeye L, Bombeke K, Vonck K, Van Roost D, et al. The effect of vagus nerve stimulation on response inhibition. *Epilepsy Behav* 2016;64:171–9.
- [9] Engineer CT, Hays SA, Kilgard MP. Vagus nerve stimulation as a potential adjuvant to behavioral therapy for autism and other neurodevelopmental disorders. *J Neurodev Disord* 2017;9(1):20.
- [10] Sun L, Peräkylä J, Holm K, Haapasalo J, Lehtimäki K, Ogawa KH, et al. Vagus nerve stimulation improves working memory performance. *J Clin Exp Neuropsychol* 2017;39(10):954–64.
- [11] Neuser MP, Teckenrump V, Kühnel A, Hallschmid M, Walter M, Kroemer NB. Vagus nerve stimulation boosts the drive to work for rewards. *Nat Commun* 2020;11(1):3555.
- [12] De Ridder DD, Kilgard M, Engineer N, Vanneste S. Placebo-controlled vagus nerve stimulation paired with tones in a patient with refractory tinnitus. *A Case Report* 2015;36(4).
- [13] Adcock KS, Chandler C, Buell EP, Solorzano BR, Loerwald KW, Borland MS, et al. Vagus nerve stimulation paired with tones restores auditory processing in a rat model of Rett syndrome. *Brain Stimul* 2020;13(6):1494–503.
- [14] Van Leusden JWR, Sellaro R, Colzato LS. Transcutaneous Vagal Nerve Stimulation (tvNS): a new neuromodulation tool in healthy humans? *Front Psychol* 2015; Feb 10;6:102. <https://doi.org/10.3389/fpsyg.2015.00102>.
- [15] Frangos E, Ellrich J, Komisaruk BR. Non-invasive access to the vagus nerve central projections via electrical stimulation of the external ear: fMRI evidence in humans. *Brain Stimul* 2015;8(3):624–36.
- [16] Mercante B, Deriu F, Rangon CM. Auricular neuromodulation: the emerging concept beyond the stimulation of vagus and trigeminal nerves. *Medicine (Baltimore)* 2018;5(1):10.
- [17] Giraudier M, Ventura-Bort C, Burger AM, Claes N, D'Agostini M, Fischer R, et al. Evidence for a modulating effect of transcutaneous auricular vagus nerve stimulation (taVNS) on salivary alpha-amylase as indirect noradrenergic marker: a pooled mega-analysis. *Brain Stimul* 2022;15(6):1378–88.
- [18] Edeline JM, Manunta Y, Hennevin E. Induction of selective plasticity in the frequency tuning of auditory cortex and auditory thalamus neurons by locus coeruleus stimulation. *Hear Res* 2011;274(1–2):75–84.
- [19] Engineer ND, Riley JR, Seale JD, Vrana WA, Shetake JA, Sudanagunta SP, et al. Reversing pathological neural activity using targeted plasticity. *Nature* 2011;470(7332):101–4.
- [20] Buell EP, Loerwald KW, Engineer CT, Borland MS, Buell JM, Kelly CA, et al. Cortical map plasticity as a function of vagus nerve stimulation rate. *Brain Stimul* 2018;11(6):1218–24.
- [21] Borland MS, Vrana WA, Moreno NA, Fogarty EA, Buell EP, Vanneste S, et al. Pairing vagus nerve stimulation with tones drives plasticity across the auditory pathway. *J Neurophysiol* 2019;122(2):659–71.
- [22] Dawson J, Liu CY, Francisco GE, Cramer SC, Wolf SL, Dixit A, et al. Vagus nerve stimulation paired with rehabilitation for upper limb motor function after ischaemic stroke (VNS-REHAB): a randomised, blinded, pivotal, device trial. *Lancet* 2021;397(10284):1545–53.
- [23] Zhang F, Deshpande A, Benson C, Smith M, Eliassen J, Fu QJ. The adaptive pattern of the auditory N1 peak revealed by standardized low-resolution brain electromagnetic tomography. *Brain Res* 2011;1400:42–52.
- [24] Budd TW, Barry RJ, Gordon E, Rennie C, Michie PT. Decrement of the N1 auditory event-related potential with stimulus repetition: habituation vs. refractoriness. *Int J Psychophysiol* 1998;31(1):51–68.
- [25] Keute M, Barth D, Liebrand M, Heinze HJ, Kraemer U, Zaehle T. Effects of transcutaneous vagus nerve stimulation (tvNS) on conflict-related behavioral performance and frontal midline theta activity. *J Cogn Enhanc* 2020;4(2):121–30.
- [26] Ventura-Bort C, Wirkner J, Genheimer H, Wendt J, Hamm AO, Weymar M. Effects of transcutaneous vagus nerve stimulation (tvNS) on the P300 and alpha-amylase level: a pilot study. *Front Hum Neurosci* 2018;12:202.
- [27] Fischer R, Ventura-Bort C, Hamm A, Weymar M. Transcutaneous vagus nerve stimulation (tvNS) enhances conflict-triggered adjustment of cognitive control. *Cognit Affect Behav Neurosci* 2018;18(4):680–93.
- [28] Borland MS, Engineer CT, Vrana WA, Moreno NA, Engineer ND, Vanneste S, et al. The interval between VNS-tone pairings determines the extent of cortical map plasticity. *Neuroscience* 2018;369:76–86.
- [29] Oostenveld R, Fries P, Maris E, Schoffelen JM. FieldTrip: open source software for advanced analysis of MEG, EEG, and invasive electrophysiological data. *Comput Intell Neurosci* 2011;2011:1–9.
- [30] Luck SJ. An introduction to the event-related potential technique. second ed. Cambridge, Massachusetts: The MIT Press; 2014. p. 406.
- [31] Oostenveld R, Stegeman DF, Praamstra P, van Oosterom A. Brain symmetry and topographic analysis of lateralized event-related potentials. *Clin Neurophysiol* 2003;114(7):1194–202.

- [32] Holmes CJ, Hoge R, Collins L, Evans AC. Enhancement of T1 MR images using registration for signal averaging. *J Comput Assist Tomogr* 1998;22(2):324–33.
- [33] Tzourio-Mazoyer N, Landeau B, Papathanassiou D, Crivello F, Etard O, Delcroix N, et al. Automated anatomical labeling of activations in SPM using a macroscopic anatomical parcellation of the MNI MRI single-subject brain. *Neuroimage* 2002;15(1):273–89.
- [34] Bates D, Mächler M, Bolker B, Walker S. Fitting linear mixed-effects models using **lme4**. *J Stat Soft* 2015;67(1):1–48. <https://doi.org/10.18637/jss.v067.i01>.
- [35] Fox John, Weisberg Sanford. *An R companion to applied regression* [internet]. third ed. Thousand Oaks CA: Sage; 2019. p. 608 Available from: <https://socialsciences.mcmaster.ca/jfox/Books/Companion/>.
- [36] Engineer CT, Engineer ND, Riley JR, Seale JD, Kilgard MP. Pairing speech sounds with vagus nerve stimulation drives stimulus-specific cortical plasticity. *Brain Stimul* 2015;8(3):637–44.
- [37] Borland MS, Vrana WA, Moreno NA, Fogarty EA, Buell EP, Sharma P, et al. Cortical map plasticity as a function of vagus nerve stimulation intensity. *Brain Stimul* 2016;9(1):117–23.
- [38] Liégeois-Chauvel C, Musolino A, Badier JM, Marquis P, Chauvel P. Evoked potentials recorded from the auditory cortex in man: evaluation and topography of the middle latency components. *Electroencephalogr Clin Neurophysiology Evoked Potentials Sect* 1994;92(3):204–14.
- [39] Zouridakis G, Simos PG, Papanicolaou AC. Multiple bilaterally asymmetric cortical sources account for the auditory N1 m component. *Brain Topogr* 1998;10(3):183–9. <https://doi.org/10.1023/a:1022246825461>.
- [40] Yvert B, Fischer C, Bertrand O, Pernier J. Localization of human supratemporal auditory areas from intracerebral auditory evoked potentials using distributed source models. *Neuroimage* 2005;28(1):140–53.
- [41] Sable JJ, Low KA, Maclin EL, Fabiani M, Gratton G. Latent inhibition mediates N1 attenuation to repeating sounds. *Psychophysiology* 2004;41(4):636–42.
- [42] Rosburg T, Mager R. The reduced auditory evoked potential component N1 after repeated stimulation: refractoriness hypothesis vs. habituation account. *Hear Res* 2021;400:108140.
- [43] Budd TW, Michie PT. Facilitation of the N1 peak of the auditory ERP at short stimulus intervals. *Neuroreport* 1994;5(18):2513–6.
- [44] Clapp WC, Kirk IJ, Hamm JP, Shepherd D, Teyler TJ. Induction of LTP in the human auditory cortex by sensory stimulation. *Eur J Neurosci* 2005;22(5):1135–40.
- [45] Bear MF, Singer W. Modulation of visual cortical plasticity by acetylcholine and noradrenaline. *Nature* 1986;320(6058):172–6.
- [46] Berridge CW, Waterhouse BD. The locus coeruleus–noradrenergic system: modulation of behavioral state and state-dependent cognitive processes. *Brain Res Rev* 2003;42(1):33–84.
- [47] Golovin RM, Ward NJ. Neuromodulatory influence of norepinephrine during developmental experience-dependent plasticity. *J Neurophysiol* 2016;116(1):1–4.
- [48] Shepard KN, Liles LC, Weinschenker D, Liu RC. Norepinephrine is necessary for experience-dependent plasticity in the developing mouse auditory cortex. *J Neurosci* 2015;35(6):2432–7.
- [49] Martins ARO, Froemke RC. Coordinated forms of noradrenergic plasticity in the locus coeruleus and primary auditory cortex. *Nat Neurosci* 2015;18(10):1483–92.
- [50] Osipova D, Takashima A, Oostenveld R, Fernandez G, Maris E, Jensen O. Theta and gamma oscillations predict encoding and retrieval of declarative memory. *J Neurosci* 2006;26(28):7523–31.
- [51] Buzsáki G. Theta rhythm of navigation: link between path integration and landmark navigation, episodic and semantic memory. *Hippocampus* 2005;15(7):827–40.
- [52] Colgin LL. Mechanisms and functions of theta rhythms. *Annu Rev Neurosci* 2013;36(1):295–312.
- [53] Hamilton HK, Roach BJ, Cavus I, Teyler TJ, Clapp WC, Ford JM, et al. Impaired potentiation of theta oscillations during a visual cortical plasticity paradigm in individuals with schizophrenia. *Front Psychiatr* 2020;11:590567.
- [54] Hyman JM, Wyble BP, Goyal V, Rossi CA, Hasselmo ME. Stimulation in hippocampal region CA1 in behaving rats yields long-term potentiation when delivered to the peak of theta and long-term depression when delivered to the trough. *J Neurosci* 2003;23(37):11725–31.
- [55] Bikbaev A. Relationship of hippocampal theta and gamma oscillations to potentiation of synaptic transmission. *Front Neurosci* 2008;2(1):56–63.
- [56] Kilgard MP, Pandya PK, Engineer ND, Moucha R. Cortical network reorganization guided by sensory input features. *Biol Cybern* 2002;87(5–6):333–43.
- [57] Kilgard MP, Merzenich MM. Cortical map reorganization enabled by nucleus basalis activity. *Science* 1998;279(5357):1714–8.
- [58] Tyler R, Cacace A, Stocking C, Tarver B, Engineer N, Martin J, et al. Vagus nerve stimulation paired with tones for the treatment of tinnitus: a prospective randomized double-blind controlled pilot study in humans. *Sci Rep* 2017;7(1):11960.
- [59] Yakunina N, Nam EC. Direct and transcutaneous vagus nerve stimulation for treatment of tinnitus: a scoping review. *Front Neurosci* 2021;15:680590.
- [60] Stegeman I, Velde HM, Robe PAJT, Stokroos RJ, Smit AL. Tinnitus treatment by vagus nerve stimulation: a systematic review. *PLoS One* 2021;16(3):e0247221.
- [61] Kraus T, Kiess O, Hösl K, Terekhin P, Kornhuber J, Forster C. CNS BOLD fMRI effects of sham-controlled transcutaneous electrical nerve stimulation in the left outer auditory canal – a pilot study. *Brain Stimul* 2013;6(5):798–804.
- [62] Rufener KS, Geyer U, Janitzky K, Heinze HJ, Zaehle T. Modulating auditory selective attention by non-invasive brain stimulation: differential effects of transcutaneous vagal nerve stimulation and transcranial random noise stimulation. *Eur J Neurosci* 2018;48(6):2301–9.
- [63] Llanos F, McHaney JR, Schuerman WL, Yi HG, Leonard MK, Chandrasekaran B. Non-invasive peripheral nerve stimulation selectively enhances speech category learning in adults. *npj Sci Learn* 2020;5(1):12.
- [64] Hulsey DR, Shedd CM, Sarker SF, Kilgard MP, Hays SA. Norepinephrine and serotonin are required for vagus nerve stimulation directed cortical plasticity. *Exp Neurol* 2019;320:112975.
- [65] Berger A, Vespa S, Dricot L, Dumoulin M, Iachim E, Doguet P, et al. How is the norepinephrine system involved in the antiepileptic effects of vagus nerve stimulation? *Front Neurosci* 2021;15:790943.
- [66] Rodenkirch C, Carmel JB, Wang Q. Rapid effects of vagus nerve stimulation on sensory processing through activation of neuromodulatory systems. *Front Neurosci* 2022 Jul 5;16:922424.

Phasic, Event-Related Transcutaneous Auricular Vagus Nerve Stimulation Modifies Behavioral, Pupillary, and Low-Frequency Oscillatory Power Responses

 Christian Wienke,¹ Marcus Grueschow,² Aiden Haghikia,^{1,3,4} and  Tino Zaehle^{1,4}

¹Otto-von-Guericke University, 39120 Magdeburg, Germany, ²Zurich Center for Neuroeconomics, Department of Economics, University of Zurich, 8006 Zurich, Switzerland, ³Deutsches Zentrum für Neurodegenerative Erkrankungen, 39120 Magdeburg, Germany, and ⁴Center for Behavioral Brain Sciences, Magdeburg, 39120, Germany

Transcutaneous auricular vagus nerve stimulation (taVNS) has been proposed to activate the locus ceruleus-noradrenaline (LC-NA) system. However, previous studies failed to find consistent modulatory effects of taVNS on LC-NA biomarkers. Previous studies suggest that phasic taVNS may be capable of modulating LC-NA biomarkers such as pupil dilation and alpha oscillations. However, it is unclear whether these effects extend beyond pure sensory vagal nerve responses. Critically, the potential of the pupillary light reflex as an additional taVNS biomarker has not been explored so far. Here, we applied phasic active and sham taVNS in 29 subjects (16 female, 13 male) while they performed an emotional Stroop task (EST) and a passive pupil light reflex task (PLRT). We recorded pupil size and brain activity dynamics using a combined Magnetoencephalography (MEG) and pupillometry design. Our results show that phasic taVNS significantly increased pupil dilation and performance during the EST. During the PLRT, active taVNS reduced and delayed pupil constriction. In the MEG, taVNS increased frontal-midline theta and alpha power during the EST, whereas occipital alpha power was reduced during both the EST and PLRT. Our findings provide evidence that phasic taVNS systematically modulates behavioral, pupillary, and electrophysiological parameters of LC-NA activity during cognitive processing. Moreover, we demonstrate for the first time that the pupillary light reflex can be used as a simple and effective proxy of taVNS efficacy. These findings have important implications for the development of noninvasive neuromodulation interventions for various cognitive and clinical applications.

Key words: EEG/MEG; noradrenalin; pupil; pupil light reflex; taVNS; transcutaneous vagus nerve stimulation

Significance Statement

taVNS has gained increasing attention as a noninvasive neuromodulation technique and is widely used in clinical and non-clinical research. Nevertheless, the exact mechanism of action of taVNS is not yet fully understood. By assessing physiology and behavior in a response conflict task in healthy humans, we demonstrate the first successful application of a phasic, noninvasive vagus nerve stimulation to improve cognitive control and to systematically modulate pupillary and electrophysiological markers of the noradrenergic system. Understanding the mechanisms of action of taVNS could optimize future clinical applications and lead to better treatments for mental disorders associated with noradrenergic dysfunction. In addition, we present a new taVNS-sensitive pupillary measure representing an easy-to-use biomarker for future taVNS studies.

Received Mar. 13, 2023; revised July 14, 2023; accepted July 23, 2023.

Author contributions: C.W. and T.Z. designed research; C.W. performed research; M.G. and A.H. contributed unpublished reagents/analytic tools; C.W. analyzed data; and C.W., M.G., and T.Z. wrote the paper.

This work was supported by European Regional Development Fund Grant ZS/2016/04/78113, the federal state of Saxony-Anhalt, and the Data Integration Center of the University Hospital Magdeburg.

The authors declare no competing financial interests.

Correspondence should be addressed to Tino Zaehle at tino.zaehle@ovgu.de.

<https://doi.org/10.1523/JNEUROSCI.0452-23.2023>

Copyright © 2023 Wienke et al.

This is an open-access article distributed under the terms of the Creative Commons Attribution 4.0 International license, which permits unrestricted use, distribution and reproduction in any medium provided that the original work is properly attributed.

Introduction

Transcutaneous auricular vagus nerve stimulation (taVNS) has gained increasing attention as a noninvasive neuromodulation technique in recent years. Since the seminal work by Peucker and Filler (2002) describing that areas of the human outer ear are exclusively innervated by the auricular branch of the vagus nerve, taVNS has been widely used in clinical and nonclinical research settings (for review, see Burger et al., 2020b; Farmer et al., 2021), but its exact working mechanisms are still not fully understood.

It has been suggested that taVNS modulates the locus ceruleus-noradrenaline (LC-NA) system, which is involved in

various cognitive and emotional processes (Kurniawan et al., 2021; Maier and Grueschow, 2021). The LC-NA system receives indirect input from the VN through projections from the brainstem nucleus tractus solitarius (NTS; Butt et al., 2020). The LC is the main source of NA in the brain (Sara, 2009) and invasive VNS (iVNS) in animals modulated LC firing and cortical NA levels (Raedt et al., 2011; Hulseley et al., 2017).

Pupil dilation (PD) has been identified as a promising indicator of noradrenergic activity given its close relation to the LC-NA system (Samuels and Szabadi, 2008a, 2008b; Joshi et al., 2016). In humans, the LC signals behavioral response conflicts, accompanied by an increase in PD (Grueschow et al., 2021). Direct LC stimulation (Joshi et al., 2016) and iVNS in animals (Mridha et al., 2021) and humans (Desbeaumes Jodoin et al., 2015) also increased PD. It is important to note, however, that NA is not the only transmitter involved in regulating PD (Reimer et al., 2016; Mridha et al., 2021). In turn, taVNS likely modulates other transmitter systems as well, given the various projections from the NTS to other core areas (Krahl and Clark, 2012; Frangos et al., 2015). Although previous studies have examined the effects of noninvasive taVNS on PD as well, the results have been inconsistent (Keute et al., 2019; D'Agostini et al., 2022), potentially because of nonoptimal stimulation parameters (Ludwig et al., 2021). These former studies often applied tonic 30 s on/30 s off stimulation (Burger et al., 2020a; D'Agostini et al., 2022), which might be ineffective in reliably modulating the PD. However, more promising results were demonstrated with short bursts (600–5000 ms) of taVNS (Sharon et al., 2021; Urbin et al., 2021; Villani et al., 2022; D'Agostini et al., 2023), but these effects on PD have largely been investigated in the absence of a specific behavioral task, that is, in response to taVNS itself (Sharon et al., 2021; Urbin et al., 2021; D'Agostini et al., 2023) or stimulation was applied before stimulus onset (Villani et al., 2022). Furthermore, studies have largely ignored the pupil light reflex (PLR), which is also influenced by NA activity (Bitsios et al., 1999; Hysek and Liechti, 2012). The PLR is the rapid constriction of the pupil in response to light and is controlled by the brainstem Edinger–Westphal nucleus (EWN; Hall and Chilcott, 2018).

In addition to pupillometry, cortical oscillations have been indicated as noradrenergic markers, including alpha oscillations as a marker for cortical arousal (Dahl et al., 2022) and frontal-midline (FM) theta power (Dippel et al., 2017) as an electrophysiological correlate of cognitive control (Cavanagh and Frank, 2014). In line with this, taVNS has been shown to decrease occipital alpha power at rest (Sharon et al., 2021) and to increase FM theta power during a cognitive control task (Keute et al., 2020).

In this study, we investigated how phasic, event-related taVNS modulates pupillary and electrophysiological markers of LC-NA activation during a response conflict task. We expected increased PD and FM theta power, as well as reduced alpha power during cognitive processing, and reduced pupil constriction and alpha power during the PLR following taVNS.

Materials and Methods

Subjects

Twenty-nine subjects (16 female) ranging in age from 18 to 40 years (mean = 26.5; SD = 6) participated in this study. All subjects provided written informed consent, reported no history of neurologic or psychiatric disease, and reported normal or corrected-to-normal vision using contact lenses. Recordings took place at Otto-von-

Guericke University, Magdeburg, Germany, and were approved by the Ethical Committee of the Otto-von-Guericke University Magdeburg. For participation, subjects were reimbursed with money or course credit.

Experimental procedure

After providing written informed consent, subjects were prepared for the MEG recording. Electrodes for the vertical and horizontal EOG were attached above and below the right eye as well as on both outer eye corners (canthus). Impedance for EOG electrodes was kept below 10 k Ω . Head shape was then digitized using a Polhemus Fastrak motion tracker. The coordinates of three anatomic landmarks (nasion, left and right preauricular point), the five head position indicator coils, and a minimum of 200 additional points on the scalp were digitized. The stimulation electrodes (see below) were then attached, and the subjects were comfortably seated in the MEG chamber.

We applied two different tasks during the same recording session: The emotional Stroop task (EST) (Grueschow et al., 2020, 2021, 2022) and a passive Pupillary Light Reflex Task (PLRT). Both tasks were performed twice by each subject, once during active taVNS and once during sham stimulation. The order of stimulation was counterbalanced across subjects (i.e., half received taVNS in the first half of the experiment and sham stimulation in the second half of the experiment or vice versa). Subjects first performed six blocks of the EST during which they were asked to categorize the emotional expression of faces (happy or fearful) while ignoring an overlaid emotional word (happy or fear). Trials were either congruent (word matches the facial expression) or incongruent (word does not match the facial expression; Fig. 1A). The color of the overlaid word was randomly chosen for each trial to avoid adaptation. Each block consisted of 20 pictures (10 congruent, 10 incongruent). Each trial started with the presentation of a gray fixation cross in the center of the screen for 2 s. After that, the fixation cross disappeared and the actual stimulus picture was presented for 1 s, after which only the fixation cross was again visible for 5 s. The fixation cross then disappeared for a variable interstimulus interval (ISI) between 1 and 4 s. Afterward, a new trial started with the presentation of the fixation cross for 2 s. Subjects were instructed to fixate the cross whenever visible on screen to avoid eye movement and to avoid blinking as much as possible. They were further instructed that they could blink during periods with no fixation cross on screen, that is, during the ISI. Pictures subtended a visual angle of $\sim 8 \times 11.4^\circ$, which does not warrant the use of saccades to identify the emotional content. The overlaid word was centered at the same x and y coordinates as the fixation cross to further reduce the potential for saccades. All face stimuli were equally distributed between congruent and incongruent conditions. Hence, the net luminance for both conditions was identical. Responses were given via button press with the left or right index finger. The assignment of which finger had to be pressed in response to which face was counterbalanced across subjects (i.e., half the subjects had to press the left index finger following a happy face and right index finger for fearful faces and vice versa in the other half of subjects). Parallel with stimulus onset, subjects received either taVNS or sham stimulation (see below). Following completion of the EST, subjects performed the PLRT (Fig. 1B). This part consisted of one block of 20 trials with passive bright light stimulation to elicit a PLR. Subjects were first dark adapted for 2 min (~ 0.14 cd/m 2) before the actual PLRT started. Each trial started with the presentation of a gray fixation cross in the center of the screen for 2 s, after which the screen turned white for 500 ms (~ 179 cd/m 2). Afterward, only the fixation cross remained on screen for 20 s followed by a variable ISI between 8 and 12 s. Subjects were again instructed to fixate the cross whenever visible on screen to avoid eye movements and blinking as much as possible. No button presses were required in this task. Again, parallel with stimulus onset, subjects received either taVNS or sham stimulation. Subsequently, both tasks were then completed again with the remaining stimulation condition. Subjects were instructed that they could take a self-paced break after each experimental block. All stimuli were presented from the experimental computer running MATLAB R2018b (MathWorks) and Psychtoolbox 3 (Brainard, 1997; Pelli, 1997; Kleiner et al., 2007).

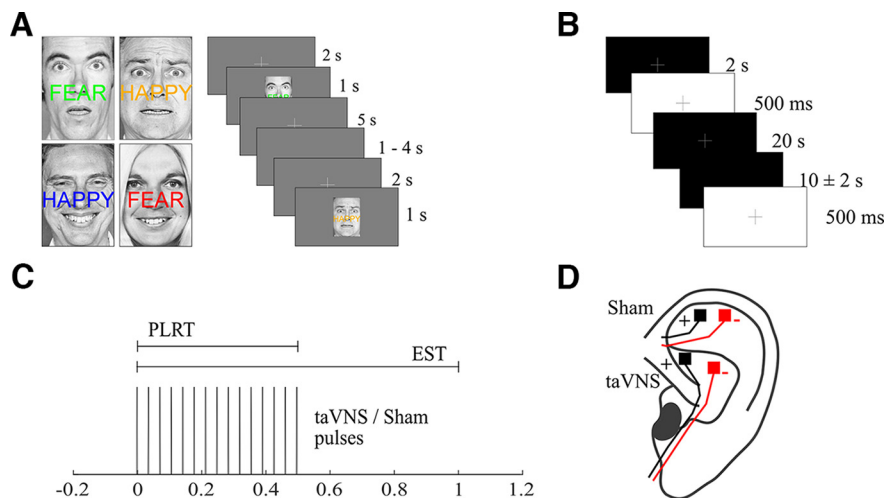


Figure 1. Paradigm. **A**, Subjects performed the EST, that is, categorizing the emotional expression of faces while ignoring the overlaid word. Each trial was either congruent or incongruent. **B**, Subjects also performed a PLRT, where they were exposed to short, bright light stimuli. **C**, Coinciding with each stimulus onset, either taVNS or sham stimulation was applied as 500 ms trains at 30 Hz. Pulse width of the monophasic square wave pulses was 200 μ s. Top, Horizontal bars show the stimulus duration during the EST and PLRT. **D**, taVNS was applied to the cymba concha region of the left ear while sham stimulation was applied to the scapha.

Electrical stimulation

Stimulation was delivered as 500 ms long trains of monophasic square wave pulses with a frequency of 30 Hz. Each pulse had a width of 200 μ s (Fig. 1C). The stimulation amplitude was set to 2 mA in line with previous studies (Capone et al., 2021; Sharon et al., 2021). We applied taVNS and sham stimulation in the same session using two Digitimer DS7A constant current stimulators outside the magnetically shielded room and two pairs of medical Ag/AgCl electrodes (Ambu Neuroline 700) cut to a size of 4 \times 4 mm. Both Digitimers were connected to the experimental computer via a DATAPixx processing unit (Vpixx Technology). For taVNS, electrodes were attached to the cymba concha and for sham stimulation to the scapha of the left ear (Fig. 1D). Although most taVNS studies use the ear lobe as the location for the sham stimulation, the scapha has been proposed as more suitable for sham stimulation (Cakmak, 2019). In both cases, the anode was placed more rostrally. Before electrode placement, both target regions were cleaned with disinfectant alcohol. A small amount of Ten20 paste (Weaver and Company) was used to ensure proper conductance. Stimulation was tested before the start of the experiment by applying single trains of 500 ms at 2 mA to ensure that stimulation worked properly and to determine whether stimulation felt uncomfortable. If the subjects reported pain or an unpleasant sensation during this test, the stimulation intensity in the respective condition was reduced in 0.1 mA steps until subjects no longer reported discomfort during stimulation. This resulted in an average stimulation intensity of 1.91 mA for taVNS (SD = 0.23) and 1.87 mA for sham (SD = 0.25). There was no statistical difference between these conditions ($t_{(28)} = 0.87$, $p = 0.39$). Of the 29 subjects, 17 rated the 2 mA in both stimulation conditions as not uncomfortable. Ten subjects rated the initial 2 mA in one stimulation condition as uncomfortable, and only two subjects rated 2 mA in both conditions as uncomfortable.

Data acquisition

Pupil diameter was recorded monocularly from the left eye using a MEG compatible EyeLink 1000 long-range mount (SR Research). The infrared camera was fixated below the video screen inside the MEG chamber. The sampling rate was set to 500 Hz. At the start of the experiment and after the first half, the camera was calibrated using the built-in five-point calibration. The entire recording session lasted \sim 65 min.

Brain activity throughout the task was recorded in a sitting position using a whole-head Elekta Neuromag TRIUX system in a magnetically shielded room (VacuumSchmelze). The sampling rate was set to 1000 Hz. An online bandpass filter was applied between 0.1 and 330 Hz. Visual stimuli were presented via rear projection using an LCD projector (DLA-G150CLE, JVC) outside the recording booth. The semitransparent screen

was placed 100 cm in front of the subjects. Responses were given using a MEG-compatible LUMItouch response system (Photon Control).

Data preprocessing

Pupillometry

Off-line preprocessing of pupil data was performed using custom scripts for MATLAB R2018b software following the recommendations from Kret and Sjak-Shie (2019). Continuous data were cut into epochs from -2 s to 5 s around stimulus onset for the EST and from -2 to 7 s for the PLRT. Trials with $>50\%$ missing data points were rejected. Subjects with $>50\%$ excluded trials in one condition were wholly excluded from statistical analyses ($N = 5$). For the remaining trials, the normalized dilation speed time series was computed to detect blinks and other artifacts. These manifest as disproportionately large changes in pupil dilation relative to the adjacent samples (Kret and Sjak-Shie, 2019). To detect dilation speed outliers, the median absolute deviation (MAD) was calculated from the normalized dilation speed time series. A threshold was then calculated by multiplying the MAD with a constant and adding the median of the normalized dilation speed time series (Kret and Sjak-Shie, 2019). This constant was set to 2.5 (Leys et al., 2013). In the first step, data points whose dilation speed exceeded this threshold were removed. To detect remaining outliers that resisted this first rejection, a smoothed trend line was then formed by linearly interpolating the resulting gaps in the pupil time series and smoothing with a 100 ms moving average. Remaining outliers in the pupil time series from this trend line were then detected as in the first step. The missing data points in the cleaned time series were then linearly interpolated. Pupil data were then z -scored, baseline corrected to the average of the 200 ms before stimulus onset, and downsampled to 100 Hz.

MEG

Off-line preprocessing of MEG data was performed using MATLAB R2018b and the FieldTrip toolbox (Oostenveld et al., 2011). In the first step, the stimulation artifact had to be cleaned from the data. Sole filtering or independent component analysis (ICA) approaches are not sufficient to sufficiently clean the stimulation artifact from the data because of nonlinear effects caused by physiological processes such as respiration and heartbeat. Thus, an autoregressive interpolation method as in Keatch et al. (2022) was used. The DATAPixx processing unit provided event markers each time a stimulation pulse was triggered. Ten milliseconds after each marker were excluded and replaced with NaNs (Not a Number). Missing data were then interpolated using the built-in MATLAB function fillgaps() with a prediction sequence length of 25 ms before and after each gap to estimate the missing values. The data

cleaned in this way were subsequently high-pass filtered at 1 Hz and low-pass filtered at 60 Hz. A band-stop filter (49–51 Hz) was applied to suppress line noise. All filters used were bidirectional infinite impulse response Butterworth filters. Continuous data were then segmented into epochs from -2 s to 5 s relative to stimulus onset. Remaining artifacts like blinks and heartbeats were removed by applying an ICA (Infomax algorithm) to the data. Components reflecting remaining artifactual activity were excluded after visual inspection. Epochs were then down-sampled to 250 Hz and baseline corrected relative to the 200 ms before stimulus onset. Average baseline values were retained for subsequent analysis to check for potential baseline differences in brain activity between conditions. Given the greater amount of interpolation necessary, we calculated spectral power using fast Fourier transformation (FFT) from a 500-ms-long Hanning tapered window directly after stimulus onset. The rationale for choosing this time window was based on the previous literature on cognitive control and theta activity, showing that an effect of conflict processing on FM theta develops within the first 500 ms after stimulus presentation (Cavanagh and Frank, 2014). We further decided to restrict this part of the analysis on the first 500 ms to avoid comparing interpolated with noninterpolated data. The advantage of the FFT approach is that it only uses the selected time window compared with a moving window method like Morlet wavelets that would incorporate activity from adjacent time points where no interpolation was applied. Frequencies were set from 2 to 14 Hz in 0.5 Hz steps.

To further investigate the effects of taVNS on longer lasting effects in the alpha range at occipital sites (Sharon et al., 2021), we also computed time-frequency representations (TFR) of these sensors using Morlet wavelets. TFRs were computed for the whole trial between -1000 and 5000 ms relative to stimulus onset in 40 ms time bins for frequencies between 2 and 14 Hz in 0.5 Hz steps. The number of cycles for the wavelet was set to five. A baseline correction using decibel transformation was applied relative to the time period from -500 to -200 ms before stimulus onset.

Statistical analyses

Statistical analyses were performed using R 4.1.2 software (<https://www.R-project.org/>; <http://www.rstudio.com/>). Linear mixed effect models (LMMs) were constructed using the lme4 package (Bates et al., 2015) in R and fitted using the restricted maximum likelihood method. Significance values for the individual predictors were obtained with the Anova() function from the car package (Fox and Weisberg, 2019) performing likelihood-ratio chi-square tests. Significant interactions between predictors were resolved by running additional LMMs with one of the predictors nested within the other. This allowed us to calculate the effect of one predictor at both levels of the other (Frömer et al., 2018). As nested models are not supported by the Anova() function, significance was determined by estimating the degrees of freedom for the t values using the Satterthwaite approximation performed in the lmerTest package (Kuznetsova et al., 2017). Cluster-based permutation testing (CBPT) was used to analyze time series and Fourier spectra between different conditions. CBPT is a standard, data driven approach to resolve the multiple comparison problem (Maris and Oostenveld, 2007). In the first step, statistical tests are performed at each time point. Adjacent time points that exceed a (uncorrected) statistical threshold are clustered. Test statistics are summed to form the empirical cluster size. In the second step, a null hypothesis distribution is formed. For that, condition labels are randomly shuffled, and the statistical tests are repeated at each time point. Again, adjacent time points exceeding the threshold level are clustered, and test statistics in the largest cluster are summed to obtain one cluster size per iteration. This shuffling and calculating of test statistics is repeated for a certain number of iterations. The empirical cluster size from the first step is then thresholded against the distribution of randomly permuted cluster sizes to obtain the p value of clusters. CBPT was performed using the permutes package (<https://CRAN.R-project.org/package=permutes>). In each permutation analysis 10,000 permutations were used to form the null hypothesis distribution. We report average and maximum effect size (Cohen's d) from each significant cluster (Meyer et al., 2021).

Behavior

Because of technical difficulties, behavioral responses from three subjects were not recorded. Thus, behavioral results are based on 26 subjects. A mixed effect logistic regression on the single-trial level was used to determine whether stimulation (taVNS vs sham), congruency (congruent vs incongruent trials), or the interaction between these two predictors affected performance. Trials were coded as one when a correct response was given in the respective trial and as zero otherwise (i.e., incorrect answers and omissions). Similarly, sham stimulation was coded as zero and taVNS as one. The face emotion (fearful vs happy) was included as covariate in the model. The trial number was also included as predictor to account for possible effects of time spent on task. Finally, to control for the small difference in stimulation intensity between taVNS and sham stimulation, we included stimulation intensity as a continuous variable in the analysis. The random effect structure contained random intercepts and slopes for stimulation and congruency across subjects as follows:

$$\text{hits} \sim \text{trialnumber} + \text{face} + \text{intensity} + \text{stimulation} * \text{congruency} + (1 + \text{stimulation} + \text{congruency} | \text{subjectID}).$$

For the reaction times (RTs), an LMM was fitted on the single-trial level with RT as outcome variable and stimulation, congruency and their interaction as fixed effect. The trial number, face emotion-condition and stimulation intensity were again included as covariates. The random effect structure contained random intercepts and slopes for stimulation and congruency across subjects as follows:

$$\text{RT} \sim \text{trialnumber} + \text{face} + \text{intensity} + \text{stimulation} * \text{congruency} + (1 + \text{stimulation} + \text{congruency} | \text{subjectID}).$$

Pupillometry

Five subjects were excluded from the analysis of pupil data because of an excessive number of excluded trials. In the remaining 24 subjects, an average of 3.57 trials were excluded (range: 0, 28; SD = 6). The number of excluded trials did not differ between conditions ($F_{(3,69)} = 0.42$, $p = 0.74$). For the EST, average pupil time series between -500 and 5000 ms were analyzed to determine whether pupil diameters differed between conditions. LMMs were fitted at each time point with average pupil diameter as outcome. Congruency (dummy coded, 0 = incongruent, 1 = congruent), stimulation (dummy coded, 0 = sham, 1 = taVNS), and their interaction were set as fixed effects. The continuous predictor stimulation intensity was again included as a covariate. Random intercepts and slopes for congruency and stimulation across subjects were set as random effects as in the following:

$$\text{pupil} \sim \text{intensity} + \text{stimulation} * \text{congruency} + (1 + \text{stimulation} + \text{congruency} | \text{subjectID})$$

For the PLRT we examined in a similar fashion the effect of the predictors stimulation (dummy coded, 0 = sham, 1 = taVNS) and stimulation intensity as fixed effect on pupil diameter at each time point between -500 and 7000 ms relative to stimulus onset. The random effect structure contained random intercepts and slopes for stimulation across subjects as follows:

$$\text{pupil} \sim \text{intensity} + \text{stimulation} + (1 + \text{stimulation} | \text{subjectID}).$$

Apart from the pupil diameter at each time point, previous pharmacological studies have shown that other dynamics of the pupil light reflex are also affected by an increase in NA, among others. These include the onset latency of the pupil light reflex, the velocity with which the pupil constricts and re-dilates, as well as the maximal constriction amplitude (Theofilopoulos et al., 1995; Bitsios et al., 1999; Hysek and Liechti,

2012). To further elucidate the effect of taVNS on dynamics of the PLR, we thus extracted the following parameters from the preprocessed and averaged PLR time series for each subject from both stimulation conditions: The peak constriction amplitude was determined as the maximal negative value in the PLR time series after stimulus onset. To determine velocity-based parameters of pupillary dynamics, we then computed the first (velocity) and second (acceleration) derivative of the PLR time series. The onset of the pupil constriction was determined as the most negative acceleration in the first period of the second derivative (Bergamin and Kardon, 2003). We then determined the peak and average constriction velocity after stimulus onset as well as the peak and average redilation velocity after the maximum of the pupil constriction. During constriction of the pupil after light onset, when the velocity is negative, the peak constriction velocity was determined as the peak negative velocity between onset of the PLR and the peak constriction amplitude. Similarly, the average constriction velocity was determined as the mean velocity between PLR onset and the maximal pupil constriction. Finally, during redilation of the pupil, when velocity is positive, the peak dilation velocity was determined as peak positive velocity after the maximal pupil constriction. The average dilation velocity was calculated as mean velocity after the maximal pupil constriction. These parameters were again analyzed using separate LMMs. The models for all dependent variables (DV) contained the predictor stimulation as well as the stimulation intensity as fixed effect and random intercepts across subjects as follows:

$$DV \sim \text{intensity} + \text{stimulation} + (1 | \text{subjectID}).$$

MEG

Seven subjects were excluded from analysis of the MEG data after visual inspection of the data from each trial and sensor. Exclusion criteria were flat or severely noise-corrupted sensors in the frontal-midline or occipital-midline region of interest (ROI). Average baseline brain activity from frontal and occipital ROIs before stimulus onset was analyzed between conditions (e.g., PLR during taVNS, congruent trials during taVNS, ...) using two LMMs. Both models contained the predictor condition as fixed effect as well as random intercepts across subjects as follows:

$$\text{Baseline}_{\text{frontal/occipital}} \sim \text{condition} + (1 | \text{subjectID}).$$

Spectral power from the remaining 22 datasets was analyzed using CBPT. For the EST, Fourier spectra from FM and occipital-midline (OM) gradiometers were first averaged and then subjected to separate permutation analysis. LMMs were fitted at each frequency point between 2 and 14 Hz with power as outcome and congruency, stimulation, and their interaction as well stimulation intensity as fixed effects. The random effect structure contained random intercepts and slopes for the congruency and stimulation across subjects as follows:

$$\text{PSD}_{\text{frontal/occipital}} \sim \text{intensity} + \text{stimulation} * \text{congruency} + (1 + \text{congruency} + \text{stimulation} | \text{subjectID}).$$

For the PLRT, spectra from OM and FM gradiometers were first averaged and then analyzed in the same way with power as outcome and stimulation intensity and stimulation as fixed effect. Random slopes and intercepts for stimulation across subjects were set as random effect as follows:

$$\text{PSD}_{\text{frontal/occipital}} \sim \text{intensity} + \text{stimulation} + (1 + \text{stimulation} | \text{subjectID}).$$

Differences between taVNS and sham stimulation in the TFRs of OM gradiometers were also analyzed using CBPT. To avoid comparing interpolated with noninterpolated time periods, we restricted the analysis to time period from 600 to 5000 ms poststimulus, that is, after the offset of stimulation where contamination from an electrical artifact can be ruled out. The CBPT was then performed using dependent sample *t* tests

as implemented in FieldTrip (Oostenveld et al., 2011) again with 10,000 permutations.

Relationship between parameters across tasks

We further investigated the relationship between taVNS-specific effects on electrophysiological and pupillometric measures between the two tasks. First, for the EST and PLRT we calculated stimulation-related changes, that is, deltas (taVNS minus sham difference) in FM and OM power spectra ($\Delta\text{PSD}_{\text{frontal}}$, $\Delta\text{PSD}_{\text{occipital}}$), the pupil diameter time series ($\Delta\text{PD}_{\text{EST}}$, $\Delta\text{PD}_{\text{PLRT}}$), the average power difference at FM and OM sensors from significant clusters during the EST and PLRT ($\Delta\text{fm.est}$, $\Delta\text{om.est}$, $\Delta\text{fm.plrt1}$, $\Delta\text{om.plrt1}$, $\Delta\text{om.plrt2}$), and the average pupil diameter difference from significant clusters indicated by the CBPT ($\Delta\text{pupil.est}$, $\Delta\text{pupil.plrt1}$, $\Delta\text{pupil.plrt2}$). Second, we analyzed whether averaged FM and OM power changes from clusters derived via CBPT in one task were predictive of FM and OM power changes in the other task. That is, at FM sensors during the EST, we analyzed whether $\Delta\text{PSD}_{\text{frontal}}$ could be predicted by $\Delta\text{fm.plrt}$. Using CBPT we tested the following model at each frequency between 2 and 14 Hz:

$$\Delta\text{PSD}_{\text{frontal}} \sim \Delta\text{fm.plrt} + (1 | \text{subjectID}).$$

Vice versa at FM sensors during the PLRT, we analyzed whether the respective $\Delta\text{PSD}_{\text{frontal}}$ could be predicted by the average power difference from the FM stimulation cluster during the EST using CBPT with the following model at each frequency between 2 and 14 Hz:

$$\Delta\text{PSD}_{\text{frontal}} \sim \Delta\text{fm.est} + (1 | \text{subjectID}).$$

At OM sensors during the EST we tested whether $\Delta\text{PSD}_{\text{occipital}}$ could be predicted by $\Delta\text{om.plrt1}$ and $\Delta\text{om.plrt2}$ again using CBPT with the following model at each time point between 2 and 14 Hz:

$$\Delta\text{PSD}_{\text{occipital}} \sim \Delta\text{om.plrt1} + \Delta\text{om.plrt2} + (1 | \text{subjectID}).$$

Vice versa at OM sensors during the PLRT, we tested whether the respective $\Delta\text{PSD}_{\text{occipital}}$ could be predicted by $\Delta\text{om.est}$ in the same way with the following model at each frequency between 2 and 14 Hz:

$$\Delta\text{PSD}_{\text{occipital}} \sim \Delta\text{om.est} + (1 | \text{subjectID}).$$

We finally tested whether stimulation-specific changes in PD during one task could be predicted by the averaged difference in PD from significant clusters in the other. That is, for EST we tested whether $\Delta\text{PD}_{\text{EST}}$ could be predicted by $\Delta\text{pupil.plrt1}$ and $\Delta\text{pupil.plrt2}$. CBPT was used to test the following model at each time point between -200 and 5000 ms:

$$\Delta\text{PD}_{\text{EST}} \sim \Delta\text{pupil.plrt1} + \Delta\text{pupil.plrt2} + (1 | \text{subjectID}).$$

Vice versa for the PLRT, we tested whether $\Delta\text{PD}_{\text{PLRT}}$ could be predicted by $\Delta\text{pupil.est}$ with the following model at each time point between -200 and 7000 ms:

$$\Delta\text{PD}_{\text{PLRT}} \sim \Delta\text{pupil.est} + (1 | \text{subjectID}).$$

Results

Behavior

Accuracy in the EST was systematically modulated by the congruency of the stimuli and taVNS. The mixed effect logistic regression revealed that the predictor congruency was a significant indicator of accuracy ($\beta = 0.92$, $p < 0.001$, Fig. 2A). This positive beta estimate corresponds to an odds ratio (OR) of 2.51, indicating that in congruent trials subjects were ~ 2.51 times more likely to give a correct response. Importantly, we also

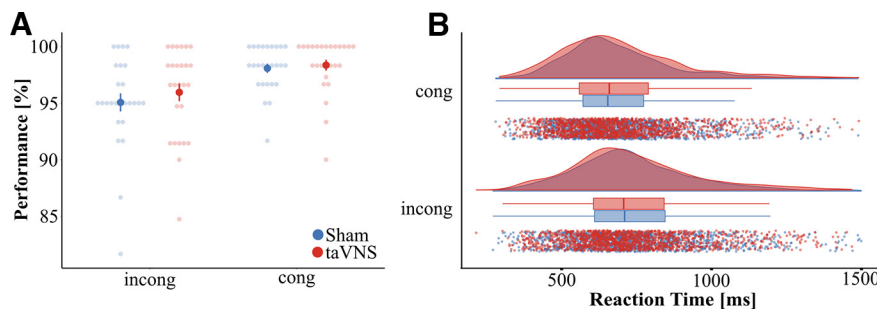


Figure 2. Behavior. **A**, During the EST, subjects made fewer errors in congruent trials and during taVNS. **B**, Subjects responded faster during congruent trials compared with incongruent trials, but no effect of stimulation and no stimulation-congruency-interaction was observed. Error bars in **A** represent SEM.

observed a significant effect of vagus nerve stimulation ($\beta = 0.44$, $p = 0.03$) corresponding to an OR of 1.55. This indicates that during taVNS, subjects were 1.55 times more likely to give a correct response than in the sham stimulation. Furthermore, we observed a significant effect of the predictor trial number ($\beta = 0.005$, $p < 0.001$), corresponding to an OR of 1.005, which indicates that accuracy slowly improved over the duration of the experiment. No significant effect was observed for the predictor face emotion ($\beta = 0.06$, $p = 0.7$), stimulation intensity ($\beta = -0.24$, $p = 0.57$), or the stimulation-by-congruency interaction ($\beta = 0.02$, $p = 0.95$).

Reaction time during the EST was significantly modulated by congruency. The LMM revealed a significant effect of the predictor congruency ($\chi_{(1)}^2 = 57.13$, $p < 0.001$; Fig. 2B). Subjects responded faster during congruent trials (mean = 699.88 ms, SD = 260.62 ms) compared with incongruent trials (mean = 753.69 ms, SD = 254.43 ms). Further, the trial number was also a significant indicator of RT ($\chi_{(1)}^2 = 75.59$, $p < 0.001$), indicating that subjects responded faster over the duration of the experiment ($\beta = -0.49$, SE = 0.06, $t = -8.6$). No effects on RTs were observed for the predictors stimulation ($\chi_{(1)}^2 = 0.37$, $p = 0.54$), face ($\chi_{(1)}^2 = 2.01$, $p = 0.16$), stimulation intensity ($\chi_{(1)}^2 = 0.43$, $p = 0.51$), or the stimulation-by-congruency interaction ($\chi_{(1)}^2 = 1.36$, $p = 0.24$).

Pupillometry

Figure 3 shows the PD and differences in pupil dilation separately for each condition during the EST and PLRT. PD during the EST was systematically modulated by congruency and stimulation. For the factor congruency, regardless of stimulation, CBPT indicated a significant difference between conditions. This corresponded to a significant cluster in the observed data between 770 and 2500 ms poststimulus ($p_{cluster} = 0.0001$; Fig. 3A, B) with greater pupil dilation during incongruent trials (mean = 0.19 z score, SD = 1.37) compared with congruent trials (mean = 0.12 z score, SD = 1.38). Cohen's d of the average pupil dilations from that cluster (d_{avg}) was 0.43, the maximal Cohen's d during that cluster (d_{max}) was 0.58 at 1280 ms poststimulus. Both congruency conditions show the well-known light reflex to the face stimuli (Grueschow et al., 2021, 2022; Fig. 3A), which is absent when both conditions are directly contrasted (Fig. 3B). The CBPT further indicated a significant effect of the predictor stimulation, corresponding to a cluster between 400 and 3200 ms poststimulus ($p_{cluster} = 0.0001$; Fig. 3C,D) with greater pupil dilation during taVNS (mean = 0.13 z score, SD = 1.35) compared with sham stimulation (mean = -0.005 z score, SD = 1.37, $d_{avg} = -0.47$, $d_{max} = -0.6$ at 2150 ms poststimulus). Furthermore, the CBPT also indicated a congruency-by-stimulation interaction corresponding to five clusters between 60 and 190 ms, 720 and 1730 ms, 1970

and 2180 ms, 3120 and 3250 ms, and 3970 and 5000 ms poststimulus (Fig. 3E,F). Figure 3F shows the difference between incongruent and congruent trials for both, sham and taVNS. For all clusters, nested LMMs were computed to resolve these interactions. However, only the model with stimulation nested in congruency for the cluster between 720 and 1730 ms indicated a trend toward a taVNS effect only during congruent trials ($\beta = 0.13$, SE = 0.07, $t_{(69)} = 1.9$, $p = 0.06$) but not during incongruent trials ($\beta = 0.07$, SE = 0.07, $t_{(69)} = 1$, $p = 0.33$). No other nested model indicated significant effects (all p values > 0.16). Finally, the CBPT indicated an effect of the factor stimulation intensity corresponding to a cluster between 860 and 5000 ms poststimulus ($p_{cluster} = 0.0001$). As stimulation intensity is a continuous variable, we report the average beta estimate from the significant cluster to provide an overview of the size and direction of the effect. This resulted in an average beta of 0.236, indicating that higher stimulation intensities were associated with higher PD.

Pupil constriction during the PLRT was also systematically modulated by stimulation and stimulation intensity. The CBPT indicated a significant effect of the continuous variable stimulation intensity corresponding to a cluster between 300 and 6500 ms poststimulus ($p_{cluster} = 0.0001$). Here, the average beta estimate was -0.299 , indicating that an increase in stimulation intensity reduced the pupil constriction. The CBPT also indicated a difference between taVNS and sham stimulation corresponding to two clusters, the first between 100 and 1200 ms and the second between 1900 and 7000 ms poststimulus (both $p_{cluster} = 0.0001$; Fig. 3G,H). Average pupil diameter in both clusters was higher (i.e., less constricted) during taVNS (cluster 1, mean = -1.85 z score, SD = 1.32; cluster 2, mean = -0.59 z score, SD = 0.93) compared with sham (cluster 1, mean = -2 z score, SD = 1.24, $d_{avg} = -0.51$, $d_{max} = -1.47$ at 340 ms; cluster 2, mean = -0.66 z score, SD = 0.89, $d_{avg} = -0.35$, $d_{max} = -0.42$ at 5180 ms). In cluster 1, the peak constriction amplitude ($\chi_{(1)}^2 = 7.56$, $p = 0.006$), the peak constriction velocity ($\chi_{(1)}^2 = 12.03$, $p = 0.0006$), and the average constriction velocity ($\chi_{(1)}^2 = 11.44$, $p = 0.0007$) were modulated by stimulation intensity but not by stimulation (all p values > 0.09). Inspection of the corresponding beta estimates indicated that higher stimulation intensities corresponded to higher (i.e., more negative) peak constriction amplitudes ($\beta = -0.59$, SE = 0.21, $t = -2.75$), higher peak constriction velocities ($\beta = -1.52$, SE = 0.44, $t = -3.47$), and higher average constriction amplitudes ($\beta = -0.82$, SE = 0.24, $t = -3.38$). The onset of the PLR was significantly modulated by stimulation ($\chi_{(1)}^2 = 9.92$, $p = 0.002$) but not by stimulation intensity ($p = 0.15$). The onset of the PLR was delayed during taVNS (mean = 197.92 ms, SD = 66.59) compared with sham stimulation (mean = 170.83 ms, SD = 62.27, $\beta = 25.3$, SE = 8.03, $t = 3.15$). In the second cluster,

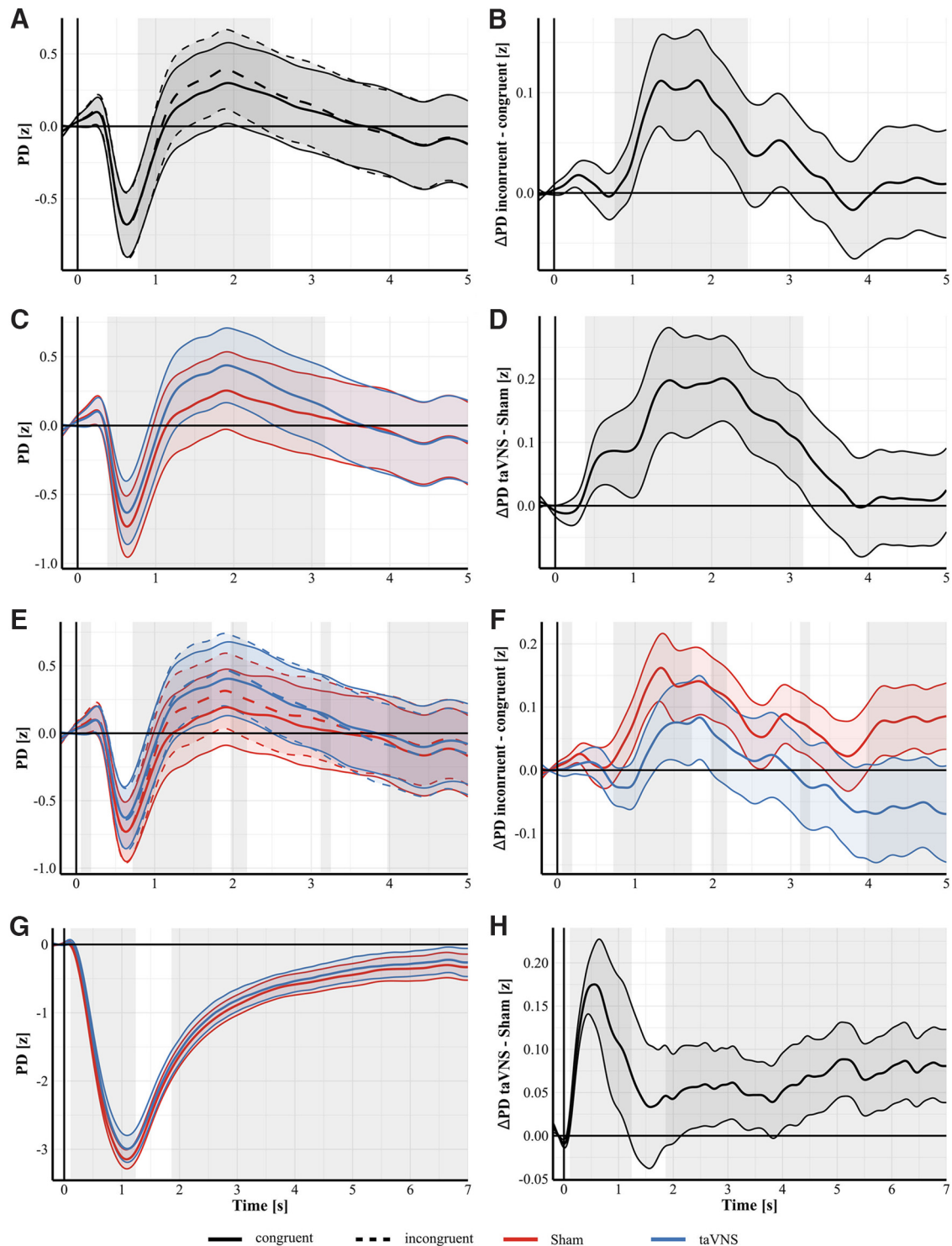


Figure 3. Pupil dilation separately for conditions (left) and difference waves (right). **A, B**, Effect of congruency. Grand average PD from the EST during incongruent (dashed lines) and congruent (solid lines) trials (**A**). Difference between incongruent and congruent trials during the EST (**B**). Permutation testing indicated a significant difference between incongruent and congruent trials corresponding to a cluster between 770 and 2500 ms poststimulus with higher PD during incongruent trials compared with congruent trials (gray shaded rectangle indicates the significant cluster). **C, D**, Effect of stimulation. Grand average PD from the EST during taVNS (blue) and Sham stimulation (red); **C**. Difference between taVNS and Sham stimulation during the EST (**D**). Permutation testing indicated a significant difference corresponding to cluster between 400 and 3200 ms poststimulus (gray shaded rectangle) with higher PD during taVNS. **E, F**, Stimulation-by-congruency interaction. Grand average PD from the EST for both congruent (solid) and incongruent (dashed) trials during taVNS (blue) and Sham (red) stimulation (**E**). Difference between incongruent and congruent trials during taVNS (blue) and Sham stimulation (red); **F**). Permutation testing indicated a significant stimulation-by-congruency interaction corresponding to five clusters in our data (gray shaded rectangles; see Pupillometry Results for details). **G, H**, Effect of stimulation during the PLRT. Grand average PD from the PLRT during taVNS (blue) and Sham stimulation (red); **G**. Difference between taVNS (blue) and Sham stimulation (red) during the PLRT (**H**). Permutation testing indicated a significant difference between taVNS and Sham stimulation corresponding to two clusters between 100 and 1200 ms and 1900 and 7000 ms poststimulus (gray shaded rectangles). PD was higher (i.e., less constricted) during taVNS compared with Sham stimulation in both clusters. Shaded areas around curves indicate SEM.

neither average nor peak dilation velocity were affected by stimulation (all p values > 0.35) or by intensity (all p values > 0.05).

MEG

Baseline brain activity at frontal and occipital sensors between conditions was analyzed using separate LMMs. Neither model revealed an effect of condition (frontal, $\chi_{(5)}^2 = 6.8$, $p = 0.23$; occipital, $\chi_{(5)}^2 = 0.51$, $p = 0.99$) indicating there were no differences in baseline brain activity. Figure 4 shows the power at FM and OM gradiometers during the EST for the different experimental conditions and their respective difference. Power at FM gradiometers during the EST was systematically modulated by congruency, stimulation, and stimulation intensity. The CBPT indicated a significant effect of the predictor stimulation intensity corresponding to a cluster between 2 and 14 Hz ($p_{cluster} = 0.0001$). The average beta estimate from that cluster was -4^{-26} , indicating a reduction in power with increasing stimulation intensity. The CBPT further indicated an effect of the predictor congruency corresponding to a cluster between 2 and 10 Hz ($p_{cluster} = 0.0001$; Fig. 4A,B). FM power within that frequency range was higher during incongruent trials (mean = $0.59 \text{ pT}^2/\text{cm}$, SD = 0.4) compared with congruent trials (mean = $0.58 \text{ pT}^2/\text{cm}$, SD = 0.39, $d_{avg} = 0.47$, $d_{max} = 0.62$ at 8.5 Hz). The CBPT also indicated an effect of the predictor stimulation corresponding to a cluster between 4 and 14 Hz ($p_{cluster} = 0.0001$; Fig. 4C,D). FM power within that frequency range was higher during taVNS (mean = $0.522 \text{ pT}^2/\text{cm}$, SD = 0.39) compared with sham stimulation (mean = $0.508 \text{ pT}^2/\text{cm}$, SD = 0.38, $d_{avg} = -0.4$, $d_{max} = 0.52$ at 7.5 Hz). Finally, the CBPT indicated a congruency-by-stimulation interaction on FM power during the EST corresponding to two clusters in our data, one between 2 and 4.5 Hz ($p_{cluster} = 0.0001$) and the second between 8.5 and 10 Hz ($p_{cluster} = 0.0003$). Nested linear mixed models were used to resolve the interaction in both clusters. For the first cluster between 2 and 4.5 Hz, neither the model with congruency nested in stimulation nor the respective model with stimulation nested in congruency revealed significant effects (all p values > 0.06). In the second cluster between 8.5 and 10 Hz, the model with stimulation nested in congruency revealed a significant effect of stimulation only during incongruent trials ($\beta = 1.73^{-26}$, SE = 6.7^{-27} , $t = 2.6$, $p = 0.01$) but not during congruent trials ($\beta = 1.18^{-26}$, SE = 6.7^{-27} , $t = 1.78$, $p = 0.07$). During incongruent trials, taVNS caused higher power (mean = $0.483 \text{ pT}^2/\text{cm}$, SD = 0.3) compared with sham (mean = $0.467 \text{ pT}^2/\text{cm}$, SD = 0.28). The corresponding model with congruency nested in stimulation revealed no significant effects (all p values > 0.14). Furthermore, no effects of stimulation intensity were observed in either of the two clusters (both p values > 0.07).

Power at OM gradiometers during the EST was also systematically modulated by congruency, stimulation, and stimulation intensity. The respective CBPT indicated an effect of the predictor stimulation intensity corresponding to a cluster in our data between 2 and 10.5 Hz ($p_{cluster} = 0.0001$). The average beta estimate from that cluster was -9.43^{-26} indicating a reduction in power in that frequency range with increasing stimulation intensity. The CBPT also indicated an effect of congruency corresponding to three clusters in our data (Fig. 4E,F). The first between 2 and 4.5 Hz ($p_{cluster} = 0.0001$), the second between 8 and 9 Hz ($p_{cluster} = 0.0085$), and the third between 11 and 12.5 Hz ($p_{cluster} = 0.0001$). In the first two clusters (between 2 and 4.5 Hz and 8 and 9 Hz) power was higher during incongruent trials (cluster 1, mean = $0.771 \text{ pT}^2/\text{cm}$, SD = 0.57; cluster 2, mean = $0.573 \text{ pT}^2/\text{cm}$, SD = 0.44) compared with congruent

trials (cluster 1, mean = $0.767 \text{ pT}^2/\text{cm}$, SD = 0.55, $d_{avg} = 0.18$, $d_{max} = 0.18$ at 4.5 Hz; cluster 2, mean = $0.57 \text{ pT}^2/\text{cm}$, SD = 0.43, $d_{avg} = 0.24$, $d_{max} = 0.27$ at 8.5 Hz). In the third cluster between 11 and 12.5 Hz power was higher during congruent trials (mean = $0.513 \text{ pT}^2/\text{cm}$, SD = 0.39) compared with incongruent trials (mean = $0.51 \text{ pT}^2/\text{cm}$, SD = 0.38, $d_{avg} = -0.11$, $d_{max} = -0.13$ at 12 Hz). The CBPT further indicated a significant effect of stimulation corresponding to a cluster between 2 and 14 Hz ($p_{cluster} = 0.0001$; Fig. 4G,H). Average OM power in that frequency range was lower during taVNS (mean = $0.61 \text{ pT}^2/\text{cm}$, SD = 0.47) compared with sham stimulation (mean = $0.64 \text{ pT}^2/\text{cm}$, SD = 0.55, $d_{avg} = 0.3$, $d_{max} = 0.48$ at 10.5 Hz). Finally, the CBPT indicated an effect of the congruency-by-stimulation interaction corresponding to two clusters in our data, one between 2 and 4.5 Hz ($p_{cluster} = 0.0001$) and one between 10.5 and 12.5 Hz ($p_{cluster} = 0.0001$). Nested models were again used to resolve the interaction with each predictor nested within the other and stimulation intensity as fixed effects. Random intercepts across subjects were set as random effects. In the first cluster neither the model with stimulation nested in congruency nor the model with congruency nested in stimulation revealed a significant effect (all p values > 0.46). In the second cluster the model with stimulation nested in congruency revealed a significant effect of stimulation only during congruent trials ($\beta = -3.42^{-26}$, SE = 1.4^{-26} , $t = -2.45$, $p = 0.01$) but not during incongruent trials ($\beta = -2.5^{-26}$, SE = 1.4^{-26} , $t = -1.8$, $p = 0.07$). Power was lower during taVNS (mean = $0.54 \text{ pT}^2/\text{cm}$, SD = 0.37) compared with sham stimulation (mean = $0.57 \text{ pT}^2/\text{cm}$, SD = 0.47).

Figure 5 shows the power at FM and OM gradiometers during the PLRT separately for the different stimulation conditions and their respective difference. Power at FM gradiometers during the PLRT was systematically modulated by stimulation. The respective CBPT indicated a significant effect of the predictor stimulation, corresponding to a cluster in our data between 3.5 and 7 Hz ($p_{cluster} = 0.0001$; Fig. 5A,B). Power was higher during taVNS (mean = $0.29 \text{ pT}^2/\text{cm}$, SD = 0.2) compared with sham stimulation (mean = $0.275 \text{ pT}^2/\text{cm}$, SD = 0.19, $d_{avg} = -0.37$, $d_{max} = -0.38$ at 5 Hz). No effect of stimulation intensity was observed. Power at OM gradiometers during the PLRT was modulated by stimulation and stimulation intensity. The respective CBPT indicated an effect of the predictor stimulation intensity corresponding to a cluster between 2 and 14 Hz ($p_{cluster} = 0.0001$). The average beta estimate from that cluster was -3.26^{-26} indicating a reduction in power in that frequency range with increasing stimulation intensity. The CBPT further indicated an effect of the predictor stimulation corresponding to two clusters in our data, one between 5.5 and 6.5 Hz and one between 10 and 12.5 Hz (Fig. 5C,D). Power in both clusters was lower during taVNS (cluster 1, mean = $0.278 \text{ pT}^2/\text{cm}$, SD = 0.18; cluster 2, mean = $0.211 \text{ pT}^2/\text{cm}$, SD = 0.13) compared with sham stimulation. (cluster 1, mean = $0.291 \text{ pT}^2/\text{cm}$, SD = 0.21, $d_{avg} = 0.34$, $d_{max} = 0.34$ at 6 Hz; cluster 2, mean = $0.226 \text{ pT}^2/\text{cm}$, SD = 0.17, $d_{avg} = 0.38$, $d_{max} = 0.41$ at 11.5 Hz).

Power at OM Gradiometers during the EST was also modulated by taVNS after stimulation offset. The CBPT between 600 and 5000 ms poststimulus indicated a difference between taVNS (Fig. 6A) and sham (Fig. 6B) corresponding to a cluster in the alpha range between ~ 8.5 and 13 Hz, ~ 1000 ms after stimulus onset and 500 ms after stimulation offset at parieto-occipital sensors ($p_{cluster} = 0.034$). During taVNS, alpha power was lower compared with sham (Fig. 6C). Figure 6D shows the time course of the averaged alpha power between 8.5 and 13 Hz. Power values from the time period between 0 and 500 ms were cut from

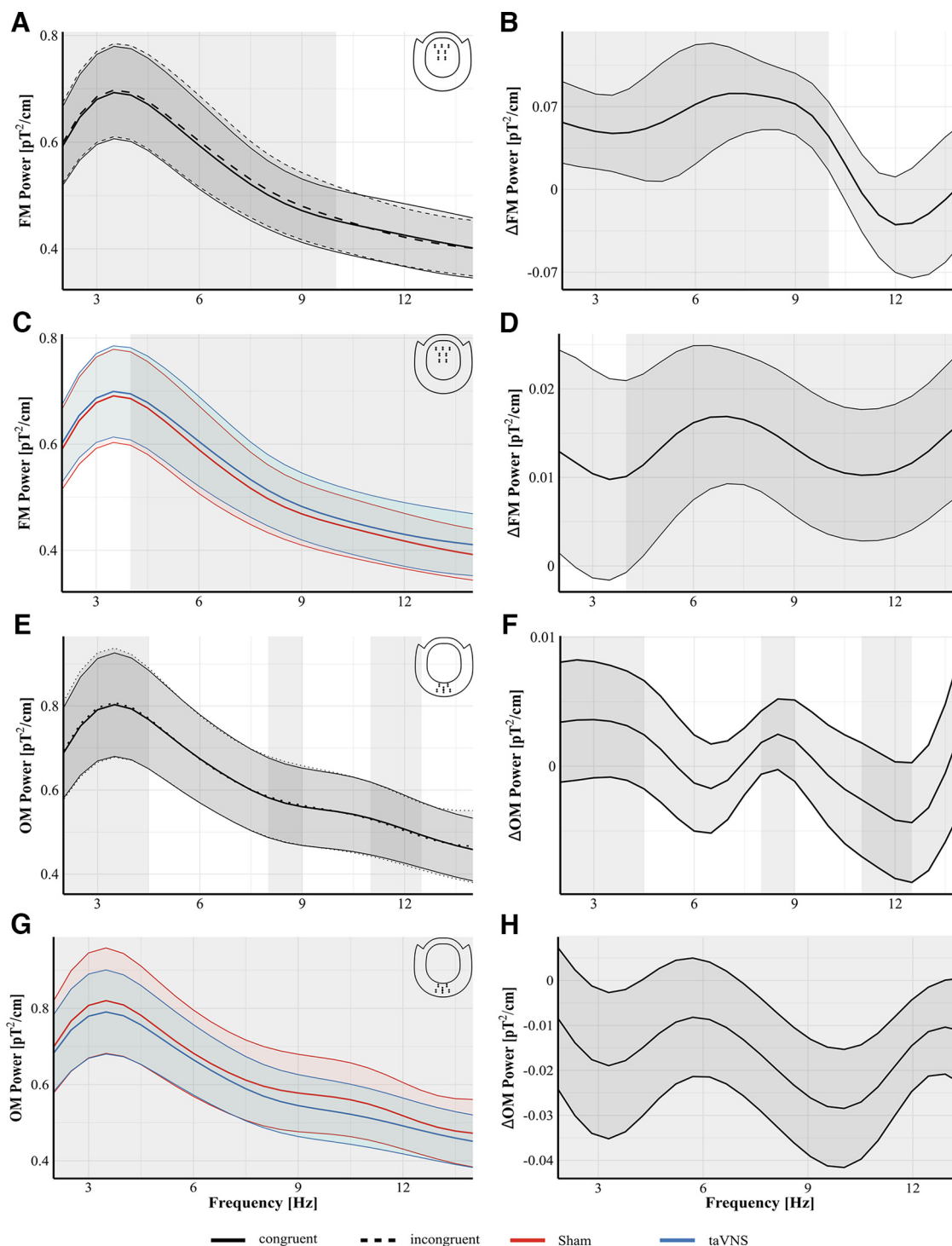


Figure 4. Fourier spectra for conditions (left) and difference waves (right) during the EST. **A, B**, Effect of congruency on FM sensors. Inset, top right (**A**), Grand average FFT at FM sensors from the EST during incongruent (dashed) and congruent (solid) trials. Difference between incongruent and congruent trials during the EST (**B**). Permutation testing indicated a significant difference between incongruent and congruent trials corresponding to a cluster between 2 and 10 Hz with higher power during incongruent trials compared with congruent trials (gray shaded rectangle indicates the significant cluster). **C, D**, Effect of stimulation on FM sensors. Inset, top right (**C**), Grand average FFT at FM sensors from the EST during taVNS (blue) and Sham stimulation (red). Difference between taVNS and Sham stimulation during the EST (**D**). Permutation testing indicated a significant difference corresponding to cluster between 4 and 14 Hz (gray shaded rectangle) with higher power during taVNS. **E, F**, Effect of congruency on OM sensors in the EST. Inset, top right (**E**), Grand average FFT at OM sensors for both congruent (solid) and incongruent (dashed) trials. Difference between incongruent and congruent trials during the EST (**F**). Permutation testing indicated a significant difference corresponding to three clusters (gray shaded rectangles; see MEG Results for details). **G, H**, Effect of stimulation on OM sensors in the EST. Inset, top right (**G**), Grand average FFT at OM sensors from the EST during taVNS (blue) and Sham stimulation (red). Difference between taVNS and Sham stimulation during the EST (**H**). Permutation testing indicated a significant difference corresponding to cluster between 2 and 14 Hz (gray shaded rectangle) with lower power during taVNS. Shaded areas around curves indicate SEM.

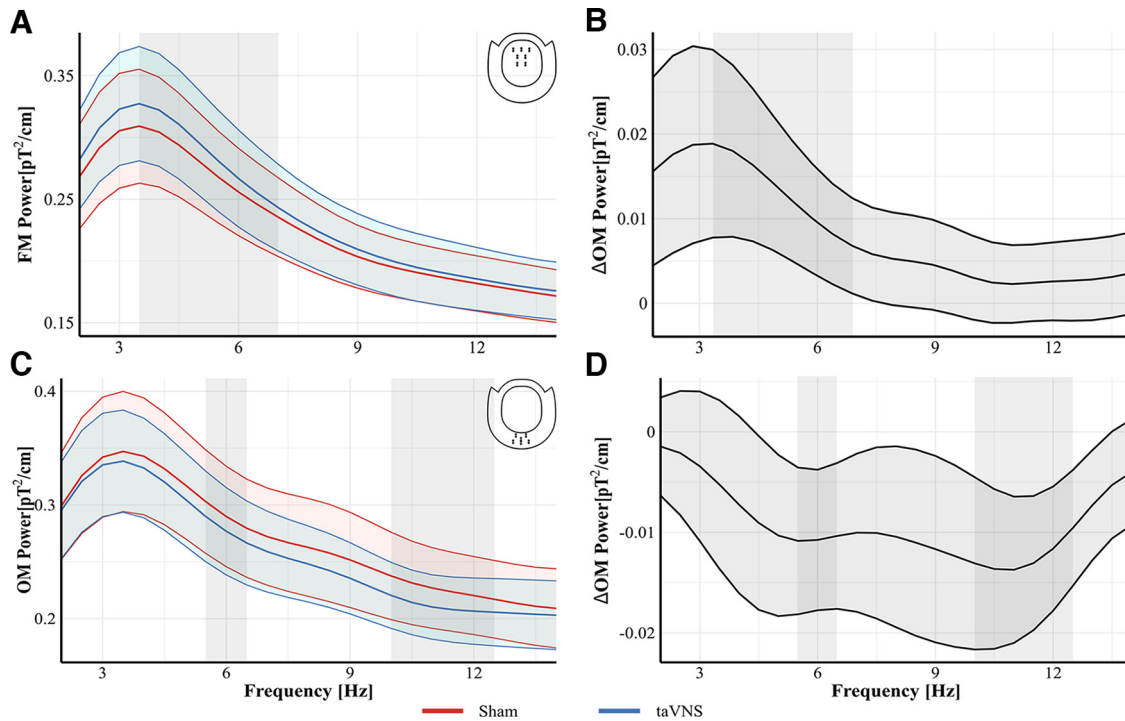


Figure 5. Fourier spectra for conditions (left) and difference waves (right) during the PLRT. **A, B**, Effect of stimulation at FM sensors during the PLRT. Inset, top right (**A**) Grand average FFT at FM sensors from the PLRT for taVNS (blue) and sham (red). Difference between taVNS and sham trials during the PLRT (**B**). Permutation testing indicated a significant difference between taVNS and sham corresponding to a cluster between 3.5 and 7 Hz (gray rectangle) with higher power during taVNS. **C, D**, Effect of stimulation at OM sensors during the PLRT. Inset, top right (**C**), Grand average FFT at OM sensors for taVNS (blue) and sham (red). Difference between taVNS and sham trials during the PLRT (**D**). Permutation testing indicated a difference between taVNS and sham corresponding to two clusters between 5.5 and 6.5 and between 10.5 and 12 Hz (gray shaded rectangle) with lower power during taVNS in both clusters. Shaded areas around curves indicate the SEM.

the data for visualization to indicate that this period was not included in this analysis. The CBPT on TFR data during the PLRT indicated no significant difference.

Relationship between parameters across tasks

Finally, we examined whether electrophysiological and pupillometric measures in one task could be predicted by the corresponding measure in the other task. For the pupil differences during the EST, CBPT indicated that neither $\Delta\text{pupil.plrt1}$ nor $\Delta\text{pupil.plrt2}$ were significant predictors for $\Delta\text{PD}_{\text{EST}}$. For the pupil differences during the PLRT, CBPT indicated also no significant effect of $\Delta\text{pupil.est}$.

For the FM power differences during the EST, CBPT indicated that $\Delta\text{fm.plrt}$ was a significant predictor over the entire analyzed frequency range between 2 and 14 Hz ($p_{\text{cluster}} = 0.0001$). The average positive beta estimate from within that cluster of 1.37^{-26} indicated that subjects with higher FM power differences during the PLRT (i.e., more power during taVNS) also exhibited higher FM power differences during the EST. Vice versa, for FM power differences during the PLRT the CBPT indicated an effect of $\Delta\text{fm.est}$ corresponding to a cluster between 2 and 14 Hz in our data ($p_{\text{cluster}} = 0.0001$). Again, the positive average beta estimate of 4.7^{-27} indicated that subjects with higher-power differences in the EST also exhibited higher-power differences in the PLRT. For the OM power differences during the EST, the respective CBPT indicated an effect of $\Delta\text{om.plrt1}$ corresponding to a cluster between 2 and 14 Hz ($p_{\text{cluster}} = 0.0001$) with an average beta estimate of -1.12^{-26} . This negative beta indicates that subjects who showed lower OM power during the PLRT ~ 6 Hz also exhibited lower OM power during the EST. Apart from that, the CBPT indicated no effect of $\Delta\text{om.plrt2}$. Finally, the CBPT on

OM power differences during the PLR indicated an effect of $\Delta\text{om.est}$ corresponding to a cluster between 2 and 6.5 Hz ($p_{\text{cluster}} = 0.0002$). The average beta estimate was -6.2^{-27} , indicating again that subjects with lower OM power in the EST also exhibited lower OM power in the PLRT.

Discussion

In this study, we show for the first time that phasic event-related taVNS systematically modulates behavioral, pupillary, and electrophysiological parameters of LC-NA activity during cognitive processing. We show that taVNS (1) increased pupil dilation and improved performance in an EST, (2) reduced the amplitude and delayed the onset of the pupil constriction of the PLR task, and (3) increased task-related theta and alpha power while reducing occipital alpha power. These results extend previous work on taVNS that has solely used task-free settings (Sharon et al., 2021; Urbin et al., 2021; D'Agostini et al., 2023) and demonstrate for the first time that taVNS systematically modulates the pupil light reflex. Finally, we show that electrophysiological parameters were associated across tasks. Higher taVNS-induced FM power in the EST was associated with higher taVNS-induced FM power in the PLRT, and lower OM power in the EST during taVNS was associated with lower OM power in the PLRT during taVNS.

Despite the stimulation duration, our study matched former taVNS studies in terms of stimulation amplitude, pulse width, and frequency. It is thus likely that longer stimulation durations like 30 s (Warren et al., 2019; Burger et al., 2020a) or continuous stimulation (Keute et al., 2019; D'Agostini et al., 2021, 2022) only modulate tonic LC firing without an effect on phasic LC activity.

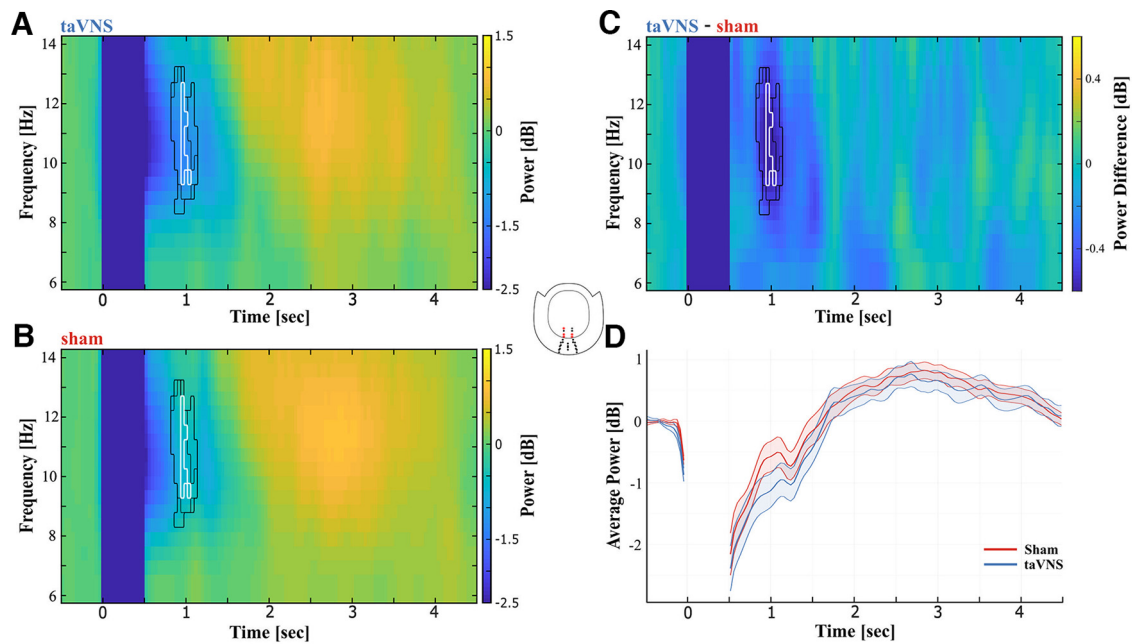


Figure 6. Differences in alpha power at occipital midline gradiometers between taVNS and sham. CBPT was performed for OM gradiometers between 600 and 5000 ms poststimulus. Inset, middle, The analysis indicated a difference between taVNS and sham in the alpha range \sim 1000 ms poststimulus at parieto-occipital sensors. Power in this cluster during taVNS was lower compared with sham stimulation. **A**, TFR from these sensors for taVNS. **B**, TFR from these sensors for sham. **C**, Difference between taVNS and sham. Black outlines in **A–C** represent the significant time-frequency cluster for each individual sensor. White outlines in **A–C** represent the overlap of time-frequency clusters that were significant in all five sensors. **D**, Time course of averaged alpha power between 8.5 and 13 Hz. The period between 0 and 500 ms was not considered in the analysis and was blanked out in the figure accordingly. The shaded area around curves indicates SEM.

Behavioral results during the EST show the expected Stroop effect, that is, an increase in RT and a decrease in accuracy during incongruent trials, indicating processing costs for conflict resolution (Botvinick et al., 2001). More importantly, we additionally observed a stimulation-specific effect on accuracy during the EST. During taVNS, subjects responded more accurately compared with sham stimulation. Remarkably, this effect was apparent despite the notable occurrence of numerous subjects achieving or closely approaching ceiling levels, denoting perfect accuracy (i.e., 100%). This might have attenuated the stimulation effect on behavioral performance. Tasks that are more difficult, or subject populations already exhibiting impaired cognitive control, might show stronger benefits on behavioral accuracy from taVNS. Interestingly, this behavioral improvement was accompanied by a stimulation-specific increase in FM theta and alpha power. Reaction times, however, were not affected by taVNS. This might be because of the fact that our sample consisted of relatively young, healthy adults, who already performed at or near optimal levels with little to no room for improvement in reaction time. Again, subject groups with already impaired cognitive control might show improved reaction times by taVNS. However, this is only speculative and needs further investigation.

Our observations further underline the potential of FM theta power as an electrophysiological marker of taVNS during cognitive processing. The increase in FM alpha power, however, was somewhat surprising, as recent studies suggest an overall reduction in cortical alpha power (Lewine et al., 2019; Sharon et al., 2021). In these studies, alpha was viewed as an idling state of low cortical arousal. However, this notion is debated (Cooper et al., 2003), for instance, by studies showing increased alpha power with increasing working memory load (Klimesch, 1999; Jensen et al., 2002). Additionally, internally directed attention has been associated with higher alpha power at frontal and central locations (Cooper et al., 2003). Thus, the observed increase in alpha

power following taVNS could be because of direct noradrenergic modulation or reflect a shift toward more internally directed attention as an indirect effect of increased LC-NA activity. However, as we did not ask participants about their focus of attention, this notion warrants further investigation. Finally, we replicated the decrease in occipital alpha power following taVNS (Sharon et al., 2021) but now in an active cognitive task with visual stimulation. We observed these taVNS-specific effects on occipital alpha power during both the EST as well as the PLRT. In both tasks, power in the alpha range at OM gradiometers was reduced following taVNS compared with sham stimulation. Although the passive PLRT might be more comparable to previous work that applied taVNS in a task-free environment (Sharon et al., 2021), we extend previous findings by the observation that a comparable decrease can also be observed during cognitive processing. This provides further evidence for the potential of occipital alpha power as an indicator of taVNS efficacy. However, these results must be interpreted with care because of our correction of the stimulation artifact. For that, we removed contaminated portions of the data and interpolated these gaps using an autoregressive function. As we used monophasic pulses, which seem to cause longer-lasting artifacts compared with biphasic pulses (Keatch et al., 2022), we had to remove larger chunks of the original data. This might have decreased our signal-to-noise ratio, which could explain the small effect sizes observed in the theta range for the congruency effect. Our observations in the alpha range however are robust and replicate recent findings (Sharon et al., 2021). Therefore, we are optimistic that we did not overcompensate during our artifact rejection approach.

Our pupil recordings during the EST show the well-known incongruency effect, that is, stronger pupil dilation during incongruent trials compared with congruent trials (Grueschow et al., 2020, 2021), further supporting the involvement of the LC-NA system in the resolution of response conflicts. Most importantly,

however, we also observed a strong stimulation-specific effect on pupil diameter. We observed increased pupil dilation following taVNS, suggesting a stimulation-induced increased level of noradrenergic tone. The LC shows two discernable activity patterns, (1) a tonic baseline activation and (2) a phasic burst-like activation following salient or behaviorally relevant stimuli. Tonic LC activity is related to baseline PD, whereas the phasic activation is reflected in transient increases in PD (Aston-Jones and Cohen, 2005). One could argue that the phasic stimulation used in our study, in contrast to the often used 30 s of taVNS, could better mimic and thus amplify the phasic activation pattern of the LC. This then leads to an amplification of phasic LC activations after relevant stimuli, which then causes an observable, transient increase in pupil diameter. The temporal dynamic of longer stimulation intervals is closer in resemblance to the tonic activation pattern without the increased effect on transient pupil dynamics. The pupil diameter is controlled by the interplay of two antagonistic muscles—the sympathetically innervated pupil dilator muscle and the parasympathetically innervated pupil sphincter muscle. Sympathetic neurons innervating the dilator muscle originate in the superior cervical ganglion. Parasympathetic innervation stems from the ciliary ganglion, which in turn receives input from the EWN (Eckstein et al., 2017; Hall and Chilcott, 2018). NA plays a key role in both systems. It reduces activity in the EWN through inhibitory α_2 -adrenoreceptor and activates the pupil dilator muscle via excitatory α_1 -adrenoreceptors (Samuels and Szabadi, 2008a, b; Hall and Chilcott, 2018). Thus, either activation of the sympathetic or inhibition of the parasympathetic route can lead to pupil dilation. This leads to three potential explanations for our results. First, through sole central inhibition of the EWN. In this case, the pupil sphincter muscle would receive less input from the EWN during taVNS. The balance between both muscles would then shift towards relatively stronger activity in the sympathetic dilator muscle. Second, through sole excitation of the pupillary dilator muscle. In this case, taVNS would only activate the sympathetic part of the pupil's innervation. However, this is highly unlikely as NA would have to be released directly at the pupil only and not in the brain. The third possible explanation is the combination of both factors, that is, simultaneously increased activity in the sympathetic and increased inhibition of the parasympathetic route. In our eyes, the first explanation is the most plausible. A study in mice investigated the pathways necessary for the pupil dilation following direct phasic LC stimulation. After surgical removal of the superior cervical ganglion and pharmacological blockage of α_2 -adrenoreceptors in the EWN through yohimbine, no pupil dilation in response to stimulation was observed. Importantly, ~ 1 h after yohimbine application, the stimulation-induced pupil dilation returned (Liu et al., 2017). This supports the idea of increased noradrenergic EWN inhibition as cause for the increased pupil dilation in our study. The same mechanism holds for the observed reduction of the PLR. Following the influx of light, activity in the EWN increases, which leads to a constriction of the pupillary sphincter muscle. During taVNS, the increased NA concentration likely inhibited activity in the EWN, which, in turn, reduced pupil constriction. The observed increase in latency of the PLR is also in line with a pharmacological study, showing that NA reuptake inhibitors prolonged the latency of PLR (Theofilopoulos et al., 1995).

Although our pupillometric results are consistent with an increased LC activation, it is necessary to note that the LC-NA system is possibly not the only neuromodulatory system involved. The NTS is an important relay station in the brainstem, with

widespread connections to, for example, the raphe nuclei or limbic and forebrain areas (Krahl and Clark, 2012; Frangos et al., 2015). Especially, cholinergic projections from the basal forebrain are also known to mediate pupil dilation in rodents (Reimer et al., 2016; Mridha et al., 2021). Hence, a cholinergic interaction cannot completely be ruled out. Although these transmitter systems have most likely only secondary effects, their potential influence warrants future investigation.

Another limitation may concern the stimulation itself. Electrophysiological recordings during active stimulation suffer from the presence of stimulation artifacts several orders of magnitudes stronger than the actual brain activity, and MEG is especially susceptible to these artifacts. Thus, the number of studies that apply stimulation while simultaneously recording brain activity is limited, and only a handful of MEG studies that applied taVNS during critical periods (e.g., onset of target stimuli) have been conducted so far (Lehtimäki et al., 2013; Hyvärinen et al., 2015; Keatch et al., 2022). Different artifact correction mechanisms, like temporal signal space separation (Taulu and Simola, 2006), have been applied, but nonlinear components of the artifact make it hard to capture. Although previous studies on simultaneous MEG and taVNS used temporal signal space separation as an artifact cleaning method (Lehtimäki et al., 2013; Hyvärinen et al., 2015), we had to realize that this method was not adequately applicable for our data as it was unable to sufficiently remove the artifact from our MEG recordings. Accordingly, we implemented an artifact-cleaning approach as demonstrated in Keatch et al. (2022), which involved the exclusion and subsequent interpolation of contaminated time points. This method has been shown to retain a good amount of information in the signal, especially at lower frequencies. However, as interpolation bears the risk of altering the original data, this method has to be used with caution. Hence, better methods are required to sufficiently clean the electrical artifact to better estimate online taVNS effects. Future work is also needed to determine, whether phasic taVNS modulates other indirect LC-NA markers, for instance salivary alpha-amylase (Giraudier et al., 2022).

In conclusion, we show compelling evidence that phasic event-related taVNS modulates pupil dilation as well as theta and alpha power likely through central noradrenergic modulation. In contrast to previous work using task-free taVNS paradigms (Sharon et al., 2021; Urbin et al., 2021; D'Agostini et al., 2023), we show that these metrics can be obtained while being engaged in a cognitive task. This has the added bonus of investigating potential taVNS effects on behavioral performance as we have done here during a cognitive control task. Finally, we also show that the PLR can effectively be used to index taVNS effects, providing an additional, easy-to-use biomarker for future taVNS studies.

References

- Aston-Jones G, Cohen JD (2005) An integrative theory of locus coeruleus-norepinephrine function: adaptive gain and optimal performance. *Annu Rev Neurosci* 28:403–450.
- Bates D, Mächler M, Bolker B, Walker S (2015) Fitting linear mixed-effects models using lme4. *J Stat Soft* 67:1–48.
- Bergamin O, Kardon RH (2003) Latency of the pupil light reflex: sample rate, stimulus intensity, and variation in normal subjects. *Invest Ophthalmol Vis Sci* 44:1546–1554.
- Bitsios P, Szabadi E, Bradshaw CM (1999) Comparison of the effects of venlafaxine, paroxetine and desipramine on the pupillary light reflex in man. *Psychopharmacology (Berl)* 143:286–292.
- Botvinick MM, Carter CS, Braver TS, Barch DM, Cohen JD (2001) Conflict monitoring and cognitive control. *Psychol Rev* 108:624–652.

- Brainard DH (1997) The Psychophysics Toolbox. *Spatial Vis* 10:433–436.
- Burger AM, Van der Does W, Brosschot JF, Verkuil B (2020a) From ear to eye? No effect of transcutaneous vagus nerve stimulation on human pupil dilation: a report of three studies. *Biol Psychol* 152:107863.
- Burger AM, D'Agostini M, Verkuil B, Van Diest I (2020b) Moving beyond belief: a narrative review of potential biomarkers for transcutaneous vagus nerve stimulation. *Psychophysiology* 57:e13571.
- Butt MF, Albusoda A, Farmer AD, Aziz Q (2020) The anatomical basis for transcutaneous auricular vagus nerve stimulation. *J Anat* 236:588–611.
- Cakmak YO (2019) Concerning auricular vagal nerve stimulation: occult neural networks. *Front Hum Neurosci* 13:421.
- Capone F, Motolese F, Di Zazzo A, Antonini M, Magliozzi A, Rossi M, Marano M, Pilato F, Musumeci G, Coassin M, Di Lazzaro V (2021) The effects of transcutaneous auricular vagal nerve stimulation on pupil size. *Clin Neurophysiol* 132:1859–1865.
- Cavanagh JF, Frank MJ (2014) Frontal theta as a mechanism for cognitive control. *Trends Cogn Sci* 18:414–421.
- Cooper NR, Croft RJ, Dominey SJJ, Burgess AP, Gruzeliier JH (2003) Paradox lost? Exploring the role of alpha oscillations during externally vs. internally directed attention and the implications for idling and inhibition hypotheses. *Int J Psychophysiol* 47:65–74.
- D'Agostini M, Burger AM, Franssen M, Claes N, Weymar M, von Leupoldt A, Van Diest I (2021) Effects of transcutaneous auricular vagus nerve stimulation on reversal learning, tonic pupil size, salivary alpha-amylase, and cortisol. *Psychophysiology* 58:e13885.
- D'Agostini M, Burger AM, Villca Ponce G, Claes S, von Leupoldt A, Van Diest I (2022) No evidence for a modulating effect of continuous transcutaneous auricular vagus nerve stimulation on markers of noradrenergic activity. *Psychophysiology* 59:e13984.
- D'Agostini M, Burger AM, Franssen M, Perkovic A, Claes S, von Leupoldt A, Murphy PR, Van Diest I (2023) Short bursts of transcutaneous auricular vagus nerve stimulation enhance evoked pupil dilation as a function of stimulation parameters. *Cortex* 159:233–253.
- Dahl MJ, Mather M, Werkle-Bergner M (2022) Noradrenergic modulation of rhythmic neural activity shapes selective attention. *Trends Cogn Sci* 26:38–52.
- Desbeaumes Jodoin V, Lespérance P, Nguyen DK, Fournier-Gosselin M-P, Richer F (2015) Effects of vagus nerve stimulation on pupillary function. *Int J Psychophysiol* 98:455–459.
- Dippel G, Mückschel M, Ziemssen T, Beste C (2017) Demands on response inhibition processes determine modulations of theta band activity in superior frontal areas and correlations with pupillometry—implications for the norepinephrine system during inhibitory control. *Neuroimage* 157:575–585.
- Eckstein MK, Guerra-Carrillo B, Miller Singley AT, Bunge SA (2017) Beyond eye gaze: what else can eyetracking reveal about cognition and cognitive development? *Dev Cogn Neurosci* 25:69–91.
- Farmer AD, et al. (2021) International consensus based review and recommendations for minimum reporting standards in research on transcutaneous vagus nerve stimulation (version 2020). *Front Hum Neurosci* 14:568051.
- Fox J, Weisberg S (2019) *An R companion to applied regression*. 3rd ed. Thousand Oaks, CA: Sage.
- Frangos E, Ellrich J, Komisaruk BR (2015) Non-invasive access to the vagus nerve central projections via electrical stimulation of the external ear: fMRI evidence in humans. *Brain Stimul* 8:624–636.
- Frömer R, Maier M, Abdel Rahman R (2018) Group-level EEG-processing pipeline for flexible single trial-based analyses including linear mixed models. *Front Neurosci* 12:48.
- Giraudier M, Ventura-Bort C, Burger AM, Claes N, D'Agostini M, Fischer R, Franssen M, Kaess M, Koenig J, Liepelt R, Nieuwenhuis S, Sommer A, Usichenko T, Van Diest I, von Leupoldt A, Warren CM, Weymar M (2022) Evidence for a modulating effect of transcutaneous auricular vagus nerve stimulation (taVNS) on salivary alpha-amylase as indirect noradrenergic marker: a pooled mega-analysis. *Brain Stimul* 15:1378–1388.
- Grueschow M, Kleim B, Ruff CC (2020) Role of the locus coeruleus arousal system in cognitive control. *J Neuroendocrinol* 32:e12890.
- Grueschow M, Stenz N, Thörn H, Ehler U, Breckwoldt J, Brodmann Maeder M, Exadaktylos AK, Bingisser R, Ruff CC, Kleim B (2021) Real-world stress resilience is associated with the responsiveness of the locus coeruleus. *Nat Commun* 12:2275.
- Grueschow M, Kleim B, Ruff CC (2022) Functional coupling of the locus coeruleus is linked to successful cognitive control. *Brain Sciences* 12:305.
- Hall C, Chilcott R (2018) Eyeing up the future of the pupillary light reflex in neurodiagnostics. *Diagnostics* 8:19.
- Hulsey DR, Riley JR, Loerwald KW, Rennaker RL, Kilgard MP, Hays SA (2017) Parametric characterization of neural activity in the locus coeruleus in response to vagus nerve stimulation. *Exp Neurol* 289:21–30.
- Hysek CM, Liechti ME (2012) Effects of MDMA alone and after pretreatment with reboxetine, duloxetine, clonidine, carvedilol, and doxazosin on pupillary light reflex. *Psychopharmacology (Berl)* 224:363–376.
- Hyvärinen P, Yrttiäho S, Lehtimäki J, Ilmoniemi RJ, Mäkitie A, Ylikoski J, Mäkelä JP, Aarnisalo AA (2015) Transcutaneous vagus nerve stimulation modulates tinnitus-related beta- and gamma-band activity. *Ear Hear* 36:e76–e85.
- Jensen O, Gelfand J, Kounios J, Lisman JE (2002) Oscillations in the alpha band (9–12 Hz) increase with memory load during retention in a short-term memory task. *Cerebral Cortex* 12:877–882.
- Joshi S, Li Y, Kalwani RM, Gold JI (2016) Relationships between pupil diameter and neuronal activity in the locus coeruleus, colliculi, and cingulate cortex. *Neuron* 89:221–234.
- Keatch C, Lambert E, Woods W, Kameneva T (2022) Measuring brain response to transcutaneous vagus nerve stimulation (tvNS) using simultaneous magnetoencephalography (MEG). *J Neural Eng* 19:026038.
- Keute M, Demirezen M, Graf A, Mueller NG, Zaehle T (2019) No modulation of pupil size and event-related pupil response by transcutaneous auricular vagus nerve stimulation (taVNS). *Sci Rep* 9:11452.
- Keute M, Barth D, Liebrand M, Heinze H-J, Kraemer U, Zaehle T (2020) Effects of transcutaneous vagus nerve stimulation (tvNS) on conflict-related behavioral performance and frontal midline theta activity. *J Cogn Enhanc* 4:121–130.
- Kleiner M, Brainard D, Pelli D, Ingling A, Murray R, Broussard C, Cornelissen F (2007) What's new in Psychtoolbox-3? *Perception* 36:1116.
- Klimesch W (1999) EEG alpha and theta oscillations reflect cognitive and memory performance: a review and analysis. *Brain Res Brain Res Rev* 29:169–195.
- Krahl S, Clark K (2012) Vagus nerve stimulation for epilepsy: a review of central mechanisms. *Surg Neurol Int* 3:S255–S259.
- Kret ME, Sjak-Shie EE (2019) Preprocessing pupil size data: guidelines and code. *Behav Res Methods* 51:1336–1342.
- Kurniawan IT, Grueschow M, Ruff CC (2021) Anticipatory energization revealed by pupil and brain activity guides human effort-based decision making. *J Neurosci* 41:6328–6342.
- Kuznetsova A, Brockhoff PB, Christensen RHB (2017) lmerTest package: tests in linear mixed effects models. *J Stat Soft* 82:1–26.
- Lehtimäki J, Hyvärinen P, Ylikoski M, Bergholm M, Mäkelä JP, Aarnisalo A, Pirvola U, Mäkitie A, Ylikoski J (2013) Transcutaneous vagus nerve stimulation in tinnitus: a pilot study. *Acta Otolaryngol* 133:378–382.
- Lewine JD, Paulson K, Banger N, Simon BJ (2019) Exploration of the impact of brief noninvasive vagal nerve stimulation on eeg and event-related potentials. *Neuromodulation* 22:564–572.
- Ley S, Ley C, Klein O, Bernard P, Licata I (2013) Detecting outliers: do not use standard deviation around the mean, use absolute deviation around the median. *J Exp Soc Psychol* 49:764–766.
- Liu Y, Rodenkirch C, Moskowitz N, Schriver B, Wang Q (2017) Dynamic lateralization of pupil dilation evoked by locus coeruleus activation results from sympathetic, not parasympathetic, contributions. *Cell Rep* 20:3099–3112.
- Ludwig M, Wienke C, Betts MJ, Zaehle T, Hämmerer D (2021) Current challenges in reliably targeting the noradrenergic locus coeruleus using transcutaneous auricular vagus nerve stimulation (taVNS). *Auton Neurosci* 236:102900.
- Maier SU, Grueschow M (2021) Pupil dilation predicts individual self-regulation success across domains. *Sci Rep* 11:14342.
- Maris E, Oostenveld R (2007) Nonparametric statistical testing of EEG- and MEG-data. *J Neurosci Methods* 164:177–190.
- Meyer M, Lamers D, Kayhan E, Hunnius S, Oostenveld R (2021) Enhancing reproducibility in developmental EEG research: BIDS, cluster-based permutation tests, and effect sizes. *Dev Cogn Neurosci* 52:101036.
- Mridha Z, de Gee JW, Shi Y, Alkashgari R, Williams J, Suminski A, Ward MP, Zhang W, McGinley MJ (2021) Graded recruitment of pupil-linked neuromodulation by parametric stimulation of the vagus nerve. *Nat Commun* 12:1539.

- Oostenveld R, Fries P, Maris E, Schoffelen J-M (2011) FieldTrip: open source software for advanced analysis of MEG, EEG, and invasive electrophysiological data. *Comput Intell Neurosci* 2011:156869–156869.
- Pelli DG (1997) The VideoToolbox software for visual psychophysics: transforming numbers into movies. *Spatial Vis* 10:437–442.
- Peuker ET, Filler TJ (2002) The nerve supply of the human auricle. *Clin Anat* 15:35–37.
- Raedt R, Clinckers R, Mollet L, Vonck K, El Tahry R, Wyckhuys T, De Herdt V, Carrette E, Wadman W, Michotte Y, Smolders I, Boon P, Meurs A (2011) Increased hippocampal noradrenaline is a biomarker for efficacy of vagus nerve stimulation in a limbic seizure model. *J Neurochem* 117:461–469.
- Reimer J, McGinley MJ, Liu Y, Rodenkirch C, Wang Q, McCormick DA, Tolia AS (2016) Pupil fluctuations track rapid changes in adrenergic and cholinergic activity in cortex. *Nat Commun* 7:13289.
- Samuels E, Szabadi E (2008a) Functional neuroanatomy of the noradrenergic locus coeruleus: its roles in the regulation of arousal and autonomic function part i: principles of functional organisation. *Curr Neuropharmacol* 6:235–253.
- Samuels E, Szabadi E (2008b) Functional neuroanatomy of the noradrenergic locus coeruleus: its roles in the regulation of arousal and autonomic function part ii: physiological and pharmacological manipulations and pathological alterations of locus coeruleus activity in humans. *Curr Neuropharmacol* 6:254–285.
- Sara SJ (2009) The locus coeruleus and noradrenergic modulation of cognition. *Nat Rev Neurosci* 10:211–223.
- Sharon O, Fahoum F, Nir Y (2021) Transcutaneous vagus nerve stimulation in humans induces pupil dilation and attenuates alpha oscillations. *J Neurosci* 41:320–330.
- Taulu S, Simola J (2006) Spatiotemporal signal space separation method for rejecting nearby interference in MEG measurements. *Phys Med Biol* 51:1759–1768.
- Theofilopoulos N, McDade G, Szabadi E, Bradshaw C (1995) Effects of reboxetine and desipramine on the kinetics of the pupillary light reflex. *Br J Clin Pharmacol* 39:251–255.
- Urbin MA, Lafe CW, Simpson TW, Wittenberg GF, Chandrasekaran B, Weber DJ (2021) Electrical stimulation of the external ear acutely activates noradrenergic mechanisms in humans. *Brain Stimul* 14:990–1001.
- Villani V, Finotti G, Di Lernia D, Tsakiris M, Azevedo RT (2022) Event-related transcutaneous vagus nerve stimulation modulates behaviour and pupillary responses during an auditory oddball task. *Psychoneuroendocrinology* 140:105719.
- Warren CM, Tona KD, Ouwerkerk L, van Paridon J, Poletiek F, van Steenbergen H, Bosch JA, Nieuwenhuis S (2019) The neuromodulatory and hormonal effects of transcutaneous vagus nerve stimulation as evidenced by salivary alpha amylase, salivary cortisol, pupil diameter, and the P3 event-related potential. *Brain Stimul* 12:635–642.